THE UNIVERSITY *of* EDINBURGH

Structure and Regulation of G-substrate in Neurodegenerative Disease

Maa Ohui Shormeh Vigbedor

Doctor of Philosophy – The University of Edinburgh – 2013

CONTENTS

Table of Figures

List of Tables

Abbreviations

ACN – Acetonitrile

AD – Alzheimer's Disease

ADHD – Attention Deficit/Hyperactivity Disorder

APS – Ammonium PerSulphate

ATP – Adenosine TriPhosphate

BSA – Bovine Serum Albumin

BS^3 - Bis [sulfosuccinimidyl] suberate

cDNA – complementary DNA

CF – Climbing Fibre

cGMP – cyclic Guanosine MonoPhosphate

cGK2 – cyclic GMP dependent protein Kinase 2

CHCA – α-Cyano-4-HydroxyCinnamic Acid

CJD – Creutzfeldt - Jakob Disease

CNS – Central Nervous System

DA – Dopaminergic

DARP-32 – Dopamine and cyclic AMP-Regulated neuronal Phosphoprotein-32

DNA – DeoxyriboNucleic Acid

DTT – DiThioThreitol

ECL – Enhanced ChemiLuminescence

EDC - 1-Ethyl-3-(3-dimethylaminopropyl) carbodiimide hydrochloride

EDTA – EthyleneDiamineTetraacetic Acid

EVC – Ellis-van Creveld syndrome

FPLC – Fast Protein Liquid Chromatography

FRET – Fluorescence Resonance Energy Transfer

GDI2 – Guanosine diphosphate Dissociation Inhibitor 2

GFAP – Glial Fibrillary Acidic Protein

GFP – Green Fluorescent Protein

GRIN1 – G-protein Regulated Inducer of Neurite Outgrowth 1

GTP – Guanosine TriPhosphate

GS – G-Substrate

HRP – Horse Radish Peroxidase

IAA - IodoAcetAmide

IPTG – IsoPropyl-beta-D-ThioGalactopyranoside

KLH – Keyhole Limpet Haemocyanin

LB – Lysogeny Broth

L-DOPA – Levo-Dopa

LTD – Long Term Depression

MALDI-tof – Matrix-Assisted Laser Desorption Ionization time-of-flight

MES - 2-(N-Morpholino) EthaneSulfonic acid

MINT – Molecular INTeractions database

MOWSE – MOlecular Weight SEarch

NEB – New England Biolabs

NMR – Nuclear Magnetic Resonance

NO – Nitric Oxide

NOESY - Nuclear Overhauser Effect SpectroscopY

NOS1 – Nitric Oxide Synthase 1

NTA - Nitriloacetic Acid

OD – Optical Density

PBS – Phosphate Buffered Saline

PC – Purkinje Cell

PCR – Polymerase Chain Reaction

PD – Parkinson's Disease

PF – Parallel Fibre

PKG – cGMP-dependent Protein Kinase

PMSF – PhenylMethaneSulfonyl Fluoride

pNPP – para NitroPhenyl Phosphate

PP1 – Protein Phosphatase 1

PP1γ – Protein Phosphatase 1 Gamma isoform

PP2A – Protein Phosphatase 2A

PP5 – Protein Phosphatase 5

PVDF - PolyVinyliDene Fluoride

SCA1 – Spinocerebellar Ataxia Type 1

sdH_2O – Sterile distilled water

SDS-PAGE – Sodium-Dodecyl Sulphate PolyacrylAmide Gel Electrophoresis

SEM – Standard Error of the Mean

TAE – Tris Acetate EDTA

TBS-T – Tris Buffered Saline with Tween-20

TOCSY – Total Correlated SpectroscopY

UV – Ultra Violet

WAD – Acrofacial Dysostosis Weyers type

DECLARATION

I DECLARE THAT THIS THESIS IS MY OWN COMPOSITION AND THAT THE WORK PRESENTED HEREIN IS MY OWN WORK UNLESS OTHERWISE STATED. THIS WORK HAS NOT BEEN SUBMITTED FOR ANY OTHER DEGREE OR PROFESSIONAL QUALIFICATION.

…….

MAA OHUI SHORMEH VIGBEDOR

ACKNOWLEDGEMENTS

I thank God for His grace and provision during my PhD.

My immense gratitude goes to Professor Alastair Aitken for his excellent supervision and to the Darwin Trust of Edinburgh for funding my studies.

I would also like to thank Professor Patricia Cohen of Dundee University for her kind gift of purified PP1 gamma and PP5 and Professors Paul Greengard and Angus Nairn of Rockefeller University for their kind gift of the phospho G-substrate antibody.

I would also like to thank Dr. Andrew Cronshaw for assistance with mass spectrometry, Mr. Juraj Bella and Dr. Andrew Herbert for assistance with NMR and Dr. Janice Bramham for help and advice on CD experiments.

I owe a debt of gratitude to my husband, Francis and to my whole family for their support and understanding during my PhD.

I would finally like to thank past and present members of the Aitken research group for interesting and useful discussions. My appreciation goes especially to Miss MunChing Lee, Miss Sylvia Ispasani and Mr. Sean McLaughlin-Stewart for collaboration in the investigation of the effect of DJ-1 on G-substrate.

ABSTRACT

G-substrate is a 23 kDa protein named as a specific substrate of cGMP-dependent protein kinase and found predominantly in cerebellar Purkinje cells. As a component of the NO/cGMP/PKG pathway, G-substrate is potentially involved in several important cellular processes and has so far been associated with a number of disease conditions: a single point mutation in G-substrate has been linked to hypercholesterolaemia, while the potent inhibition of PP2A by phosphorylated G-substrate possibly influences Tau protein hyperphosphorylation and contributes to Alzheimer's disease pathology. Conversely, overexpression of G-substrate protein in dopaminergic neurons has been found to protect neurons from Parkinson's disease toxins, making G-substrate a possible target of interventions for mitigating the debilitating effects of Parkinson's disease on patients.

A shorter splice variant, which only retains one of the phosphorylatable threonine motifs, has recently been described for G-substrate and given the importance of phosphorylation to its action as a phosphatase inhibitor, this study focuses on determining whether both variants of the protein exhibit similar levels of phosphatase inhibition and interact with the same/similar proteins *in vivo*. We were also interested in determining whether the 51 amino acid section absent from short G-substrate resulted in any significant differences in protein structure, which potentially has implications on functions *in vivo*.

My results indicate the association of G-substrate with a wide range of proteins involved in processes including cell cycle regulation, endocytosis and signalling and the two variants do not always interact with the same proteins. Among these interactors is the PARK 7/ DJ-1 protease, which like G-substrate has been shown to be neuroprotective. I have found that G-substrate is proteolysed by DJ-1 in its active form and interactions between these two proteins is affected by the anti-vertigo drug Tanganil. Phosphatase inhibition studies suggest that the G-substrate variants affect phosphatase activity to different extents under similar conditions, while NMR and circular dichroism structural studies suggest that in solution, the full length G-substrate variant is slightly more compactly folded.

Understanding the details of G-substrate action in the cell will lead to a better understanding of its roles including the protection of dopaminergic neurons from Parkinson's disease toxins and shed more light on the intricacies of the NO/cGMP/PKG signalling pathway as a whole, thus providing important information that might help improve strategies for dealing with conditions involving this pathway and help develop interventions for diseases such as Alzheimer's and Parkinson's.

Chapter 1: Introduction

1.1 G-substrate

Human G-substrate, an acid and heat stable protein (1) also known as protein phosphatase 1 regulatory subunit 17 (C7 orf 16), is located in the 7p15 region of chromosome 7(2). The G-substrate gene (Ensembl ID: ENSG00000106341.6) encodes three transcripts; PPP1R17-001, PPP1R17-002 and PPP1R17-003 (**Error! eference source not found.**). PPP1R17-003 encodes a processed transcript with no known protein product while the other two transcripts are protein coding. PPP1R17-001 codes for isoform 1 of the protein, which is 155 amino acids long. The protein coded for by PPP1R17-002 is a 104 amino acid protein, with identical N- and C-termini to isoform 1, but missing a 51 amino acid section containing the first phosphorylation motif of full length G-substrate (Figure 1.2). Phosphorylation of the threonine residue retained in the short isoform was found by Aitken and coworkers to be essential for the phosphatase inhibition activity of full length G-substrate (3) The G-substrate gene is conserved across several species, with protein sequences from human, chimpanzee, rat, mouse and chicken showing large areas of homology with almost complete identity at the phosphorylation motifs (Figure 1.3).

Online subcellular localization prediction using WoLF PSORT (4) revealed the existence of a possible endoplasmic reticulum (ER) membrane retention signal – a 'KKXX-like' motif represented by the sequence DKIA in the C-terminal region and one of two peroxisomal targeting signal (PTS2) of the consensus (R/K)-(L/I/V)-X5-(Q/H)-(L/I/V),within the sequence KLDPRCSHL located near the N-terminal region of both full length and short G-substrate. The presence of these signals suggests that *in vivo*, some G-substrate protein might exist localized to the ER, suggesting a role in either fatty acid or protein synthesis depending on whether localization is to the smooth or rough ER. The additional presence of a peroxisomal targeting sequence, however, might indicate that G-substrate is localized to the smooth rather than the rough ER. Peroxisomes, which are thought to originate from the ER (5), represent a class of ubiquitous and essential cell organelles characterized by the presence of a proteinaceous matrix surrounded by a single membrane and are involved in fatty acid (FA) beta-oxidation in virtually all organisms. Peroxisomes of higher eukaryotes are, in addition, involved in a number of functions not shared by peroxisomes in lower

eukaryotes, including ether phospholipid biosynthesis, FA alpha-oxidation, and glyoxylate detoxification.

Defects in peroxisomal biogenesis or protein recruitment have been linked with a number of diseases including Zellweger spectrum disorders, X-linked adrenoleukodystrophy (X-ALD) and Refsum disease (phytanoyl-CoA hydroxylase deficiency) (6).

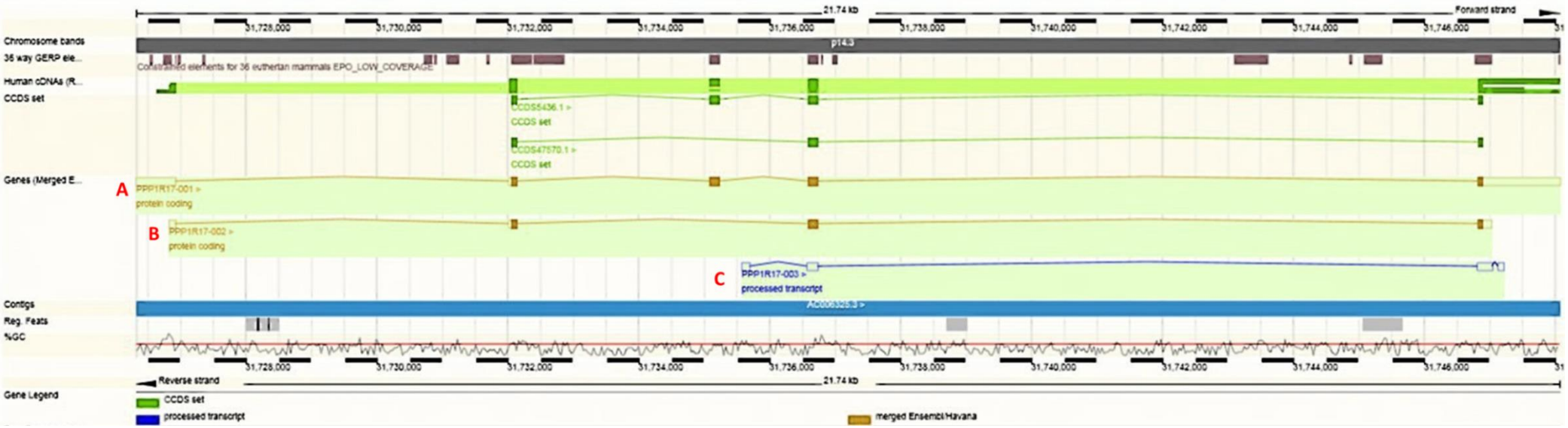

Figure 1.1: Ensembl image showing transcripts of the G-substrate gene.

A and **B** represent translated mRNA transcripts for G-substrate variants 1 and 2 respectively, while **C** represents an untranslated transcript of the G-substrate gene

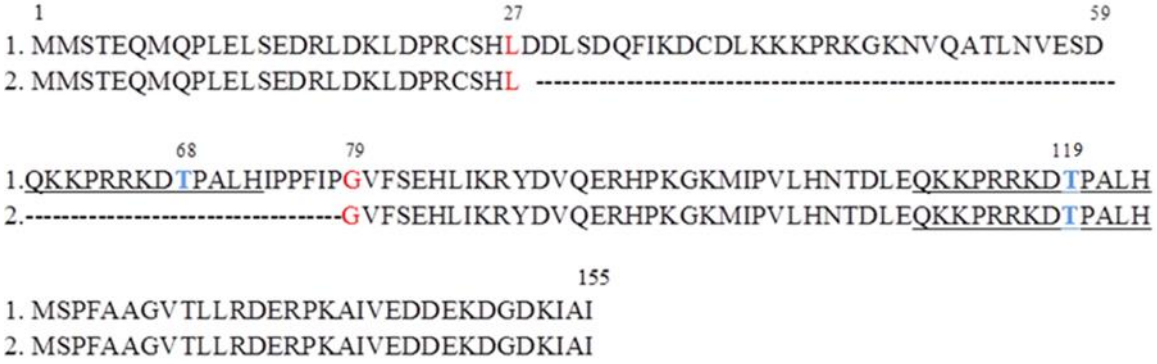

Figure 1.2: Alignment of human G-substrate isoforms.

The phosphorylation motif is underlined, T represents phosphorylatable threonine residues, residues in red flank area deleted from the full length protein, 1=full length G-substrate and 2=short G-substrate

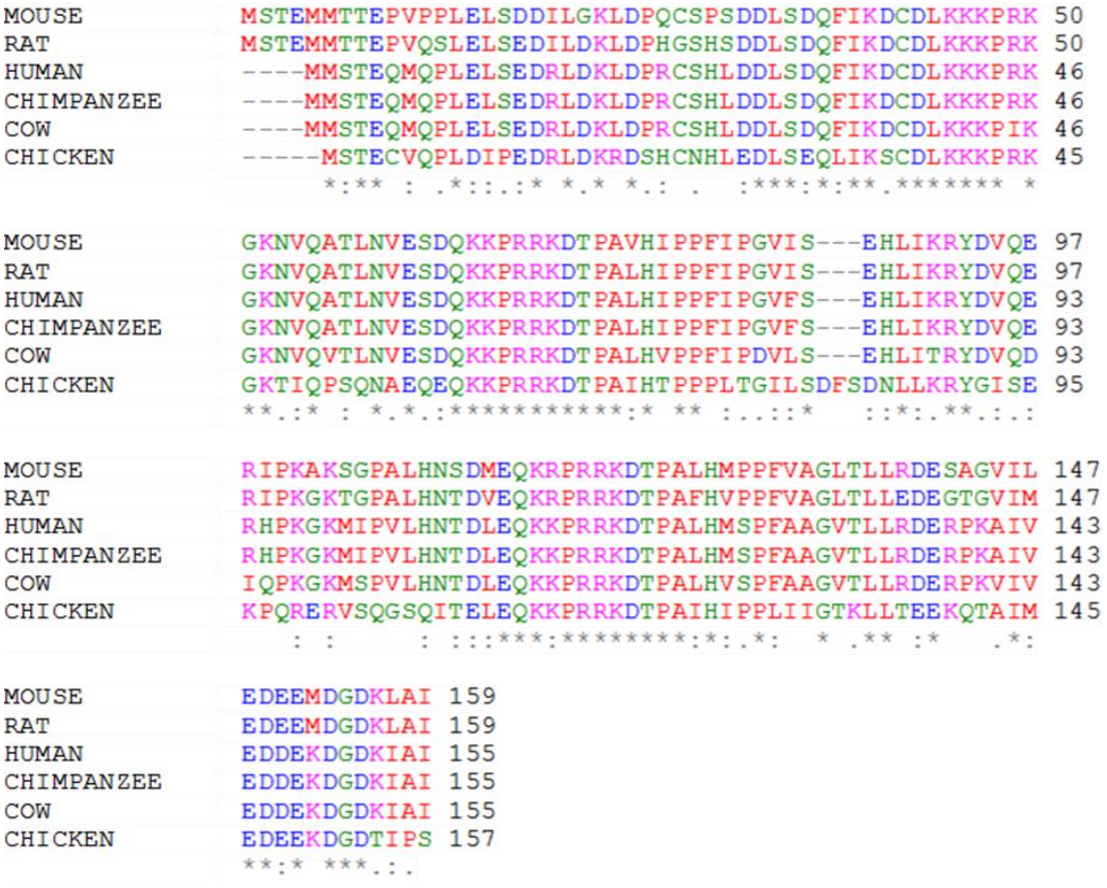

Figure 1.3: Alignment of canonical G-substrate sequences from mouse, rat, human, chimpanzee, cow and chicken.

1.1.1 Discovery of G-substrate

G-substrate was discovered during an investigation to identify endogenous substrates of cyclic guanosine monophosphate (cGMP)-dependent protein kinase (cGK) in mammalian brain. It was discovered that G-substrate, a soluble protein with an apparent molecular weight of 23,000 from rabbit cerebellum, was rapidly phosphorylated by cGK, while the presence of types I and II cyclic adenosine monophosphate (cAMP)-dependent protein kinases (PKA) failed to significantly increase the amount of phosphate incorporated into the protein (1).

1.1.2 G-substrate Localization

G-substrate contains three clusters of basic amino acids ---**KKKPR/IKGK**---**KKPRRK**DT(Pi)PA---**KKPRRK**DT(Pi)PA---, the second and third of which possess identical amino acid sequences and occur adjacent to the phosphorylatable threonine residues originally described by Aitken and co-workers through direct protein sequencing of G-substrate purified from rabbit cerebellum [3]. Although no specific function has been determined for these amino acid clusters, it has been suggested that these clusters could represent potential nuclear localization signals (NLSs), which are characterized by clusters of basic amino acids. It is also possible that the presence of a number of hydrophobic amino acids interspersed in short sequences might represent a nuclear export sequence (NES).The presence of both NLSs and NESs (Figure 1.4) suggests that G-substrate may shuttle between the cytoplasm and the nucleus, a possibility supported by the observation that studies of cerebellar Purkinje cells in brain slices show G-substrate in both the cytosol and the nucleus of the Purkinje cells. The location of NLSs near the phosphorylation sites of G-substrate could result in the phosphorylation state of the protein determining the location of the protein; it is likely that upon phosphorylation, the negative charge introduced by the $PO4^{2-}$ group might disrupt the structure of the amino acid clusters, interfering with their ability to bind to shuttling proteins and resulting in the retention of phosphorylated G-substrate either in the nucleus or in the cytoplasm.

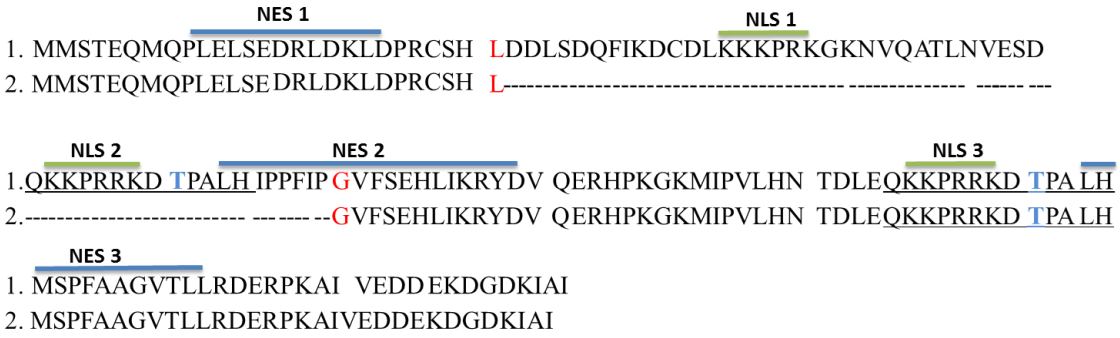

Figure 1.4: Alignment of human G-substrate isoforms showing positions of NESs and NLSs. Blue and green lines show amino acids making up respective signals, **T** represents phosphorylatable threonine residues, 1=full length G-substrate and 2=short G-substrate

While several regions of rabbit brain including the hippocampus, caudate and cerebral cortex were investigated by Schlichter and coworkers in 1978, the 23,000 molecular weight band representing G-substrate was only found in the cerebellar fractions (7). Endo and co-workers later confirmed that G-substrate was localized almost exclusively to the Purkinje cells of the cerebellum (8). Low levels of G-substrate have also been detected in the paraventricular region of the hypothalamus and the pons/medulla (9). A small proportion of G-substrate has also been found to co-express with other signalling components of the NO-cGMP-cGK pathway in the retinas of adult mice and rats, where it is located in a subpopulation of amacrine cells and in C38-positive retinal ganglion cells (RGCs), but not in alpha RGC's (10).

1.1.2.1 The Cerebellum

The cerebellum is located beneath the cerebrum and behind the brain stem (Figure 1.5) and accounts for approximately 10 % of the volume of the brain (11). Despite its relatively small size, the cerebellum is thought to contain over half the total number of neurons in the brain (12).

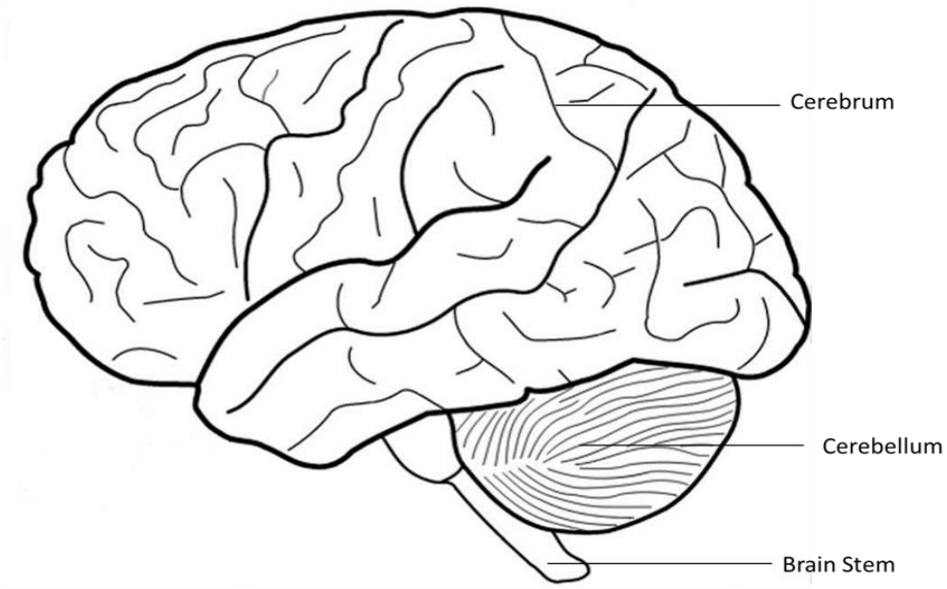

Figure 1.5: A lateral view of the human brain showing its main features

The cerebellum possesses three major functional divisions (Figure 1.6): the spinocerebellum, in the vermis and intermediate part of the cerebellar hemispheres is involved in ongoing maintenance of tone, execution, and control of axial and proximal (vermis) and distal movements; the cerebrocerebellum, in the lateral part of the hemisphere is involved in initiation, motor planning, and timing of coordinated movements (13); and the vestibulocerebellum in the flocculonodular lobe is involved in axial control and balance and positional reflexes. The NO/cGMP/PKG pathway, of which G-substrate is a member has been shown to be essential in the induction of cerebellar long term depression (LTD) (14) and LTD-dependent motor learning. This includes the vestibule-ocular reflex adaptation controlled by this part of the cerebellum. In addition, we have evidence that the drug Tanganil, affects the interaction between the Parkinson's disease protein, Park7/DJ-1 and G-substrate (see section 7.4.2). Tanganil has been shown to target the vestibular system (15).

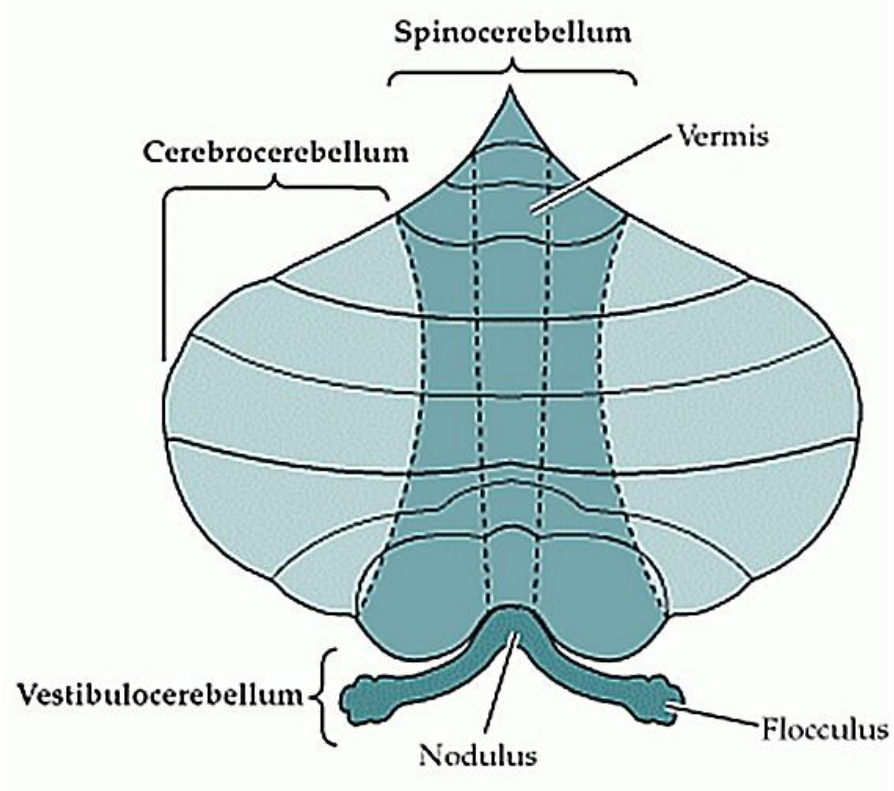

Figure 1.6: Flattened view of the cerebellar surface illustrating the three major subdivisions (16).

The cerebellar cortex is divided into three distinct cellular layers with specific cellular composition (Figure 1.7). The molecular layer is the outermost layer and is primarily made up of Purkinje cell dendrites and granule cell axons (parallel fibres). The molecular layer also contains the stellate and basket cell interneurons (17). Next is the Purkinje cell layer, which is mainly made up of a monolayer of Purkinje cell somata. The Purkinje cell layer also contains the cell bodies of Candelabrum cells and Bergmann Glia (18). Lastly, bordering the medullary centre of the cerebellum is the granular (granule cell) layer. The small granule cells comprise the great majority of this layer within which the somata of the Golgi cell, Lugaro cell interneurons and the unipolar brush cells are also located.

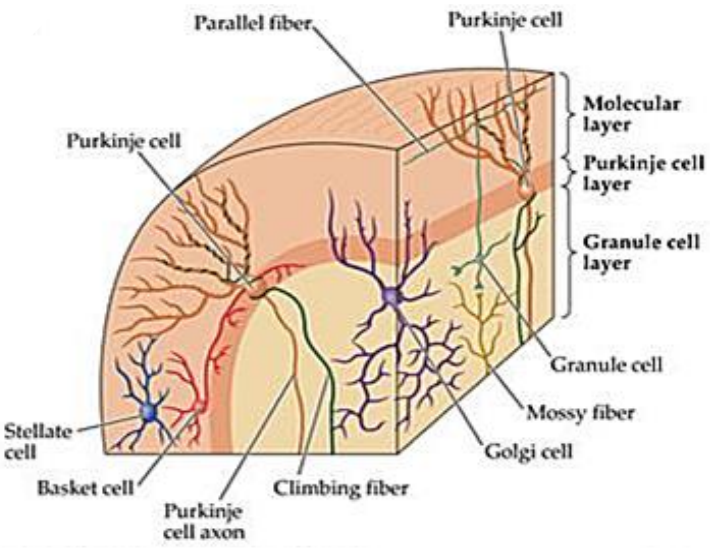

Figure 1.7: The Three Cellular Layers of the Cerebellar Cortex (18).

Purkinje cells form the sole output of the cerebellar cortex (19) and are consequently extremely important for the function and development of the cerebellum. Diseases and disorders affecting the function of Purkinje cells result in severe sensory-motor defects such as ataxia, altered motor learning, and possibly cognitive defects (20). As mentioned in section 1.1.2 above, the majority of G-substrate is located in the Purkinje cells, where it is found in the dendrites, somata and axons, suggesting an important role for this protein in Purkinje cell and ultimately cerebellar function.

1.1.2.2 G-substrate Expression is Age-dependent

In 2002 Iida and coworkers, using a fluorescence differential display PCR method, identified G-substrate as one of five genes expressed in an age-dependent manner in the brains of 3-day- to 15-month-old mice (21). Quantitative PCR analyses revealed that the expression of G-substrate mRNA was quite low in the brains of 3-day- and 1-week-old mice, but was modest in 2-week- to 9-month-old mice. The highest expression of G-substrate was observed in 15-month-old mice, which had mRNA levels approximately twice that of 6- and 9-month-old mice. The notable increase in G-substrate expression in the brains of 2-week-old mice corresponds to the maturation of cerebellar neuronal circuitry (22-24), including the maturation of the cerebellar Purkinje cells where G-substrate is most abundant. This age-dependent

increase in G-substrate expression suggests the possibility of G-substrate contributing physiologically to mechanisms that might compensate for the age-dependent decline in motor function (25,26), since the cerebellum plays an important role in controlling motor function.

1.1.3 G-substrate Polymorphisms

Natural variations in amino acid composition occur at positions 10 (R to L) and 12 (V to L) (27). One single nucleotide polymorphism (SNP), involving the substitution of a tyrosine residue with a cytosine residue in the 5' promoter region of the G-substrate gene (–1323T>C), has been linked to hypercholesterolemia in subjects studied in East-Central Japan. The T-allele was found to result in hypercholesterolemia approximately two-fold higher than in individuals lacking the T-allele with individuals carrying the T-allele showing total cholesterol levels approximately 14 % higher than those without it (28).

1.1.4 Phosphorylation of G-substrate

G-substrate is phosphorylated exclusively on two threonine residues (Thr 68 – site 1 and Thr 119 – site 2 in humans) successfully by both cyclic AMP- and cyclic MP-dependent protein kinases (29). These serine/threonine protein kinases are very much alike, showing highly similar amino acid compositions and hydrodynamic shapes among other things. PKA and cGK also share a number of *in vitro* substrates including glycogen synthase, pyruvate kinase and cardiac troponin–1 with the *in vitro* phosphorylation of such shared substrates generally proceeding more rapidly with PKA. In spite of their similarities, these two kinases also exhibit several major differences, which support suggestions that they regulate distinct physiological processes. These include their sensitivities to and mechanisms of activation by cyclic nucleotides, immunochemical cross-reactivity, and tissue distributions among others. Perhaps the most significant difference between these kinases is the fact that all the functional domains of cGK are found on a single polypeptide chain, whereas PKA has separate regulatory (cAMP binding) and catalytic chains.

1.1.4.1 Cyclic GMP-dependent Protein Kinase

G-substrate was discovered and named as a specific substrate of cGK. Mammalian cGK exists as three isoforms encoded on two genes. Human PRKG1, located on chromosome 10, encodes the soluble isoform I of cGK. The amino terminus (first 90 to 100 residues) of cGK I is encoded by two alternative exons, producing cGK isoforms Iα and Iβ. cGK I has been found at high concentrations in all types of smooth muscle, hippocampal neurons, the lateral amygdala, platelets and cerebellar Purkinje cells (30) and is most likely the isoform with which cerebellar G-substrate interacts. PRKG2 is located on chromosome 4 and encodes the membrane-bound isoform 2 (cGK II), which is expressed in prostate, small intestine, colon, thymus and prostate. cGK phosphorylates both sites of G-substrate at similar rates, yielding a V_{max} of 2.2 µmol/min/mg and a K_m of 0.21µM. The high degree of specificity exhibited by cGK towards G-substrate is purported to be a result of selective substrate binding rather than catalytic efficacy (29).The two isoforms of cGK exist as homodimers, held together by leucine zippers in the N-terminus and have similar domain structures made up of an N-terminal regulatory domain containing a dimerization and an autoinhibitory region, two tandem cGMP-binding domains and a C-terminal catalytic domain (Figure 1.8).

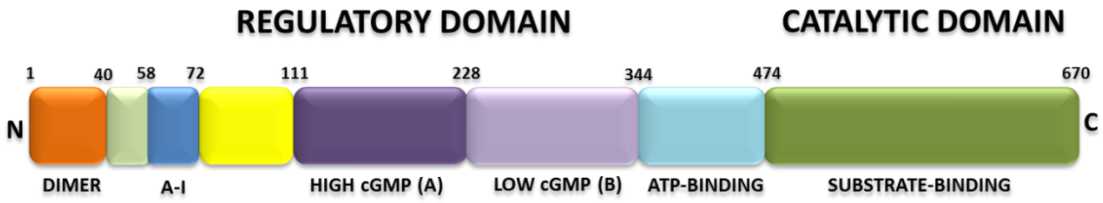

Figure 1.8: A schematic representation of the functional domain structure of a monomer of cGK.

'N' and 'C' refer to the N- and C-termini respectively. 'Dimer' represents the dimerization domain and 'A-I' represents the autoinhibitory domain. Numbers indicate amino acid residues in the polypeptide chain.

In the absence of cGMP, cGKs exist in a conformation which has their catalytic/substrate binding domains bound to an autoinhibitory/ pseudo substrate domain, making them unable to bind substrates and effect catalysis (Figure 1.9). Upon cGMP binding, the apo-enzyme structure effectively unfurls and frees the catalytic domain for substrate phosphorylation (31). Research has shown that the two cGMP-binding sites contribute differently to activation of cGK I and cGK II. Binding of cGMP to the high affinity sites alone was found to result in partial activation of cGK I kinase activity, which was further activated upon binding of high concentrations of cGMP to its low affinity sites. In cGK II, occupation of the high affinity site had no effect on the kinase's ability to phosphorylate its targets, implying that occupation of the low affinity cGMP-binding site was required for effective activation of cGK I.

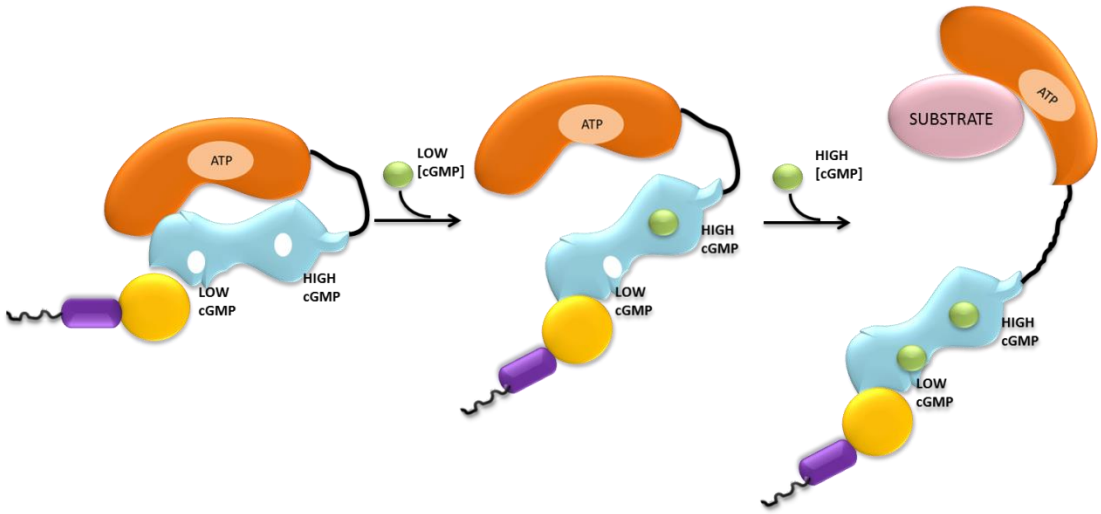

Figure 1.9: An illustration of mode of activation of cGK by cGMP.
Image is adapted from Taylor et al. (32). The kinase is shown as a monomer for simplicity.

1.1.4.2 Cyclic AMP-dependent Protein Kinase

Although G-substrate is successfully phosphorylated by both cGK and cAK, phosphorylation by cAK occurs at a much lower rate, yielding a V_{max} of 2.3 pmol/min/mg and a K_m of 5.8 µM. Furthermore, unlike cGK, cAK phosphorylates

the two threonine residues of G-substrate at different rates, with site 2 being phosphorylated 4 times more slowly than site 1(3). cAK occurs naturally as a quaternary structure made up of two regulatory (R) and two catalytic (C) subunits. R subunits exist as two major forms, R I and R II, each of which has two subtypes, alpha and beta. All four subtypes of the cAK regulatory subunit are encoded by different genes. The catalytic subunit exists as three isoforms, alpha, beta and gamma, encoded on chromosomes 19, 1 and 9 respectively. The different isotypes of cAK subunits are believed to facilitate targeting to tissues and cells. Regulatory subunits contain two cAMP binding domains, an auto inhibitory domain and a dimerization domain at the N-terminal position. A typical catalytic subunit contains and ATP binding site, a site at which the regulatory subunit binds and the active site of the enzyme (Figure 1.10). Interestingly, although cGK and cAK have a number of substrates in common, the positions of the high and low affinity cyclic nucleotide binding sites, which are vital to their activation, are reversed in these two kinases.

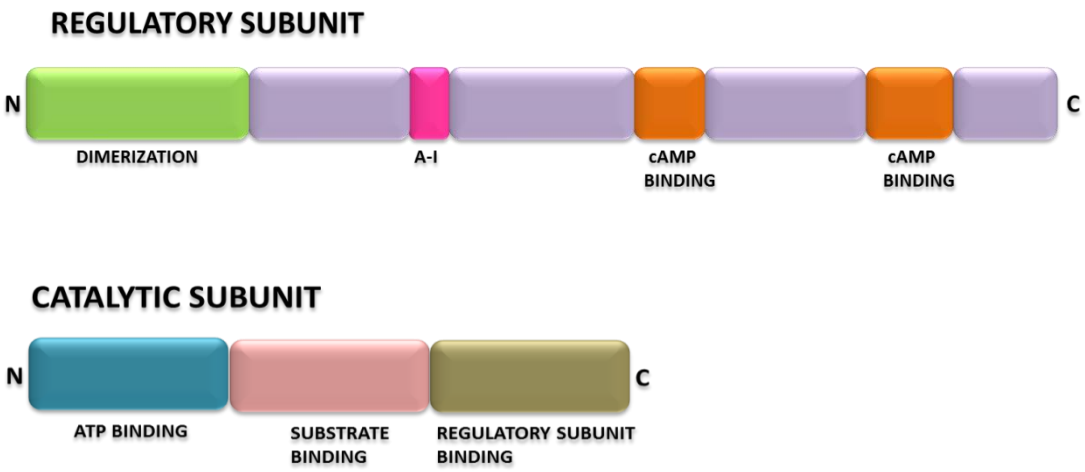

Figure 1.10: A schematic representation of typical domain architecture of cAK regulatory and catalytic subunits.

'N' and 'C' refer to the N- and C-termini respectively and 'A-I' represents the autoinhibitory domain.

The cAK holoenzyme exists as a 'dimer of dimers' – each dimer consists of a catalytic subunit bound to a regulatory subunit and the two dimers interact at their dimerization domains to form a tetrad, the inactive cAK enzyme. Upon cAMP

binding, the catalytic subunits dissociate from the regulatory subunits, free and active and able to phosphorylate its substrates (Figure 1.11).

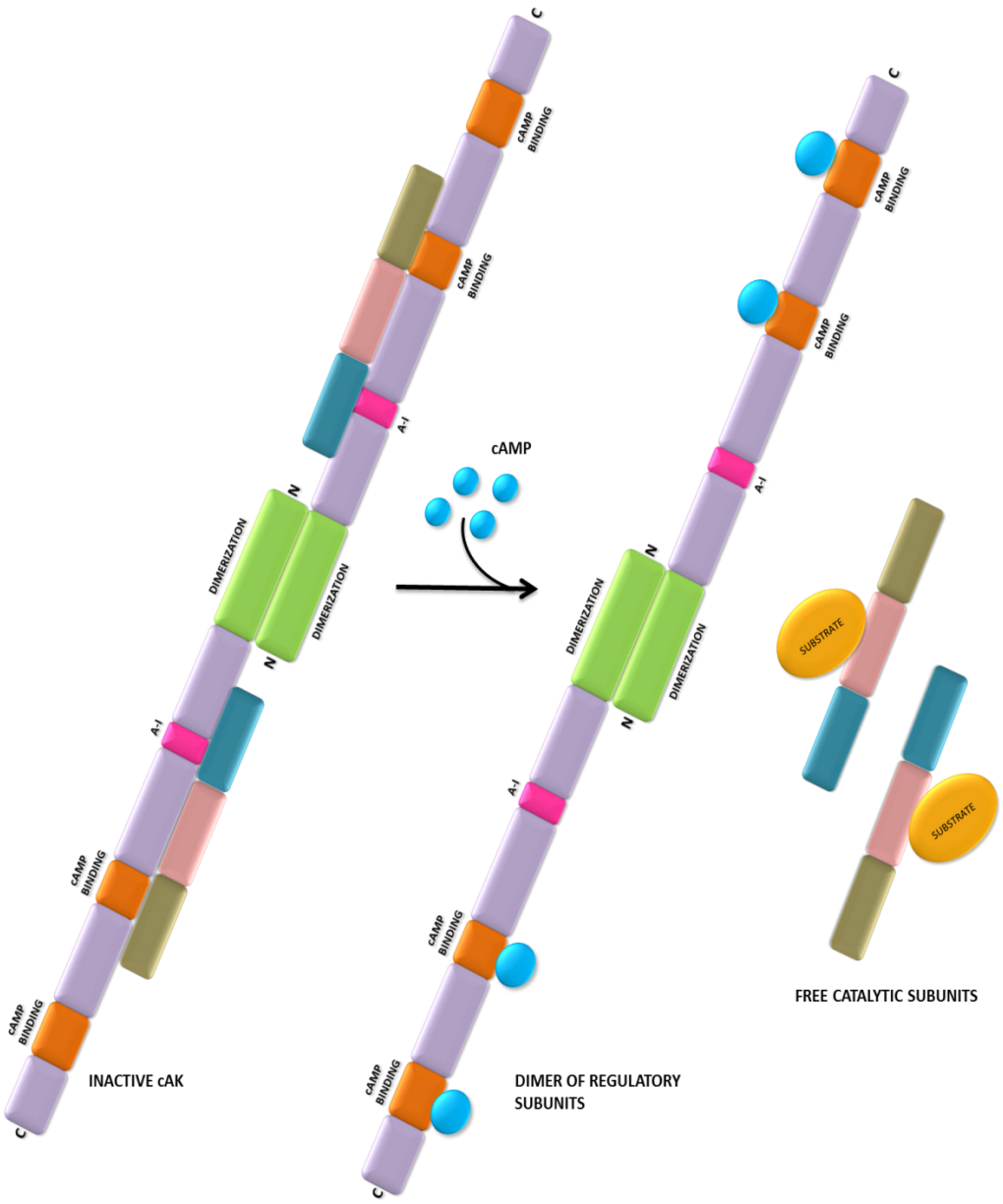

Figure 1.11: An illustration of cAK activation by cAMP.

1.1.5 Phosphatase Inhibition by Phospho G-substrate

Phospho-G-substrate is known to effectively inhibit protein phosphatase 1 (PP1) and protein phosphatase 2A (PP2A) upon phosphorylation at two threonine residues. PP1 and PP2A have been found to catalyze about 90 % of the phospho-protein

dephosphorylations that occur in the eukaryotic cell. Mammals are thought to contain as many as 650 distinct PP1 complexes and approximately 70 PP2A holoenzymes (33), suggesting that PP1 catalyzes the majority of protein dephosphorylation events in the mammalian cell. Work done by Hall and coworkers (9) and by Endo and coworkers (8) suggest that phospho-G-substrate inhibits one of these phosphatases more effectively than the other. These investigations were, however, carried out under different conditions with Endo and coworkers using PP2Ac to assay the protein phosphatase inhibitory activities of human and rat G-substrate while Hall and coworkers used $PP2A_1$ to assay the protein phosphatase inhibitory activity of mouse G-substrate. It is therefore also probable that the differences observed could be due to the unique effects of the different conditions used by the two groups on the reaction dynamics. Further investigation is therefore necessary to confirm the existence of any differences in the ability of G-substrate to inhibit these phosphatases and to determine whether G-substrate protein purified from different species affect these and other phosphatases differently.

1.1.5.1 Protein Phosphatase 1

PP1 plays important roles in the control of glycogen metabolism, muscle contraction, cell progression, neuronal activities, RNA splicing, mitosis, apoptosis, protein synthesis, and the regulation of membrane receptors and channels (34) The human genome, like other mammalian genomes, contains three PP1-encoding genes. These genes encode four different catalytic subunits: PP1α, located on chromosome 11, PP1β, also known as PP1δ, which is located on chromosome 2 and the splice variants PP1γ1 and PP1γ2 located on chromosome 12. These isoforms of PP1c are thought to have about 85 % similarity, differing mainly in their N- and C-termini and exhibiting a similarly broad substrate similarity as free PP1 isoforms. The targeting of the PP1 catalytic subunit to particular cellular locations and its specificity towards its wide range of targets has been shown to result mainly from interactions with a large number of regulatory subunits including activity modulators, chaperones and inhibitors (35). A number of docking/interacting motifs/domains have been described for PP1 interactions with regulatory proteins.

The primary motif, referred to as the RVxF domain, generally conforms with the consensus sequence K/R K/R V/I x F/W, where x is any residue other than phenylalanine, isoleucine, methionine, tyrosine, aspartic acid, or proline (36). This sequence is thought to bind in an extended conformation to a PP1 hydrophobic groove about 20 Å (~ 2.1 nm) away from the active site and function mainly to anchor interacting proteins to PP1. This brings PP1 close to its interacting proteins and promotes secondary interactions that contribute to PP1 isoform selection, determination of activity and substrate specificity of the holoenzyme.

Other interacting/docking domains currently identified include the ΦΦ pocket described for interactions with the RNA-binding protein nuclear inhibitor of PP1 (NIPP1) (37). This hydrophobic pocket is formed by PP1 residues Leu_{75}, Tyr_{78}, Met_{282}, Ile_{295}, Leu_{296}, and Lys_{297} and regulatory proteins access via two sequential hydrophobic (ΦΦ) residues, Ile_{209} and Ile_{210} of NIPP1. A similar but not identical interaction with PP1 has been observed involving residues Val_{458} and Phe_{459} of spinophilin, an actin-binding PP1 regulator highly enriched in dendritic spines.

The SILK motif, which contains the consensus sequence G/S I L R/K has been found in seven of the vertebrate PP1 interactors currently identified. This motif is usually positioned N-terminal to the RVxF sequence and like the RVxF domain, does not affect the conformation of the PP1 enzyme, but contributes to the effective anchoring of PP1 to interacting proteins (38).

The protein MYPT1 (myosin phosphatase target subunit 1/protein phosphatase 1 regulatory subunit 12A), which is involved in the regulation of the interaction between actin and myosin, contains a PP1 interaction motif at its N-terminus that adheres to the consensus sequence R x x Q V/I/L K/R x Y/W, where x can be any residue. This motif is referred to as the myosin phosphatase N-terminal element or MyPhoNE lies within a five-turn α-helix, which faces hydrophobic residues in a shallow hydrophobic cleft on PP1 and is present in six other PP1 interacting proteins (39).

A number of PP1 interacting proteins, including MYPT1 and the neurabins, which target PP1 to dendritic spines, are thought to possess isoform-specific docking sites since they interact with PP1 in an isoform-dependent manner. It is suspected that

these isoform-specific docking domains may be found around the N- and C-termini of the PP1 isoforms since they differ mainly at these termini.

Interestingly, none of the currently described PP1 docking domains has been found in either isoform of human g-substrate. The section of g-substrate protein (both full length and short isoforms) most similar to the classical RVxF domain is a region just upstream of the phosphorylation motif at site 1. This section reads N- to C- terminus as FSEHLIKR, but when read C- to N- terminus, appears to contain a possible RVxF (**RKIL**HES**F**) domain, although the last two residues of this possible RVxF domain (red) are separated by three amino acid residues (blue).

Both variants of G-substrate possess a number of pairs of hydrophobic residues that could function as possible ΦΦ regions. These include the first two methionines of both isoforms, M_1, M2. Full length g-substrate possesses two identical sequential hydrophobic amino acid pairs, $F_{34,}$ I_{35} and $F_{76,}$ I_{77}, both of which are absent from the short variant because they fall in the region of full length G-substrate absent from the short protein. In addition to the above pairs, both full length and short G-substrate possess six identical hydrophobic amino acid pairs that could function as ΦΦ regions (Figure 1.12); Val_{80} Phe_{81}, Leu_{85} Ile_{86}, Met_{100} Ile_{101}, Val_{103} Leu_{104}, Leu_{133} Leu_{134} and Ile_{142} Val_{143} in the full length protein and Val_{29} Phe_{30}, Leu_{34} Ile_{35}, Met_{49} Ile_{50}, Val_{52} Leu_{53}, Leu_{82} Leu_{83} and Ile_{91} Val_{92} in short g-substrate.

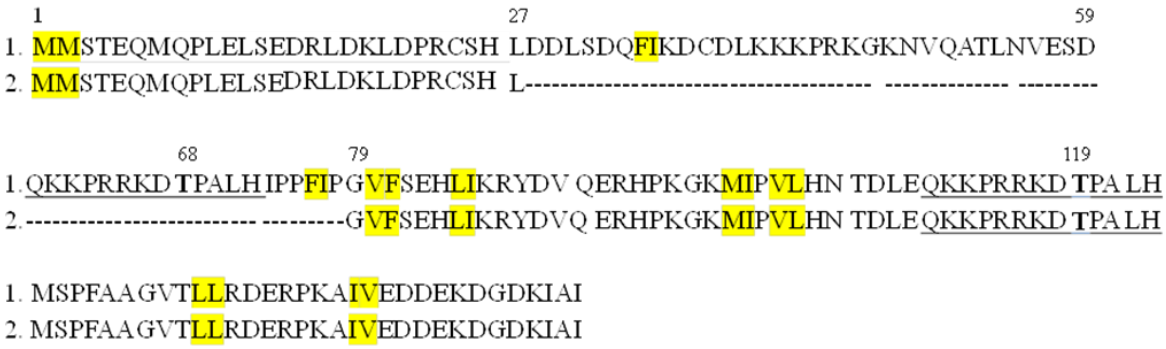

Figure 1.12: Alignment of human G-substrate isoforms with possible ΦΦ domains highlighted.
The phosphorylation motif is underlined, sequential hydrophobic amino acid pairs (ΦΦ) are highlighted, 1=full length G-substrate and 2=short G-substrate

1.1.5.2 Protein Phosphatase 2A

The heterotrimeric PP2A holoenzyme results from the assembly of a common heterodimeric core enzyme with a regulatory subunit. The heterodimeric core comprises a 36 kDa catalytic subunit (subunit C) and a 65 kDa scaffolding subunit (subunit A, also known as PR65). This core enzyme associates with a variety of regulatory subunits including viral proteins, cell signalling molecules and three accepted families of regulatory B subunits – the B, B' and B'' families. A fourth family of B subunits, the B''' family, which includes SG2NA, the striatins, and mMOB1 has been described, although controversies exist as to whether these subunits always associate with the core heterodimer or are only regulated by association with the heterodimer (40) The C subunit is encoded by two genes, PPP2CA and PPP2CB, which share 97 % identity and binds stably to the carboxyl-terminal region of the A subunit. The A subunit is encoded by two genes, PPP2R1A and PPP2R1B, and forms a rod-shaped polypeptide consisting of 15 imperfect repeats. The B subunits bind to repeats 1 to 10 (the amino-terminal region) of the A subunit while the C subunits bind to repeats 11-15 (Figure 1.13).

The large number of regulatory subunits PP2A associates with may provide a molecular basis as to how this enzyme can appropriately regulate numerous cellular processes, sometimes in seemingly antagonistic ways. PP2A can, for example, regulate the MAP kinase pathway both positively by dephosphorylating some of the inhibitory sites on Raf-1 and negatively by reversing some of the phosphorylation events downstream of Raf-1 (41). So far, PP2A has been implicated in the regulation of signal transduction, growth, development, metabolism, cell cycle progression and transformation.

Protein phosphatase 2A has been classified as a tumour suppressor due to its role in the regulation of cell proliferation pathways. This is normally brought about by PP2A 'switching off' signals turned on by phosphorylation. The protein Myc, for example, is an important regulator of cell proliferation, which is amplified in many human cancers and stabilised upon phosphorylation by extracellular-regulated kinase (ERK) (42). Upon dephosphorylation by PP2A Myc is targeted for degradation by polyubiquitination, reducing its abundance in the cell and affecting proliferation.

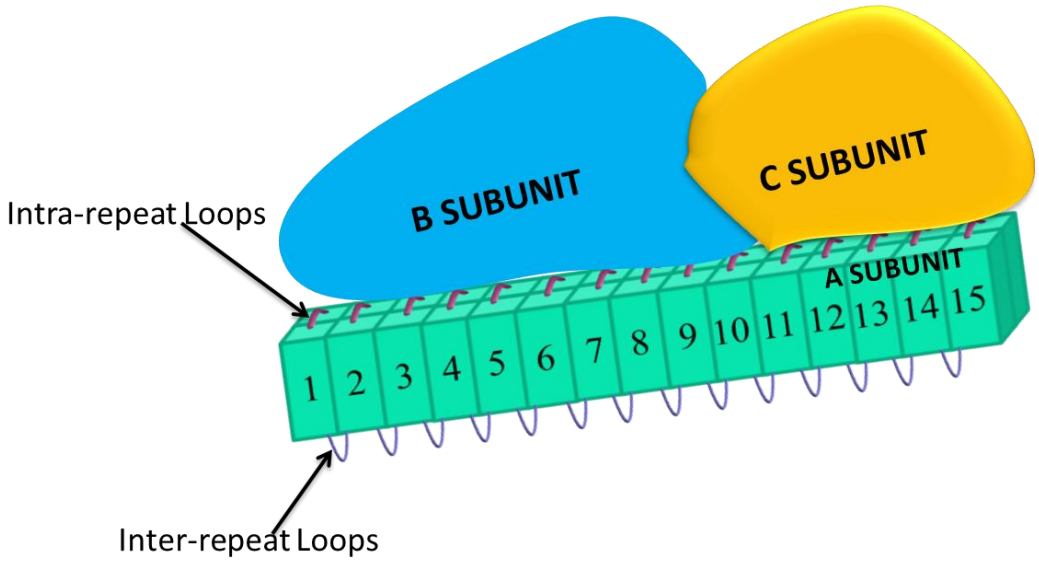

Figure 1.13: A model of the PP2A holoenzyme

1.1.6 G-substrate Structure

In the initial study by Aswad and Greengard (1), assessment with Sephadex G-100 gave a Stoke's radius of 31Å, suggesting a molecular weight of 54KDa for the G-substrate protein. SDS-PAGE analysis, however, indicated an apparent molecular weight of 23 kDa and further sedimentation coefficient analysis indicated that of G-substrate has a molecular weight of 21.7 kDa. These results suggested that the protein occupied a much larger space than was expected based on its amino acid sequence and led to predictions that the G-substrate protein existed in an asymmetric, unfolded tertiary structure. A largely unfolded secondary structure is consistent with fact that G-substrate possesses a large number of proline residues (14 in the full length and 8 in the short protein) which, due to their side-chain structure destabilize α helix and β strand conformations. To date no solution structures exist for G-substrate and the best model available (www.pdb.org) is a model of residues 12 to 96 of the full length protein based on a structure that possesses only 29 % similarity to the section of G-substrate modeled (Figure 1.14).

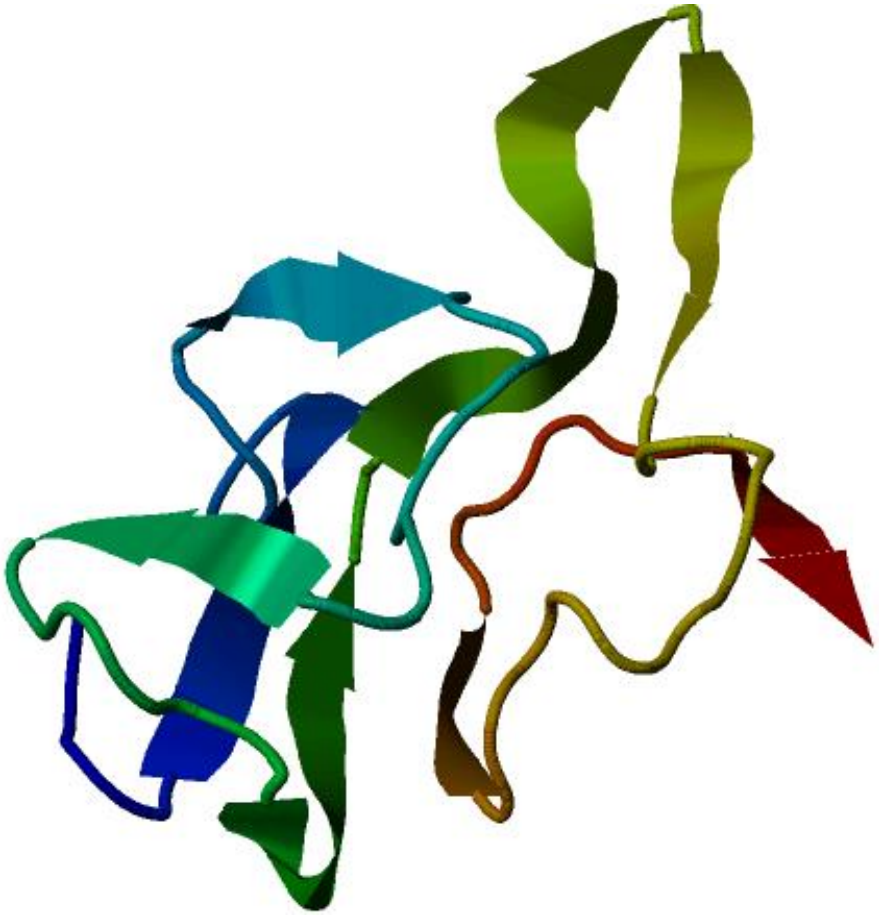

Figure 1.14: Model of G-substrate

Model is based on a structure of the human toll-like receptor 3 (TLR3) ectodomain (PDB accession: 1ziwA)

In this study, an attempt was made to study the structure of G-substrate using analytical ultracentrifugation, circular dichroism and nuclear magnetic resonance spectroscopy.

1.1.6.1 Analytical Ultracentrifugation

Analytical ultracentrifugation (AUC) makes it possible to monitor the sedimentation of macromolecules in a centrifugal field in order to characterize their hydrodynamic and thermodynamic properties in solution, without the need for matrices or surfaces. AUC is important for the study of protein interactions and protein self-association

and can exploit optical systems including absorbance, interference and fluorescence to precisely and objectively observe sedimentation in real time.

AUC can be used to obtain two complementary views of solution behaviour. Sedimentation velocity (SV) provides first-principle, hydrodynamic information about the size and shape of molecules (43) while sedimentation equilibrium (SE) provides first principle, thermodynamic information about the solution molar masses, stoichiometries, association constants, and solution nonideality (44). Data obtained from AUC experiments can be analysed using a large number of data analysis packages available for both SV and SE (45).

1.1.6.2 Circular Dichroism Spectroscopy

Circular Dichroism (CD) is a nondestructive spectroscopic technique for the evaluation of protein conformation and stability under varying conditions of temperature and ionic strength, and in the presence of solutes or small molecules. CD is relatively easy to operate, requires small amount of sample and data analyses are fast.

In conventional CD instruments a far-UV spectrum is collected from 180 to 250 nm, although further information is available in the vacuum UV region (<180 nm) which can be collected using synchrotron radiation CD (SRCD). A CD signal will be observed when a chromophore is chiral (optically active). A molecule can be intrinsically chiral because of its structure, for example, a C atom with 4 different substituents, or the disulphide bond which is chiral because of the dihedral angles of the C–S–S–C chain of atoms. Molecules can also be chiral when they are covalently linked to a chiral centre in the molecule or when placed in an asymmetric environment due to the 3-dimensional structure adopted by the molecule (46).

A number of algorithms exist which use the data from far UV CD spectra to provide an estimation of the secondary structure composition of proteins. Most procedures employ basis datasets comprising the CD spectra of proteins of various fold types whose structures have been solved by X-ray crystallography. The different types of regular secondary structure found in proteins give rise to characteristic CD spectra in the far UV (Figure 1.15) (47).

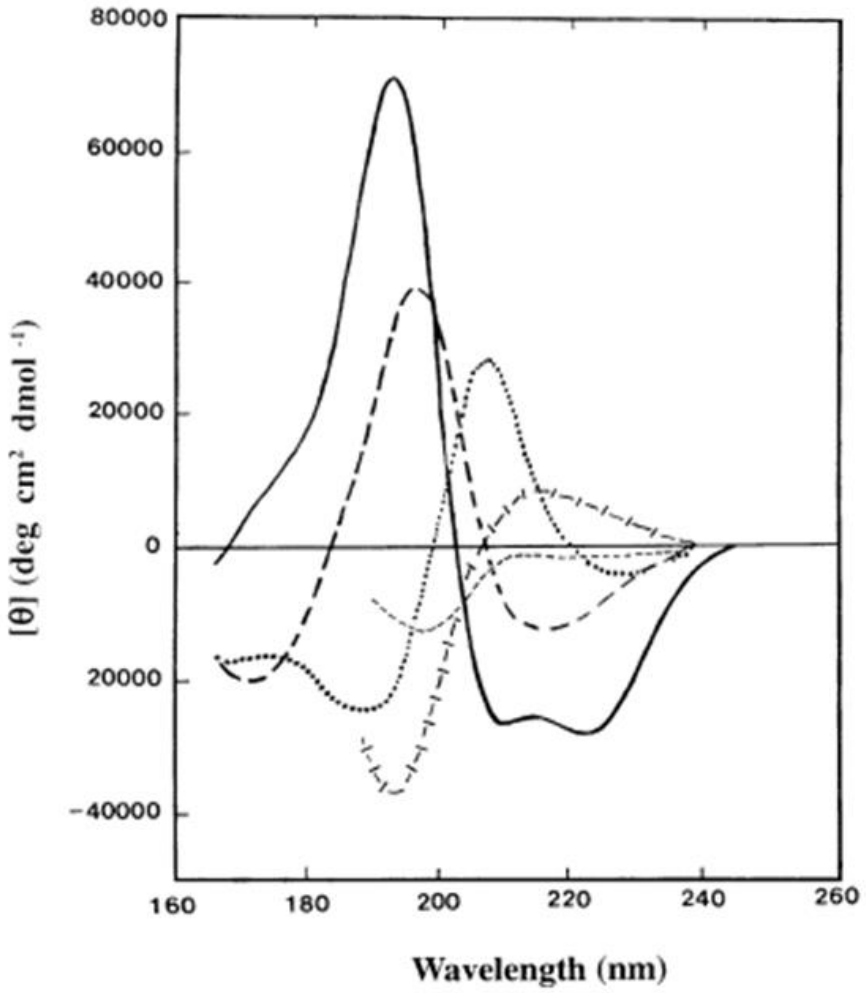

Figure 1.15: Far UV CD spectra associated with various secondary structure types taken from Kelly et al., 2005 (46).

Solid line, a-helix; long dashed line, anti-parallel h-sheet; dotted line, type I h-turn; cross dashed line, extended 31-helix or poly (Pro) II helix; short dashed line, irregular structure

1.1.6.3 Nuclear Magnetic Resonance Spectroscopy

Nuclear magnetic resonance spectroscopy (NMR) exploits the magnetic properties of certain atoms when placed in a very strong magnetic field to determine the physical and chemical properties of atoms or the molecules within which the atoms exist. This non-destructive technique is able to provide detailed information about the structure, dynamics, reaction state, and chemical environment of molecules. The NMR phenomenon is based on the fact that nuclei of atoms have magnetic properties that can be utilized to yield chemical information. The main nuclei exploited in NMR are

^{1}H, ^{15}N, ^{13}C and ^{31}P. While ^{1}H and ^{31}P are highly abundant isotopes, ^{15}N and ^{13}C are present at levels below 1 % and studies involving these nuclei generally require isotopic enrichment by production of the molecule from media that has been enriched in these isotopes. NMR experiments can be 1 dimensional, involving only one nucleus, for example a proton (^{1}H), or multi-dimensional, involving a combination of nuclei. Typically, a pulse of radiofrequency (RF) radiation is used to cause nuclei in a magnetic field to flip into the higher-energy alignment. The resultant RF pulse simultaneously excites nuclei in all local environments, all of which re-emit RF radiation at their respective resonance frequencies, creating an interference pattern in the resulting RF emission versus time, known as a free-induction decay (FID). The frequencies are extracted from the FID by a Fourier transform of the time-based data (48). In order to compare spectra from NMR machines of different magnetic field strength, the frequency of resonance is plotted as a chemical shift, which represents the resonance frequency of a particular nucleus compared to that of a standard molecule scaled to the magnetic field strength of the NMR spectrometer and reported as parts per million, ppm because the chemical shift changes associated with electron density differences are about one millionth as large as the external magnetic field used in an NMR spectrometer. The use NMR, including exploitation of techniques such as the nuclear Overhauser enhancement (NOE) effect, which makes it possible to determine distances between atoms in molecules that are near each other in three-dimensional space (49) is extremely valuable in determining the three dimensional structure of a protein in solution.

It is possible, using the combination of structural analysis methods described, to obtain valuable information on the structure of G-substrate and potentially achieve a solution structure for G-substrate using NMR spectroscopy.

1.1.7 G-substrate in Neurodegenerative Diseases

The occurrence of the majority of G-substrate protein in cerebellar Purkinje cells, which are the only output neurons of the cerebellar cortex, suggests that G-substrate might play a vital role in the successful execution of Purkinje cell and subsequently cerebellar function. Despite making up only about 10 % of total volume, the cerebellum has been found to contain over 50 % of the brain's neurons. An interesting analogy by Marr (50) compares the cerebellum to a language translator between data in the cerebrum and command sequences needed by the muscles. The main functions of the cerebellum include control of motor movement coordination, balance, equilibrium and muscle tone. G-substrate is part of the NO/cGMP/PKG pathway, which contributes to the process of long term depression (LTD), the phenomenon thought to be the cellular mechanism for cerebellar motor learning and it has been suggested that G-substrate is responsible for the induction of LTD in the cerebellum (51). Given the importance of the cerebellum and its connections to other parts of the brain, the involvement of cerebellar proteins in several diseases of the brain is not completely unexpected.

1.1.7.1 Alzheimer's Disease

Alzheimer's disease (AD) is currently the most common form of progressive dementia known and affects several million people worldwide. This neurodegenerative disease, named after Alois Alzheimer, the German psychiatrist and neuropathologist who first described it in 1907, is characterized by the accumulation of β-amyloid plaques and neurofibrillary tangles in the brains of sufferers. The neurodegeneration associated with AD has been found to begin in the hippocampus, although the disease ultimately affects all parts of the brain. The exact pattern of neurodegeneration, however, differs from individual to individual.

Cases of AD are mostly sporadic, although a small proportion, about 5-10 %, has been found to occur through autosomal-dominant inheritance. Symptoms of sporadic AD usually present around the age of 65, while approximately half of inherited AD cases are classified as 'early onset', presenting before the age of 65 (52).

The current requirement for AD diagnosis in humans is the presence of neurofibrillary tangles in the brain. Since this can only be determined post mortem, prompt and definite diagnosis of the disease is rarely achieved. It has been shown that a large proportion of the neurofibrillary tangles found in AD brains is made up of hyper phosphorylated Tau protein. Under normal conditions, Tau is a neuron-specific microtubule associated protein which is thought to be involved in the establishment and maintenance of neuronal polarity (53). The ability to determine what key events lead to tau hyper phosphorylation and its effects *in vivo* might make it possible to diagnose AD earlier and consequently reduce the impact it has on the lives of patients. The phosphorylation status of tau is regulated by PP2A and it has been shown that the PP2A holoenzyme that targets tau carries the Bβ regulatory subunit (41). In addition, studies of tau hyper phosphorylation induced by starvation in mouse brains showed that the inhibition of PP2A had a greater effect on tau hyper phosphorylation than the presence of some key tau kinases including cdk5 and TPK1/GSK3β (54). This indicates that PP2A inhibition is probably the dominant factor in the induction of tau hyper phosphorylation. PP2A represents a possible link between G-substrate and tau protein and subsequently AD. It is possible that the inhibitory effect of G-substrate on PP2A could contribute to the hyper phosphorylation of tau protein that results in the aggregation of the protein into the neurofibrillary tangles that are the hallmark of AD.

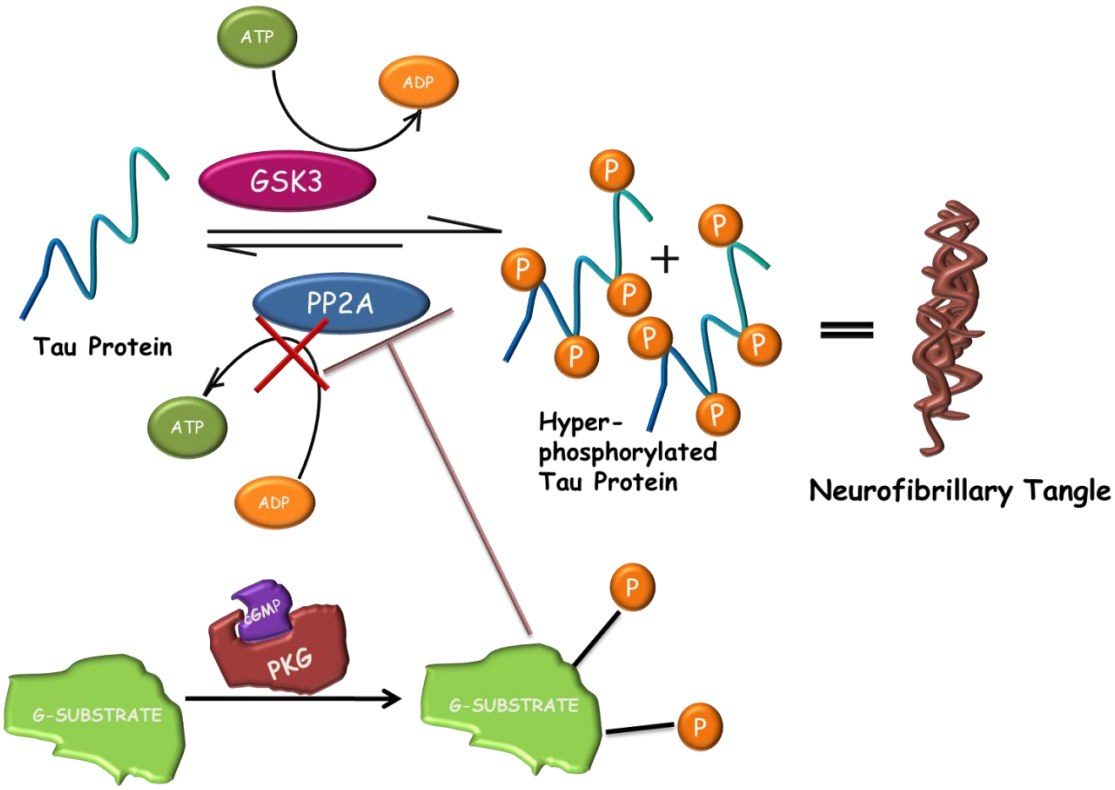

Figure 1.16: A model of the possible contribution of G-substrate to neurofibrillary tangle formation.

Phosphorylated G-substrate inhibits the PP2A holoenzyme, which is consequently ineffective in the catalysis of tau dephosphorylation. This results in the accumulation of hyper phosphorylated tau protein, which facilitates aggregation and the formation of neurofibrillary tangles.

1.1.7.2 Parkinson's disease (PD)

Parkinson's disease is named after the English physician James Parkinson, who in his 1817 publication entitled 'An Essay on the Shaking Palsy', described the disease and contributed to its establishment as a recognized medical condition. PD occurs when dopaminergic neurons in the substantia nigra are lost, decreasing dopamine levels in the brain. The classic disease symptoms begin to show when about 60 – 80 % of dopaminergic neurons are impaired or destroyed and dopamine levels decrease to between 20 and 50 % of normal levels. The hallmark of PD is the permanent degeneration of the dopaminergic neurons in the substantia nigra pars compacta (SNc), which leads to the characteristic movement disorders of this condition. PD results in the presence of intracellular inclusions, including Lewy bodies, in various areas of the brain, including the SNc, hypothalamus, brain stem, hippocampus and the cortex (55) and is defined pathologically by the presence of α-synuclein-positive

Lewy bodies in surviving nigral neurons combined with nigral cell loss and intact striatal neurons (56). Typical symptoms of PD, which are thought to occur more as a result of the decrease in dopamine production than the loss of neuronal cells, include resting tremor, muscle rigidity, bradikinesia (slowness in the execution of movement) and postural instability. Most PD cases are thought to be sporadic and present around 60 years of age. However, a small proportion of cases have currently been linked to mutations in a number of human genes including park1/SNCA, park2/parkin, park3, park4, park5/UCHL1, park6/PINK1, park7/DJ-1 and park8 (57). Most of these mutations results in disease onset that is earlier than in sporadic PD, with mutations in the E3 ubiquitin ligase, parkin resulting in disease onset as early as in teenage years and park7/DJ-1 mutations resulting in disease onset from 20 years of age. Despite the disease being known for almost 2 centuries the molecular mechanisms underlying PD are poorly understood and as a result there is currently no treatment for this devastating disease.

Although G-substrate has not yet been determined to play a direct role in PD pathophysiology, research performed by Chung and coworkers (21) has suggested that the overexpression of G-substrate protects some dopaminergic neurons from the effects of PD toxins. A10 cells of the ventral tegmental area, which possess about three times more g-substrate than the adjacent A9 cells of the SNc, were found to be less susceptible to PD toxins than the A9 neurons. Observations that G-substrate overexpression also results in a decrease in PP2A activity raised the possibility that G-substrate mediates neuroprotective effects by inhibiting serine/threonine protein phosphatase activities. Given the adverse effects of PD on patients, further investigation into the mechanisms by which this differential expression of G-substrate in adjacent neuronal cells results in differences in susceptibility to the toxic effects of PD might yield information to make possible the exploitation of G-substrate overexpression in the mitigation of the effects of PD on the brain and result in a better prognosis and a much better quality of life for patients.

1.1.7.3 Spinocerebellar Ataxia type 1 (SCA1)

Spinocerebellar ataxia (SCA) generally refers to a group of about twenty autosomal dominant cerebellar ataxias (ADCA). ADCAs have been classified clinically into three groups (58). SCA1, SCA2 and SCA3 belong to the ADCA I group and together with SCAs 6, 7 and 17 form part of the family of polyglutamine (polyQ) repeat diseases, which contains about nine known members all of which are genetically inherited, neurodegenerative diseases with similar pathogenesis and symptoms. Other members of this family include dentatorubral pallidoluysian atrophy (DRPLA) and Huntingtons's disease (HD) (59). The other SCAs have been found to arise from a variety of different genetic mutations. SCA1, the first spinocerebellar ataxia to be described, is a late onset neurodegenerative disorder, symptoms of which include peripheral neuropathy, oculomotor abnormalities and cognitive impairment, at varying degrees of severity (60).

The protein involved in SCA1 is encoded by the ATXN1 (formerly SCA1) gene. The ATXN1 gene encodes a 792-830 residue protein, ataxin-1 (61), which contains the coding region for a polyglutamine (polyQ) tract formed by between 6 and 44 CAG repeats in normal alleles. Because of this variation, the product of the ATXN1 gene varies considerably in length depending on the length of the polyQ tract. When the number of repeats in non-disease proteins is greater than 20, the tract contains CAT (histidine) nucleotide interruptions to maintain its stability (62). In disease alleles, the number of repeats is between 39 and 82 and the CAT interruptions are significantly absent. An inverse correlation has been identified between the number of CAG repeats in the polyQ tract and the age of onset of the disease (63) – as the number of polyQ repeats increases, the age of onset of SCA1 decreases and the disease progresses more rapidly, resulting in a much younger age of death. Parental transmission has also been found to affect the length of the polyQ tract, with paternal transmission increasing repeat number in 63 % of cases studied, while maternal transmission either decreased the number of repeats or left the number unchanged in 69 % of cases studied (62).

Decreased expression of G-substrate mRNA was observed in the gene profiling of the mice with spinocerebellar ataxia type 1 (SCA1) (64). In this study, the gene expression pattern of the SCA1 "ataxic" transgenic mouse line (B05-ataxin-1[82Q])

was compared with those of two "non-ataxic" lines (A02-ataxin-1[30Q] and K772T-[82Q]). In addition to G-substrate, expression levels of homer homologue 3 (Homer-3), carbonic anhydrase-like sequence, excitatory amino acid transporter 4 (EAAT4), inositol 1,4,5-trisphosphate receptor, type 1 (IP_3R1), Purkinje cell protein 1, sarcoplasmic/endoplasmic reticulum calcium ATPase 3 (SERCA3), homeotic protein Gtx and one expressed sequence tag (AI842002) were also significantly altered in the cerebellum. The observation that G-substrate expression is reduced in SCA1 presents the possibility that the reduction in G-substrate expression deprives the affected cells of the neuroprotective effects of G-substrate in a situation similar to that observed in the A9 dopaminergic cells in PD (21). It is also possible, however, that the significant decrease in G-substrate mRNA observed is merely a consequence of the loss of Purkinje cells, within which most of G-substrate is located, in the cerebellar of the ataxic mice. Further investigation into the possible role of G-substrate in SCA1 will provide further vital information on the details of G-substrate activity in the cerebellum and the possibility of exploiting G-substrate in the development of remedies against this debilitating disease.

1.2 Aims

In view of the neuroprotective function of G-substrate and the importance of the pathway within which it is found to the regulation of cellular processes in the brain, this study aimed to clone and express the recently described short isoform of G-substrate and investigate whether the two isoforms of G-substrate affect PP1 and PP2A, the two phosphatases known to be inhibited by the full length protein, in similar ways and whether the two isoforms interact with the same types of rat brain proteins. In addition, due to the importance of protein structure to biological function, this study also aimed at obtaining structural information for both isoforms of G-substrate to shed more light on whether or not they are likely to perform the same functions *in vivo*.

Chapter 2: Materials and Methods

2.1 DNA Manipulation

2.1.1 Polymerase Chain Reaction (PCR)

Polymerase chain reactions with pTrc plasmids carrying the Gsbs gene as template were performed on a PCR Sprint Thermal Cycler (Thermo Scientific) using the cycling conditions shown in Table 2.1.

Table 2.1: PCR cycling conditions for Gsbs gene mutation

Event	Temperature	Duration	Number of Cycles
Initial Denaturation	98 °C	2 min 30 sec	1
Denaturation	98 °C	10 sec	30
Annealing	56.4 °C	30 sec	
Extension	72 °C	2 min 30 sec	
Final Extension	72 °C	8 min	1

Table 2.2: Components of a typical PCR

Component	Volume (µl)	Final Concentration
sdH_2O	32.5	-
5x PCR Buffer	10.0	1 x
dNTP Mix	4.0	200 µM of each dNTP
Sense Primer	1.0	0.5 µM
Antisense Primer	1.0	0.5 µM
Template DNA	1.0	10 ng
Phusion DNA Polymerase	0.5	1 U

PCR reactions were typically set up in a volume of 50µl and contained the components shown in Table 2.2.

2.1.2 Restriction Enzyme Digestion

DNA digestion with restriction enzymes was employed in both the preparation and analysis of plasmid DNA during cloning.

2.1.2.1 *Ale*I Digests

Digestion of mutant Gsbs containing restriction sites for *AleI* was carried out at 37 °C for 15 min using FastDigest™ *AleI* (Fermentas). Reaction components for the digestion are shown in Table 2.3. The enzyme was inactivated after the digestion reaction by incubation at 65 °C.

Table 2.3: Components of a typical *AleI* digestion reaction

Component	Volume (µl)	Final Concentration
Nuclease-free Water	16	-
10x FastDigest™ Buffer	3	1 x
DNA	10	~ 0.2 µg
FastDigest™ *Ale*I	1	1 FastDigest™ Unit (FDU)

2.1.2.2 Analytical Digests

Plasmid digestion with *EcoRI* (NEB) was routinely employed to produce linearized plasmids for more accurate size determination using agarose gel electrophoresis. The reaction components of a typical analytical digest are shown in Table 2.4.

Table 2.4: Components of a typical *EcoR*I digestion reaction

Component	Volume (µl)	Final Concentration
Nuclease-free Water	16.3	-
10x Buffer	2.0	1 x
Acetylated BSA	0.2	2 µg
DNA	1.0	0.2 µg
*EcoR*I	0.5	5 U

2.1.2.3 Ligation of DNA

Following restriction digests, ligations catalysed by T4 DNA Ligase (NEB) were performed. A typical 10 µl ligation reaction involved incubating the components shown in Table 2.5 at 16 °C overnight.

Table 2.5: Components of a typical ligation reaction

Component	Volume (µl)	Final Concentration
Nuclease-free Water	3	-
10x Ligase Buffer	1	1 x
DNA	5	~ 0.1 µg
T4 DNA Ligase	1	-

2.1.3 Agarose Gel Electrophoresis

Agarose gels were used at 1 % and prepared by heating 0.5 g of molecular biology grade agarose (Sigma) in 50 ml of Tris Acetate EDTA (TAE) buffer. After cooling the agarose, 5 µl of SYBR® Safe DNA stain (Life Technologies) was added and the gel mixture poured into a mould. The gel was submerged in TAE buffer and after loading DNA samples prepared with 6x loading dye (Promega), run at 200 volts for 45.min. After adequate separation, DNA fragments were visualized using a UV transilluminator (UVP).

2.1.4 Gel Extraction of DNA

Extraction of DNA from agarose gels was performed using either the QIAquick gel extraction kit (Qiagen) or the Gel Purification Kit (Promega). The procedure was, in each case, carried out according to the manufacturer's instructions.

2.2 Production of Chemically Competent *Escherichia coli*

Escherichia coli bacteria were used throughout this project. Top10 cells (Life Technologies) were routinely used for DNA production, while BL21 Star™ (DE3) pLysS (Life Technologies) and Rosetta 2 (Novagen) cells were used for protein production. Chemically competent cells were produced based on a modified version of the method developed by Hanahan (65). Between 5 and 10 ml of LB broth supplemented with the appropriate antibiotics was inoculated with a single colony of the appropriate cell line and incubated overnight at 37 °C while shaking at 220 rpm. This overnight culture was used to inoculate 200 ml of pre-warmed LB broth supplemented with the appropriate antibiotics and grown to an optical density (OD) at 600 nm of between 0.4 and 0.7. The total volume was then divided into 50 ml fractions and incubated on ice for 20 min. The fractions were then centrifuged at 4500 g at 4 °C for 10 min. Harvested cells were resuspended in 10 ml of ice-cold 100 mM $CaCl_2$. The mixtures were combined and incubated on ice for 2 h. The competent cells were harvested by centrifuging at 4500 g at 4 °C for 10 min and resuspended in 2 ml of ice-cold 100 mM $CaCl_2$ containing 20 % (v/v) glycerol. Aliquots of 50 µl were stored at -80 °C until required.

2.3 Transformation of *Escherichia coli* Bacteria

Chemically competent bacteria were transformed with plasmid vectors carrying genes of interest as follows: approximately 1 µg of plasmid DNA was added to 50 µl of chemically competent cells and the mixture incubated on ice for 30 min. The mixture was then incubated at 42 °C for 30 sec and returned to the ice for 2 min. After recovery on ice, 250 µl of SOC. medium was added to the transformed cells. The cells were then incubated at 37 °C, while shaking at 225 rpm for 1 h. LB agar

plates supplemented with the appropriate antibiotics were spread with the transformed cells and incubated at 37 °C overnight. Negative controls without DNA and positive controls with control plasmids were also set up.

2.4 Small Scale 'Mini-Preps' of Plasmid DNA

Ten ml of LB media supplemented with the appropriate antibiotics was inoculated with one bacterial colony (carrying the desired plasmid DNA) and incubated overnight at 37 °C while shaking at 220 rpm. The culture was subsequently centrifuged for 5 min at 13,000 rpm (16,060 g) in a bench top centrifuge to pellet the bacteria. Plasmid DNA was purified using the QIAquick mini-prep kit (Qiagen) according to the manufacturer's instructions. Purified plasmid DNA was eluted in 50 µl of nuclease-free water and stored at -80 °C.

2.5 Quantification of Plasmid DNA

The concentration of plasmid DNA was determined using a NanoDrop™ 1000 Spectrophotometer (Thermo Scientific). The absorbance of 1 µl of DNA was measured at 260 nm using nuclease-free water as a blank and the concentration given in units of ng/µl. The purity of each DNA sample was given as a ratio of absorbance at 260 nm and 280 nm, with a ratio of ~1.8 regarded as 'pure'.

2.6 Expression and Purification of ^{15}N-Labeled Protein

G-substrate protein containing the heavier ^{15}N isotope of nitrogen was expressed and purified for structural analysis by nuclear magnetic resonance spectroscopy (NMR). Uniform ^{15}N isotope enrichment of the recombinant protein was achieved by growing *E. coli* bacteria in 5x M9 minimal growth medium enriched with ^{15}N labeled ammonium sulphate.

2.6.1 Overexpression of ^{15}N labeled G-substrate

Starter cultures of Rosetta 2 *E. coli* cells transformed with pTricHisA vectors carrying the gene for human G-substrate were prepared by inoculating 10 ml of LB containing ampicillin at 100 ng/L and chloramphenicol at 34 ng/L with a glycerol stock of the cells. The culture was incubated at 37 °C for 16 h while shaking at 220 rpm.

Five hundred ml of 5x M9 minimal growth medium (components shown in Table 2.6) was inoculated with 4 ml of the starter culture and incubated at 37 °C with shaking at 220 rpm. Overexpression of the protein was induced with 1 mM of IPTG when the optical density (OD) at 600 nm reached 0.6. After induction, the bacterial culture was grown for a further 5 h after which cells were harvested by centrifuging at 5000 rpm (4,080 g) for 30 min in a Sorvall GS-3 rotor.

2.6.2 Purification of ^{15}N labeled G-substrate

Harvested cells were resuspended in lysis buffer and incubated on ice for 30 min. Resuspended cells were then taken through five cycles in a sonic bath at 10 microns (15 sec on and 15 sec off) and centrifuged for 45 min at 13000 rpm (27,138 g) in a Sorvall SS-34 rotor.

The supernatant from centrifugation was applied to a gravity flow column containing NTA agarose beads charged with nickel ions and the G-substrate protein eluted with increasing concentrations of imidazole. Fractions with high G-substrate concentration and low contamination were pooled and further purified by cation exchange on a column with a sulphonic acid functional group (MonoS 5/50 column) (Amersham Biosciences).

Protein fractions were analyzed by SDS-PAGE and coomassie blue staining. G-substrate protein fractions with low contamination were buffer exchanged into 20 mM HEPES at pH 7.5 and concentrated for analysis by NMR spectroscopy.

Table 2.6: Composition of growth media and buffers used in the expression and purification of ^{15}N G-substrate

Preparation	Components	Concentration
5x M9 Growth Medium	Thiamine	0.02 g/L
	PTM_1 Salts	0.01 % (v/v)
	Isogro-^{15}N (Sigma-Aldrich)	0.5 g/L
	5x M9 Salts	20 % (v/v)
	Glucose	4.0 g/L
	Magnesium sulphate	2 mM
	Calcium chloride	0.1 mM
	Ammonium-^{15}N chloride (Sigma-Aldrich)	1.25 g/L
PTM_1 Salts	Copper sulphate pentahydrate	24 mM
	Sodium iodide	534 µM
	Manganese sulphate pentahydrate	17.8 mM
	Sodium molybdate dihydrate	827 µM
	Boric acid	323 µM
	Cobalt chloride hexahydrate	147 mM
	Zinc chloride	147 mM
	Ferrous sulphate heptahydrate	234 mM
	Biotin	1.64 mM
	Sulphuric acid	188 mM
5x M9 Salts	Sodium phosphate, dibasic heptahydrate	64 g/L
	Potassium phosphate monobasic	15 g/L
	Sodium chloride	2.5 g/L
Lysis buffer	Sodium phosphate, monobasic	50 mM
	Sodium chloride	300 mM
	Imidazole	10 mM
	Lysozyme	0.2 mg/ml
	Complete protease inhibitor	1 tablet

2.7 Sodium Dodecyl Sulphate Polyacrylamide Gel Electrophoresis

Proteins were routinely separated by size under denaturing conditions by sodium dodecyl sulphate polyacrylamide gel electrophoresis (SDS-PAGE) based on the method of King and Laemmli (66) Polyacrylamide gels of varying concentration were used according to the size of protein to be analyzed. Mini-PROTEAN Tetra Cell apparatus (BioRad) was employed for running mini gels. Vertical slab gels were

produced using 5 ml of resolving gel and overlaid with 2 ml of stacking gel (Table 2.7). Gels were fitted into the tank, which was then filled with SDS running buffer. Protein samples were prepared for SDS-PAGE by boiling for 5 min in Laemmli buffer. The protein samples were then loaded into wells created in the stacking gel and separated by running at 120 volts for approximately 45 min. PrecisionPlus Protein Markers (BioRad) were typically run alongside the protein samples to give an idea of protein size. Proteins were then visualized by staining with coomassie blue stain.

Table 2.7: Buffers for SDS-PAGE

Buffer	**Components**	**Concentration**
Stacking Gel	Acrylamide Tris-HCl, pH 6.8 SDS Ammonium persulphate (APS) TEMED	5 % (w/v) 0.125 M 0.1 % (w/v) 0.1 % (w/v) 0.04 % (v/v)
Resolving Gel	Acrylamide Tris-HCl, pH 8.8 SDS APS TEMED	10-15 % (w/v) 0.375 M 0.1 % (w/v) 0.1 % (w/v) 0.1 % (w/v)
Laemmli Buffer	Tris-HCl, pH 6.8 Glycerol SDS β-mercaptoethanol Bromophenol Blue	0.15 M 30 % (v/v) 6 % (w/v) 15 % (v/v) 0.1 % (w/v)
SDS Running Buffer	Glycine Tris SDS	0.2 M 0.025 M 0.1 % (w/v)
Coomassie Blue Stain	Acetic acid Methanol Coomassie Brilliant Blue (G250/R250)	10 % (v/v) 45 % (v/v) 0.2 % (w/v)
Destain	Acetic acid Methanol	10 % (v/v) 30 % (v/v)

2.8 Western Blotting

Immunoblotting using antibodies specific to the proteins of interest was employed in the identification of recombinant proteins produced as well as proteins purified from tissue. Both nitrocellulose and polyvinylidene fluoride (PVDF) membranes were used with PVDF membranes showing better endurance for stripping and re-probing than nitrocellulose membranes.

Table 2.8: Buffers for western blotting

Buffer	Components	Concentration
Towbin Transfer Buffer	Glycine Tris Methanol	0.192 M 0.025 M 20 % (v/v)
Ponceau S stain	Ponceau S Trichloroacetic acid	0.1 % (w/v) 3 % (w/v)
TBS-Tween (TBS-T)	Tris-HCl, pH 7.5 NaCl Tween-20	0.02 M 0.137 M 0.1 % (v/v)
Blocking Buffer	Non-fat dried milk (Marvel)	5 % (w/v) in TBS-T
Stripping Buffer	Glycine-HCl, pH 2.0 SDS	0.025 M 1 % (w/v)
Phosphate Buffered Saline (PBS) pH 7.4	Sodium phosphate Potassium phosphate Potassium chloride Sodium chloride	10 mM 1.8 mM 2.7 mM 137 mM

2.8.1 Nitrocellulose membrane

Following separation by SDS-PAGE, the gel, membrane and blotting paper were immersed for 5 min in Towbin transfer buffer (Table 2.8). Proteins were transferred from the gel to the nitrocellulose membrane by applying a constant current of 0.2 A for 45 min using the Trans-blot SD semi-dry transfer apparatus (BioRad). Transfer efficiency was checked by staining the membrane with Ponceau S stain. After destaining with distilled water, the membrane was incubated for 1 h with blocking

buffer. The membrane was subsequently washed 3 times for 5 min each time with TBS-T and incubated for 1 h in primary antibody diluted to the appropriate concentration in blocking buffer. The membrane was washed again in TBS-T and incubated in the appropriate secondary antibody conjugated to horse radish peroxidase for 1 h at room temperature. The secondary antibody was also diluted to the appropriate concentration in blocking buffer. Following incubation in secondary antibody, the membrane was again washed in TBS-T and then incubated in the enhanced chemiluminescence (ECL) system (Millipore) for 5 min. Protein bands were visualised by exposing the membrane to autoradiographic film (Kodak) and developing the film using an MI-5 Automatic X-ray film Processor (Medical Index GmbH).

2.8.2 PVDF membrane

Due to their hydrophobicity, PVDF membranes had to be pre-wet in 100 % methanol prior to use. Transfer of proteins to the membrane, incubation with antibodies and visualization of protein bands were carried out as described in the section above (2.8.1)

2.9 Dimerization of DJ-1

The extent of dimerization of the DJ-1 constructs was analyzed using the crosslinking reagent Bis [sulfosuccinimidyl] suberate (BS^3); 4 mM of BS^3 was incubated with 10 μg of each DJ-1 construct and the reactions incubated at room temperature for 3 h. The samples were subsequently run on 12 % SDS-PAGE and analyzed with ImageJ software. To test the effect of Tanganil on dimerization of the DJ-1 constructs, the reaction described above was repeated for each construct with the addition of 5 mM of Tanganil to each reaction.

2.10 Purification of Protein Phosphatases from Rat Muscle

The catalytic subunits of protein phosphatases 1 and 2-A were purified using an adaptation of the method described by Tung *et al*. (67)

2.10.1 Preparation of Muscle Extract

Skeletal muscle from 34 rats were homogenized in buffer A containing 1 mM PMSF, 4 µg/ml Leupeptin and 1 mM Benzamidine and centrifuged at 5,000 rpm (4,080 g) for 30 min at 4 °C in a Sorvall GS-3 rotor. The pH of the lysate was adjusted to 6.1 using acetic acid and the extract incubated at 4 °C for 15 min. The lysate was re-centrifuged at 5,000 rpm (4,080 g) for 30 min and the pH of the supernatant adjusted to 7.2 with sodium hydroxide. Three hundred and fifty grams of solid ammonium sulphate was added for each litre of supernatant and the suspension incubated at 4 °C for 30 min. The suspension was then centrifuged at 5,000 rpm (4,080 g) for 40 min and the supernatant discarded. The precipitate was suspended in solution D. Five volumes of ethanol containing PMSF at 1 mM were added and the mixture centrifuged immediately 5,000 rpm (4,080 g) for 5 min. The supernatant was discarded and the precipitate extracted with solution D (without glycerol). After centrifuging at 13,000 rpm (27,138 g) for 15 min in a Sorvall SS-34 rotor, the supernatant was stored on ice and the precipitate re-extracted with solution D (without glycerol). The supernatants from the two extractions were combined and the pH adjusted to 7.2 with sodium hydroxide. Four hundred and thirty grams of solid ammonium sulphate was added per litre of supernatant and the suspension incubated for 30 min at 4 °C. The suspension was centrifuged for 40 min at 13,000 rpm (27,138 g) and the pellet suspended in solution D. After buffer exchanging 5 times into buffer D, the solution was diluted with an equal volume of solution D.

Table 2.9: Buffers and Solutions used in phosphatase purification from rat muscle

Solution	Components	Concentration
Buffer A	EDTA EGTA, pH 7.0	2 mM 2 mM
Solution A	Tris-HCl, pH 7.0 EGTA 2-mercaptoethanol	50 mM 0.1 mM 0.1 % (v/v)
Solution B	Sodium glycerol 1-phosphate EDTA 2-mercaptoethanol	50 mM 2 mM 0.1 % (v/v)
Solution C	Tris-HCl, pH 7.5 EGTA Glycerol	5 mM 0.1 mM 10 % (v/v)
Solution D	Tris-HCl, pH 7.5 EGTA Glycerol	20 mM 0.1 mM 10 % (v/v)
Solution E	Tris-HCl, pH 7.0 EGTA Glycerol	20 mM 0.1 mM 10 % (v/v)

2.10.2 Affinity Purification with PolyD-Lysine Sepharose

The resultant solution was affinity purified by batch treatment with poly D-lysine Sepharose and catalytic subunits of PP2-A and PP1 eluted with 250 mM and 500 mM respectively of NaCl in solution D.

2.10.2.1 Preparation of Poly D-Lysine Sepharose

Poly D-Lysine-Sepharose was prepared using ECH Sepharose®4B (Pharmacia Biotech), Poly D-Lysine hydrobromide (Sigma-Aldrich) and 1-Ethyl-3-(3-dimethylaminopropyl) carbodiimide hydrochloride (EDC) (Pierce, now Thermo Scientific). The pH of 5 ml of sterile water was adjusted to 5 using acetic acid. After dissolving 2.5 mg of poly D-lysine and 95.85 mg of EDC in the water, 2 ml of ECH Sepharose®4B gel were added to the solution and the mixture incubated at 4 °C with end to end rotation. After 45 min, the pH of the mixture was adjusted to 5 with dilute sodium hydroxide and the mixture left to rotate at 4 °C for 16 h. Following ligand

coupling, the Sepharose beads were washed with 3 cycles of alternating pH consisting of a wash with 0.1M sodium acetate buffer at pH 4 containing 0.5 M sodium chloride followed by a wash with 0.1 M Tris-HCl buffer at pH 8 containing 0.5 M sodium chloride. This was followed by a wash with distilled water to neutralize the pH of the beads.

2.10.3 Anion-Exchange Chromatography

Each fraction was further purified by anion exchange using a MonoQ column on an AKTAprime FPLC system. A gradient over 35 ml from 0 to 500 mM of sodium chloride in buffer E (without glycerol) was run and 500 µl fractions collected.

2.11 Phosphatase Activity Assays

The activity of tissue extracts and purified phosphatases were determined using either the SensoLyte pNitrophenyl Phosphatase kit from Anaspec or an adaptation of the method by Li et al. (68)

2.11.1 SensoLyte pNitrophenyl Phosphate Phosphatase Assay

Phosphatase activity was determined using the SensoLyte pNitrophenyl Phosphatase kit (Anaspec) according to the manufacturer's instructions. The presence and activity of a phosphatase was determined by the ability of the extract to produce p-nitrophenol by dephosphorylating the reaction substrate, p-nitrophenyl phosphate (pNPP). The pNPP was provided as a solution with this kit and as a result it is not possible to determine what other chemicals the preparation might have contained. The extent of dephosphorylation was determined by measuring absorbance at 405 nm with a Wallac Victor^2 plate reader (PerkinElmer). Components of the substrate solution used with this kit are shown in Table 2.10.

Table 2.10: Components of pNPP substrate solutions used with SensoLyte kit

Component	Volume in 1ml
Assay Buffer [1]	987 µl
pNPP Stock Solution	10 µl
DTT	3 µl

2.11.2 Alternative pNitrophenyl Phosphate Assay

Determination of phosphatase activity was alternatively carried out using a preparation of pNPP adapted from Li *et al.*(68). Table 2.11 shows the components of this pNPP substrate solution.

Table 2.11: pNPP substrate solution components

Component	Concentration
pNPP	20 mM
$MgCl_2$	20 mM
Tris-HCl, pH 8.5	50 mM
DTT	1 mM
sdH_2O	-

2.12 G-substrate Interacting Proteins

G-substrate interacting proteins from rat brain were investigated by incubating G-substrate protein bound to magnetic beads with extracts prepared from rat brain, separating proteins bound to G-substrate by SDS-PAGE and identifying the interacting proteins by MALDI-tof mass spectrometry. Controls for each investigation were prepared by binding bovine serum albumin (BSA) in experiments involving G-substrate protein or ethanolamine in experiments involving the G-

[1] Assay buffers were prepared according to instructions contained in the kit.

substrate phosphopeptide, to the magnetic beads and following the same procedures for the G-substrate bound beads.

2.12.1 Preparation of Rat Brain Extract

Protein extracts from rat brain were prepared by homogenizing minced brains from male Sprague-Dawley rats in sucrose buffer (Table 2.12) containing complete protease inhibitor tablets (Roche). The homogenate was centrifuged for 30 min at 50,000 rpm (109,000 g) in a TL-100 rotor (Beckman) and the supernatant filtered using a 0.22 µm syringe driven filter (Millipore) prior to use.

2.12.2 Coupling of G-substrate protein to Magnetic Beads

Dynabeads® M-280 Tosylactivated magnetic beads (Invitrogen) were washed three times in PBS and incubated with G-substrate protein in the presence of high salt buffer. Coupling was achieved after rotating the mixture end to end for 16 h at 37 °C. The magnetic beads were subsequently incubated with blocking buffer for 1 h at room temperature and washed three times in PBS.

2.12.3 Coupling of G-substrate phospho-peptide to Magnetic Beads

Amine groups of Dynabeads® M-270 Amine magnetic beads (Invitrogen) were carboxymethylated by incubating the beads in 2 M iodoacetic acid in the presence of 1-ethyl-3-(3-dimethylaminopropyl) carbodiimide hydrochloride (EDC) for 2 h at 37 °C in the dark. The beads were then washed three times in PBS and incubated with a G-substrate phospho peptide of amino acid sequence CDQKKPRRKD[pT]PAL-amide for 1 h at 37 °C. Excess iodoacetyl groups on the beads were blocked with a 7.5 mg/ml solution of L-cysteine after which the beads were washed three times in PBS.

Table 2.12: Buffers used in the study of G-substrate interacting proteins

Buffer	Components	Concentration
Sucrose Buffer	Sucrose HEPES EDTA	250mM 10mM 1mM
Phosphate Buffered Saline (PBS) pH 7.4	Sodium phosphate Potassium phosphate Potassium chloride Sodium chloride	10mM 1.8mM 2.7mM 137mM
High Salt Buffer	Ammonium sulphate Sodium phosphate Potassium phosphate Potassium chloride Sodium chloride	1.2M 10mM 1.8mM 2.7mM 137mM
Blocking Buffer	Bovine serum albumin (BSA) Sodium phosphate Potassium phosphate Potassium chloride Sodium chloride	0.1% (w/v) 10mM 1.8mM 2.7mM 137mM
Wash Buffer	Ammonium bicarbonate Acetonitrile	100mM 50%
Reducing Solution	DTT Ammonium bicarbonate Acetonitrile	20mM 100mM 50%
Alkylating Solution	Iodoacetamide (IAA) Ammonium bicarbonate Acetonitrile	50mM 100mM 50%
Low Wash Buffer	Ammonium bicarbonate Acetonitrile	20mM 50%
Trypsin Solution	Trypsin Ammonium bicarbonate	0.57µM 50mM

2.12.4 Interaction of G-substrate with Rat Brain Proteins

Filtered rat brain extract was incubated with magnetic beads coupled to G-substrate protein for 16 h at 4 °C to allow interaction between the G-substrate protein and any of its usual interacting proteins present in the extract.

2.12.5 Analysis of Interacting Proteins

After allowing sufficient time for interacting proteins to bind to the G-substrate coupled magnetic beads, the beads were washed three times in PBS and boiled for 5 min in Laemmli buffer. After boiling, the protein sample was separated from the beads using a magnet and analyzed by SDS-PAGE. Proteins present were visualized by staining with coomassie blue stain.

2.12.6 In-gel Digestion of Proteins

Protein bands were excised from the polyacrylamide gel and incubated three times in wash buffer at room temperature for 30 min each time to remove SDS. The proteins contained in the bands were then reduced by incubating the gel bands in reducing solution for 1 h at room temperature. The bands were washed three times in wash buffer and cysteine residues in the proteins alkylated by incubating the gel bands in alkylating solution for 20 min at room temperature in the dark. The gel bands were washed three times in low wash buffer following alkylation and covered in 100 % acetonitrile until they turned white. The acetonitrile was then removed and the gel pieces allowed to dry at room temperature. The dry gel pieces were immersed in trypsin solution and kept at 4 °C until the gel pieces were completely swollen. Complete digestion of proteins was achieved after incubation at 32 °C for 16 h. Tryptic digests were sonicated for 10 min and zip-tipped (C_{18} Zip-Tip, Millipore) to reduce salt concentration in the samples.

2.12.7 MALDI-tof Mass Spectrometry of Digested Proteins

To obtain mass spectra, 1 µl of the tryptic digest was mixed with 1 µl of 10 mg/ml α-Cyano-4-hydroxycinnamic acid (CHCA) matrix and analysed using a Voyager DE-STR MALDI-tof mass spectrometer (Applied Biosystems). Processed spectral peaks were searched against non-redundant databases at the National Center for Biotechnology Information (NCBI) and Swissprot using Protein Prospector MSFit and Mascot PMF (Matrix Science) Parameters used during the database searches

included a maximum of 1 missed cleavage per peptide and a mass tolerance of 100 ppm. Proteins with significant MOWSE scores ($p<0.05$) are reported.

2.13 Circular Dichroism

CD analysis was performed on a J-810 spectropolarimeter (JASCO) at 25 °C, using a 0.1 cm cuvette (Starna), and with wavelengths in the far UV-range of 185–280 nm. Each CD spectrum represents the average of five scans (data pitch: 0.1 nm; scan speed: 10 nm/min; response time: 2s) and was corrected by subtraction of the respective spectrum obtained for its desalted buffer solution (five-scan average accumulation). The obtained raw spectrum signal was then converted from ellipticity (millidegrees) into mean residue ellipticity (degrees cm^2 per dmol per residue), to allow for concentration and protein size-independent spectrum measurement for comparison purposes, using the Spectra Manager software. The spectra were then submitted to DICHROWEB (69) for deconvolution into secondary structure components utilizing the analysis programs CDSSTR or CONTINLL (70-72) with reference sets ‘Datasets 7’ and SP175.

2.14 Nuclear Magnetic Resonance Spectroscopy (NMR)

Samples for NMR were prepared in D_2O at 10 %. NMR experiments were recorded at 278 K on a Bruker Avance III 800 MHz spectrometer equipped with a TCI cryoprobe. All NMR spectra were processed with TopSpin (Bruker). Spectra were recorded for 1D proton, 2D nuclear overhauser effect spectroscopy (NOESY) and 2D total correlated spectroscopy (TOCSY) experiments.

Chapter 3: Expression, Purification and Phosphorylation of G-substrate

3.1 Full Length G-substrate

Full length G-substrate cDNA was obtained as an IMAGE-clone (id: BI915027) from the IMAGE Consortium (Genome Systems, St. Louis). The G-substrate gene was cloned into pTrc His A (Invitrogen) using the *BamHI* and *XhoI* sites (Figure 3.1). DNA sequencing of the cloning product confirmed the recombinant protein was in frame.

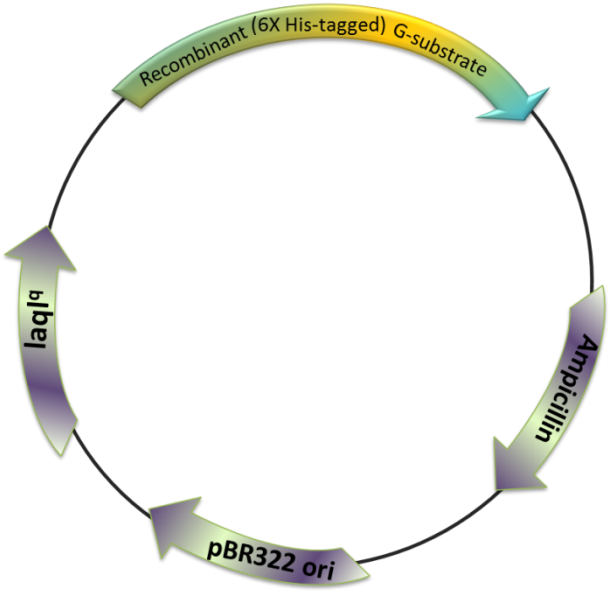

Figure 3.1: A Plasmid Map for Full Length G-substrate in pTrc HisA

The resulting protein possessed an N-terminal 6X-Histidine tag and was 190 amino acids long with a molecular weight of 21,750.6 Da.

The hexa-histidine tagged G-substrate protein was first purified by Immobilized-Metal Affinity Chromatography (IMAC) on an NTA resin charged with nickel ions. Aliquots of the Ni-NTA IMAC elution fractions were analysed by SDS-PAGE and Coomassie staining. Fractions with high protein concentration and low contamination were pooled and further purified by Cation-exchange Chromatography on a column with a sulphonic acid functional group (MonoS)

(Amersham Biosciences) with a salt (NaCl) gradient of 0 M to 1 M over 25 ml of buffer (Figure 3.2). Peak fractions were analysed by SDS-PAGE and pooled. The pooled fractions were buffer exchanged into 10 mM of 2-(N-morpholino) ethanesulfonic acid (MES) at pH 6.0 and concentrated using a vivaspin-20 column (GE Healthcare).

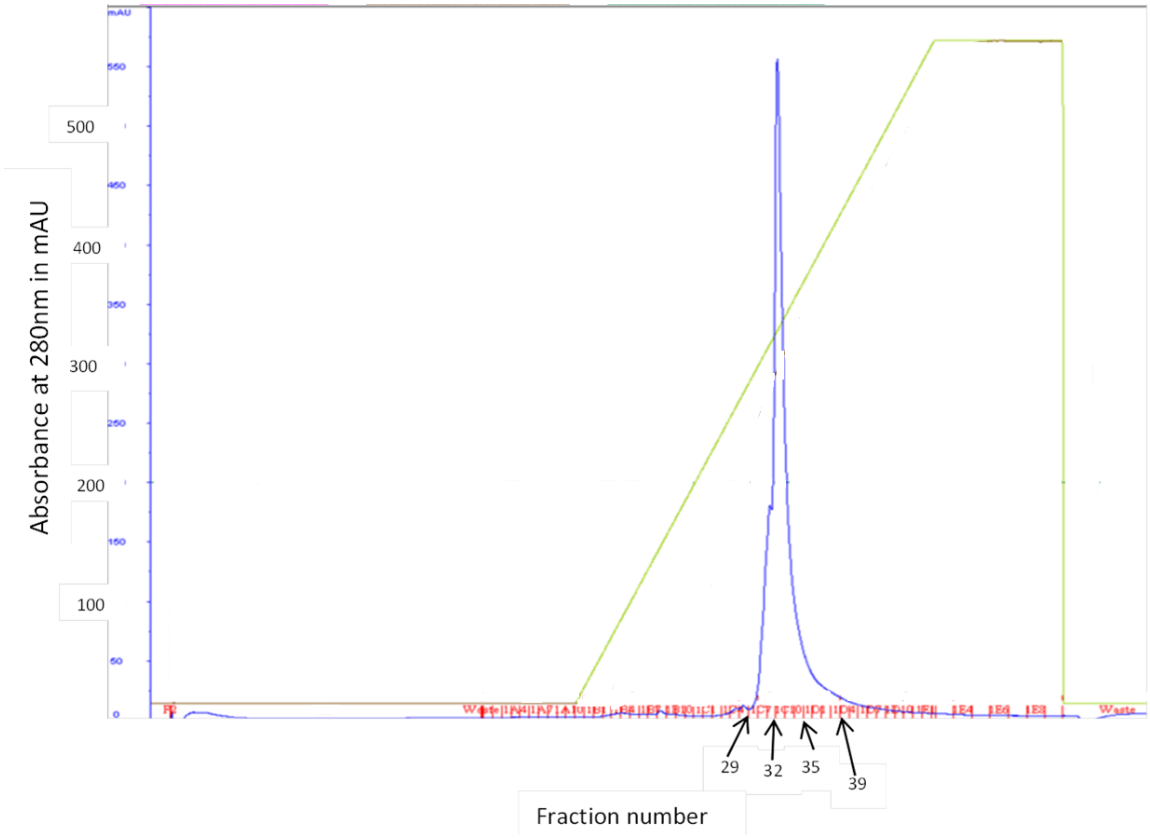

Figure 3.2: Chromatogram from Cation Exchange of Recombinant Full Length G-substrate Protein on a MonoS column.

Green line represents salt gradient and peak represents purified full length G-substrate.

G-substrate protein identity was verified by western blotting (Figure 3.3) using an antibody raised in sheep against the epitope QKKPRRKDTPALH, which represents the phosphorylation motif of G-substrate.

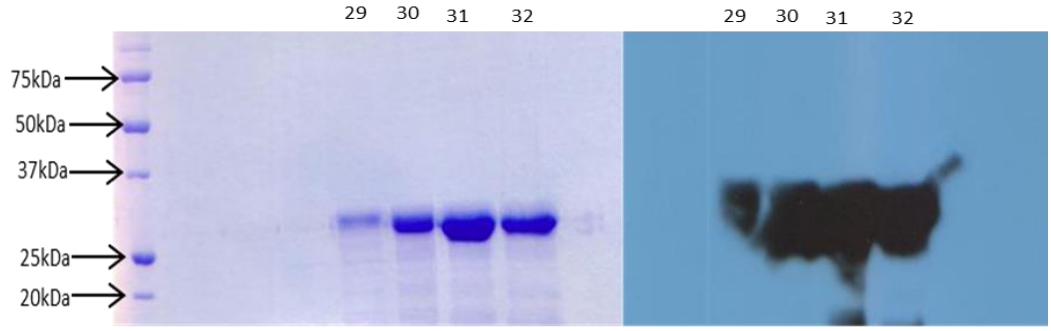

Figure 3.3: Purification of Recombinant Full Length G-substrate Protein.
SDS-PAGE (L) and Western Blot (R) Images of Fractions from Cation Exchange of purified full length G-substrate. Numbers above lanes indicate fraction numbers of eluents.

3.2 G-substrate 'Variant 2'

Recombinant G-substrate 'variant 2' DNA was produced by deleting the appropriate section from the full length G-substrate DNA as follows.

3.2.1 G-substrate 'Variant 2' Cloning

Four point mutations were introduced into the nucleotide sequence (Figure 3.4) of full length G-substrate contained in a pTrc HisA vector by polymerase chain reaction (PCR) using the primer sequences :

5'AGATCACCTAAGTGGCTGCAACGAGGGTC3' and

5'TTTCCACCCAGGTGTGTTTTCAGAACATT3'

The mutations incorporated into the nucleotide sequence of full length G-substrate were A191G, A337C, T338A and A339C. These mutations introduced recognition sites for *AleI* to the regions flanking the portion of full length G-substrate that was absent in G-substrate 'variant 2'.

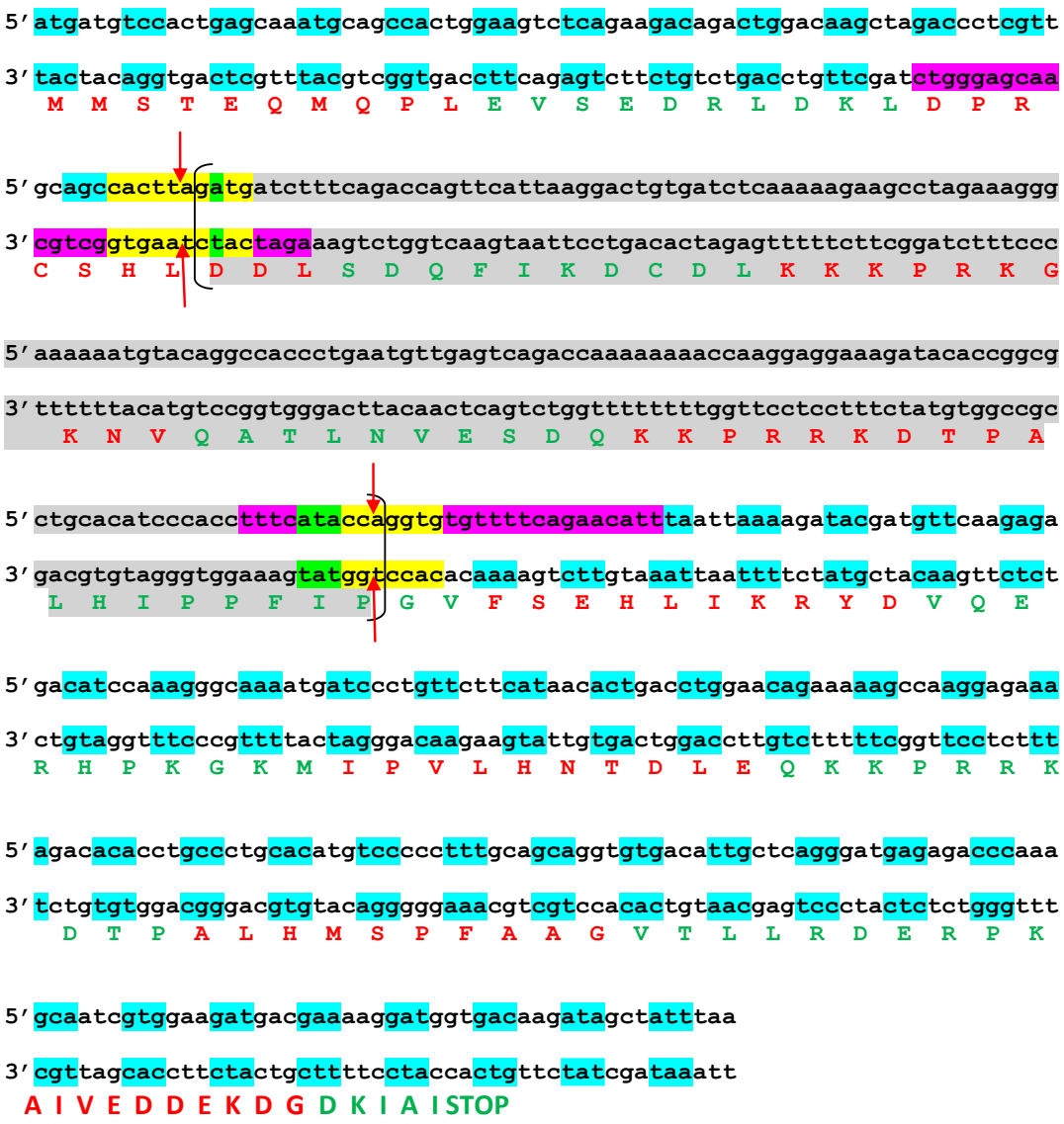

Figure 3.4: Nucleotide sequence of G-substrate.

Portions of the full length protein absent in the short isoform are highlighted in grey, mutation sites in green, areas spanned by the oligonucleotide primers in pink and recognition sites for Ale1 in yellow. The sites of deletion are identified with red arrows ⇵.

The PCR product was cleaned up using the Wizard SV Gel and PCR clean-up system (Promega) and subjected to *Ale*I digestion (see section 2.1.2) for 15 min at 37 °C. The enzyme was inactivated by incubating the mixture at 65 °C for 5 min and the digestion product cleaned up with the Wizard SV Gel and PCR clean-up system. After ligation with T4 DNA ligase (Promega), the mutant plasmids were transformed into competent Top10 cells (NEB) and grown overnight at 37°C on LB plates containing ampicillin at 100 ng/ml. Plasmid DNA was extracted from single colonies using the Qiaprep miniprep kit (Qiagen) and sequenced using the pTrc HisA vector primers 5'GAGGTATATATTAATGTATCG3' and 5'GATTTAATCTGTATCAGG3'.

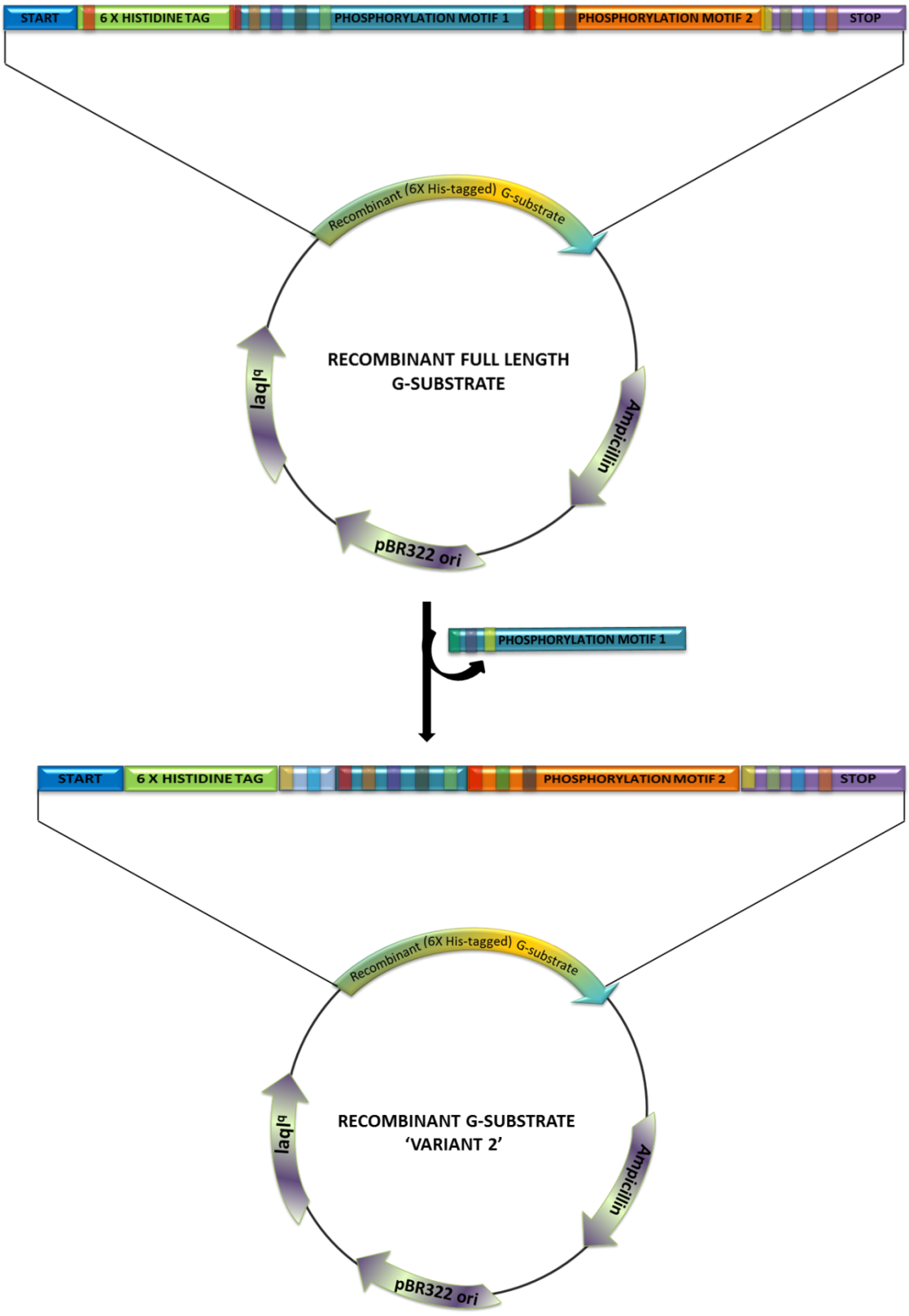

Figure 3.5: Schematic Representation of Short G-substrate Cloning.

In silico translation of the DNA sequence of the mutant plasmid yielded a 144 amino acid protein, which represented recombinant full length G-substrate with 51 amino acids deleted between leucine–61 and glycine–111 (Figure 3.6), a situation identical to that observed in the amino acid sequences of full length and 'variant 2' human G-substrate protein.

```
F/L         1 -----MGGSHHHHHHGMASMTGGQQMGRDLYDDDDKDRWGSMSTEQMQPL     45
                    .||||||||||||||||||||||||||||||||||||||||||||
 V2         1 GTGKTWGGSHHHHHHGMASMTGGQQMGRDLYDDDDKDRWGSMSTEQMQPL     50

F/L        46 EVSEDRLDKLDPRCSHLDDLSDQFIKDCDLKKKPRKGKNVQATLNVESDQ     95
              ||||||||||||||||
 V2        51 EVSEDRLDKLDPRCSHL--------------------------------     67

F/L        96 KKPRRKDTPALHIPPFIPGVFSEHLIKRYDVQERHPKGKMIPVLHNTDLE    145
                              ||||||||||||||||||||||||||||||||
 V2        68 ------------------GVFSEHLIKRYDVQERHPKGKMIPVLHNTDLE     99

F/L       146 QKKPRRKDTPALHMSPFAAGVTLLRDERPKAIVEDDEKDGDKIAI    190
              ||||||||||||||||||||||||||||||||||||||||||||
 V2       100 QKKPRRKDTPALHMSPFAAGVTLLRDERPKAIVEDDEKDGDKIAI    144
```

Figure 3.6: Amino acid sequences of Recombinant Full Length G-substrate (F/L) and Short G-substrate (V2)

3.2.2 G-substrate 'Variant 2' Expression and Purification

The pTrc HisA plasmids containing recombinant short G-substrate were transformed into BL21 Star™ (DE3) pLysS cells and grown on LB plates containing chloramphenicol at 34 ng/ml, ampicillin at 100 ng/ml and tetracycline at 12.5 ng/ml. A 10 ml starter culture was inoculated with a single colony from the plates and grown overnight at 37 °C with shaking. G-substrate 'variant 2' protein was expressed in a 1 l culture of LB broth containing antibiotics as above and inoculated with the 10 ml starter culture. Overexpression of the protein was induced with 1 mM of IPTG at an optical density (OD) at 600 nm of between 0.6 and 0.8. After induction, the bacterial cultures were grown for a further 4h after which cells were harvested by centrifuging at 5000 rpm (4,080 g) for 30 min in a Sorvall GS-3 rotor.

Harvested cells were resuspended in lysis buffer (50 mM NaH_2PO_4, 300 mM NaCl, 10 mM Imidazole, 0.2 mg/ml Lysozyme and a complete protease inhibitor tablet (Roche)) and incubated on ice for 30 min. Resuspended cells were then taken through five cycles in a sonic bath at 10 microns (15 sec on and 15 sec off) and centrifuged for 45 min at 13000 rpm (27,138 g) in a Sorvall SS-34 rotor.

The supernatant from centrifugation was applied to a gravity flow column containing NTA agarose beads charged with nickel ions and the G-substrate 'variant 2' protein eluted with increasing concentrations of imidazole. The His-tagged G-substrate 'variant 2' was further purified by anion exchange on a column with a quaternary ammonium functional group (MonoQ 5/50 column) (Amersham Biosciences)

.

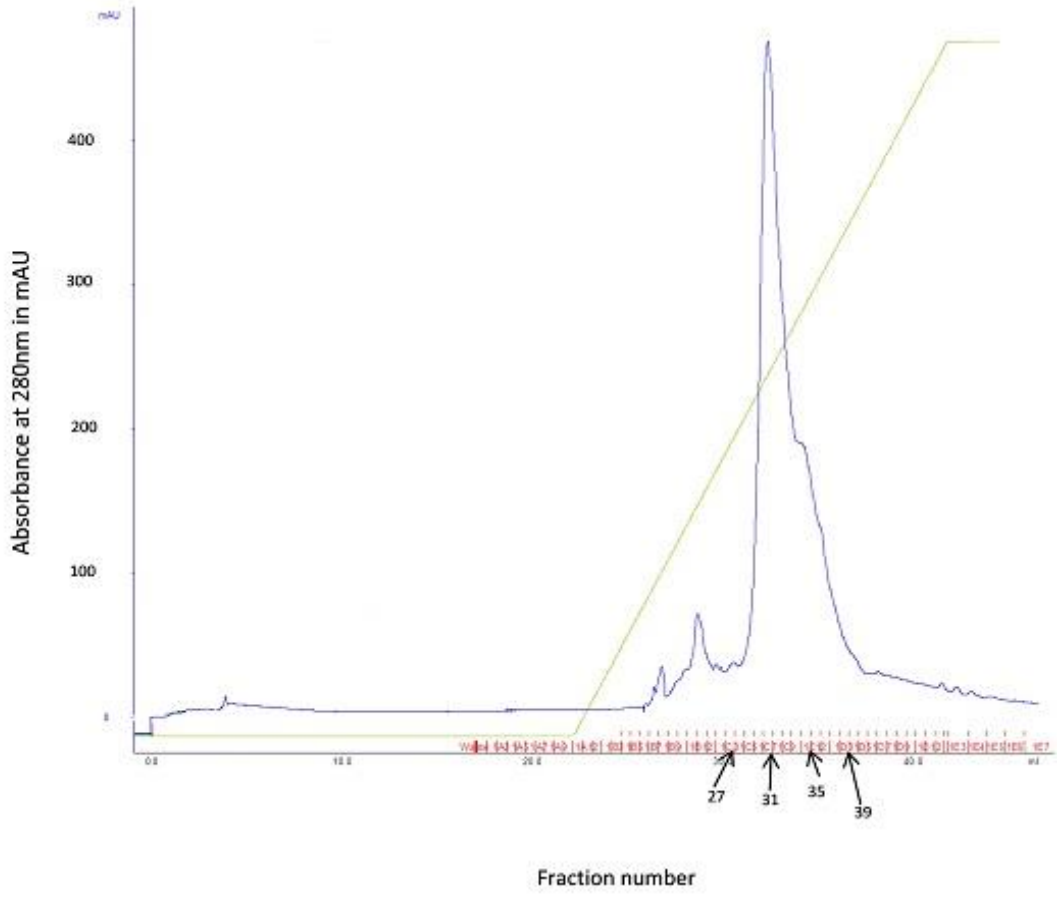

Figure 3.7: Chromatogram from Anion Exchange of Recombinant Short G-substrate.
Green line represents salt gradient and peak represents purified short G-substrate.

Fractions were analyzed by SDS-PAGE and the identity of G-substrate verified by immunoblotting using an antibody raised against the phosphorylation motif of G-substrate (Figure 3.8).

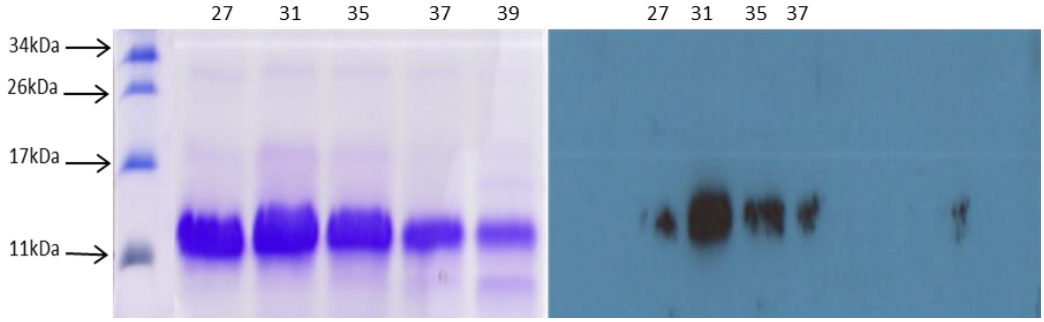

Figure 3.8: Purification of Recombinant Short G-substrate Protein.
SDS-PAGE (L) and Western Blot (R) Images of Fractions from Anion Exchange of Recombinant Short G-substrate. Numbers above lanes indicate fraction numbers of eluents.

3.3 Phosphorylation of G-substrate

G-substrate protein was identified and named as the first endogenous substrate of cyclicGMP-dependent protein kinase in the brain (1). Aitken and co-workers (3) have shown that G-substrate is also phosphorylated by cylicAMP-dependent protein kinase, although less rapidly and with a preference for T119 over T68 (Figure 3.9) (residue numbering as for human G-substrate). Phosphorylation of both variants of G-substrate was catalysed by the catalytic subunit cAMP-dependent G-substrate (see sections 3.3.1 and 3.3.2), which was more readily available commercially than cGMP-dependent protein kinase.

Figure 3.9: Amino Acid Sequences of G-substrate Isoforms.
Full Length (top) and Short G-substrate (bottom) showing the positions of the phosphorylation motifs (green) and the phosphorylateable threonines (orange).

3.3.1 Full Length G-substrate Phosphorylation

Phosphorylation of Full Length G-substrate was carried out in 10mM $MgCl_2$, 50mM Tris-HCL, pH 7.5, 200µM ATP. About 500µg of full length G-substrate was incubated under the conditions above with 250units of cAMP-dependent protein kinase. The phosphorylation reaction was incubated at 30°C for 1 h. After phosphorylation, the PKA was inactivated by incubation at 65°C for 20 min and phosphorylation of G-substrate was confirmed by MALDI-tof mass spectroscopy. Phosphorylation is observed in a mass spectrum as a mass shift of 80 Daltons per phosphorylated amino acid. Full length G-substrate possesses two phosphorylateable threonines as shown in Figure 3.9 and as a result shows a mass shift of 160 Daltons when both phosphorylateable threonines have been phosphorylated. Figure 3.10 shows the mass spectra of full length G-substrate before and after phosphorylation.

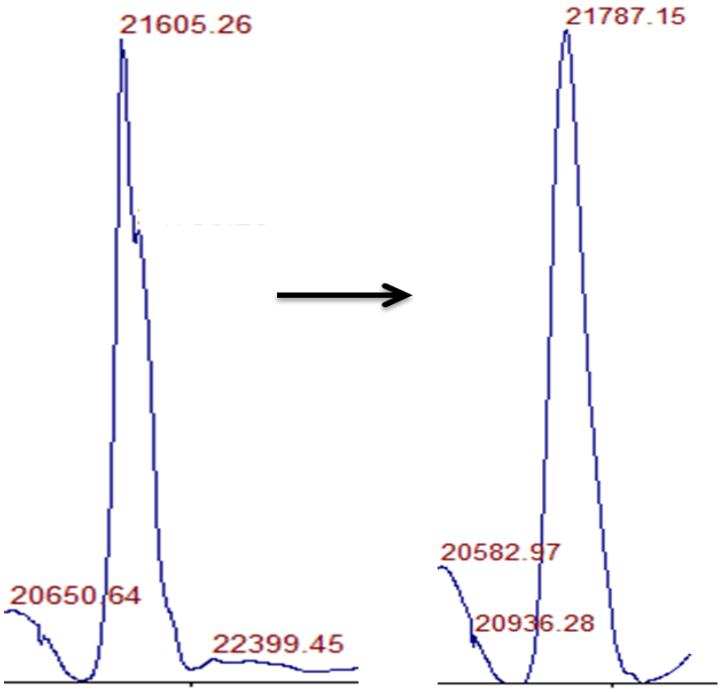

Figure 3.10: Full Length G-substrate Phosphorylation.

Maldi-tof mass spectra of Full length G-substrate before (left) and after (right) phosphorylation

3.3.2 G-substrate 'Variant 2' Phosphorylation

Phosphorylation of G-substrate 'Variant 2' was carried out in 10mM $MgCl_2$, 50mM Tris-HCL, pH 7.5, 200µM ATP and 125units of cAMP-dependent protein kinase. The phosphorylation reaction was incubated at 30°C for 1 h, after which the PKA was inactivated by incubation at 65°C for 20 min and phosphorylation of G-substrate was confirmed by MALDI-tof mass spectroscopy. Since short G-substrate possesses only one phosphorylateable threonine as shown in Figure 3.9, the phosphorylated short protein shows a mass shift of 80 daltons when it is phosphorylated. Figure 3.11 shows the mass spectra of short G-substrate before and after phosphorylation.

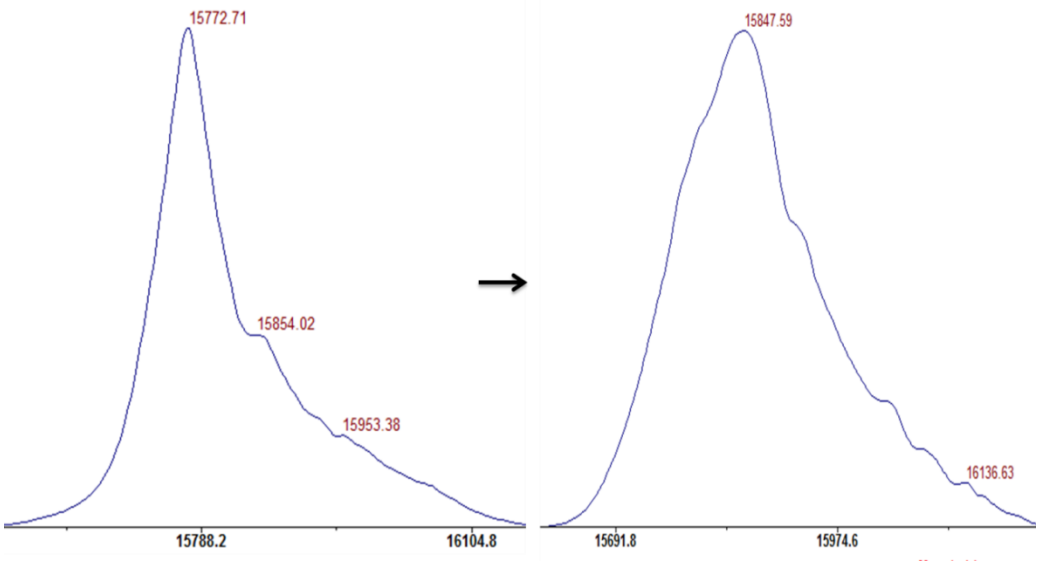

Figure 3.11: Short G-substrate Phosphorylation.

Maldi-tof mass spectra of Short G-substrate before (left) and after (right) phosphorylation.

3.3.3 Confirmation of G-substrate Phosphorylation

To ensure that the phosphorylation observed by mass spectrometry actually occurs on the threonine residues within the phosphorylation motifs of both isoforms of the protein and not on the other serine and threonine residues present, western blot analysis of the phosphorylated isoforms of G-substrate was carried out using an antibody raised against a phosphorylated peptide with amino acid sequence identical to the phosphorylation motifs of the proteins. This phospho G-substrate antibody was a kind gift from Professors Paul Greengard and Angus Nairn (Rockefeller University). Results from western blotting (Figure 3.12) confirmed that phosphorylation had occurred on the correct residues.

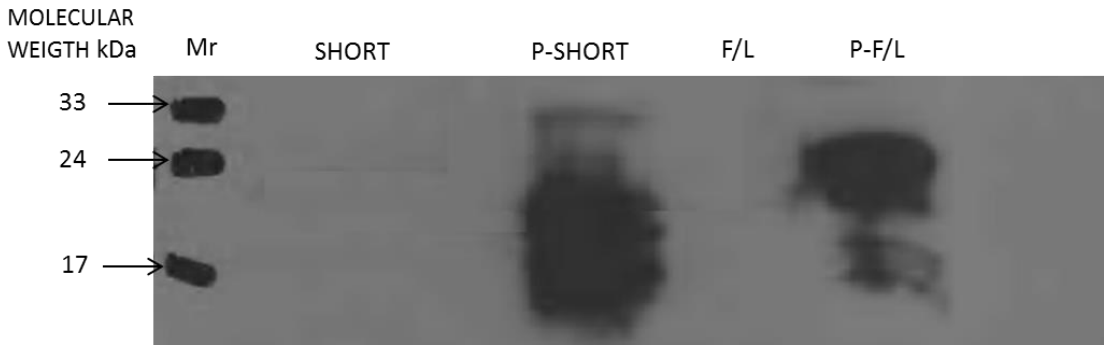

Figure 3.12: Western Blot of Phosphorylated G-substrate Isoforms.

3.4 Discussion

G-substrate protein was successfully expressed and purified. Protein yield was enhanced by the use of Rosetta2 *E. coli* cells, which made those human codons usually rare in *E. coli* bacteria available during translation. In the production of the short G-substrate protein, BL21 Star™ (DE3) pLysS cells, which served the same purpose, were used.

Both isoforms of G-substrate were found to run at molecular weights different from their predicted weights on SDS-PAGE. Analysis by MALDI-tof mass spectrometry, however, showed the proteins had the correct molecular weight.

Western blot analysis of 'variant 2' G-substrate showed bands that were less intense than those obtained for full length G-substrate even when comparable amounts of the proteins were used. This is most likely due to the possession by short G-substrate of one phosphorylation motif while full length G-substrate possesses two. It is possible that since the antibody used in the western blot analysis was raised against the phosphorylation motif, the full length protein, which potentially binds two molecules, will give a stronger signal than the short protein, which potentially binds only one antibody molecule.

Both isoforms of G-substrate were successfully phosphorylated with the catalytic subunit of cAMP-dependent protein kinase. The fact that the full length protein possessed twice as many phosphorylation sites as the short isoform was evidenced by

the requirement of approximately double the enzyme concentration to effect complete phosphorylation within the times observed for the short isoform.

Phosphorylation was detected by MALD-tof mass spectrometry as an 80 kDa shift in mass for every phosphate group added to the isoforms, resulting in a shift of 80 kDa for the short protein and 160 kDa for the full length protein.

Western blot analysis using an antibody raised against the phosphorylation motif of G-substrate, which is identical in both variants confirmed that phosphorylation had occurred on the correct threonine residues.

Chapter 4: Phosphatase Inhibition by Phosphorylated G-substrate

Inhibition of protein phosphatase activity by G-substrate protein has been studied extensively. Opinions differ, however, regarding which protein phosphatase, PP1 or PP2A is inhibited by G-substrate most effectively. Although it has been established that phosphorylated full length G-substrate does inhibit PP1 and PP2A, the role of the short G-substrate isoform as a phosphatase inhibitor has yet to be established. The experiments in this section are described in section 2.11 and were designed to investigate the effects of both phosphorylated and unphosphorylated short G-substrate on protein phosphatase activity and to compare the phosphatase inhibitory effect of this form of G-substrate to that of full length G-substrate.

In order to eliminate the effect of any p-nitrophenol present at the start of the reactions and ensure that all p-nitrophenol measured is due to the dephosphorylation of pNPP, the absorbance values at time zero for each reaction were subtracted from the absorbance values obtained for subsequent time points. As a result, curves showing the effects of the different forms of G-substrate on the activities of the phosphatases investigated show activity values starting at t = 2.5 min for assays investigating PP1 gamma and PP5 activities and at t = 5 min for all other assays. In these curves, relative activity values below the control indicate and inhibition of phosphatase activity while relative activity above the control suggests and enhancement of phosphatase activity.

Where the effects of different concentrations of the G-substrate variants on phosphatase activity are presented as histograms, the values plotted are taken at t = 25 mins for all the experiments conducted because at this point, the phosphatase activities of the different phosphatases were found to be optimum under all the conditions used.

In all the curves shown in this section, each point represents the mean of two values taken from two identical reactions under the same conditions. Experiments for all the results shown in this chapter were repeated on at least two different occasions with consistent results for every occasion.

4.1 Inhibition of Total Phosphatase Activity of Rat Brain Extract

Protein extracts were prepared from the brains of male Sprague Dawley rats according to the protocol described in 'Materials and Methods' in a buffer containing Triton X-100 and protease inhibitors. Protein phosphatase assays were performed using the SensoLyte pNPP Protein Phosphatase Assay Kit (Colorimetric) from Anaspec. Experiments were set up to select the activity of either protein phosphatase 1 or protein phosphatase 2A in the rat brain extract. Phosphatase activity was determined by monitoring the release of p-nitrophenol at 405nm using a Wallac 1420 VICTOR^2 plate reader from Perkin Elmer.

4.1.1 Inhibition of Rat Brain PP1 Activity

Assays of rat brain PP1 confirmed the fact that phosphorylated full length (F/L) G-substrate reduces the activity of PP1 in the brain. Dephosphorylation assays (Figure 4.1) performed in the presence of the phosphorylated full length protein showed phosphatase activity below that of the uninhibited control within 25 min of commencing the reaction, with phosphatase activity dipping to less than 30 % within 1 hr. The unphosphorylated full length protein, however, did not reduce phosphatase activity and instead seemed to enhance PP1 activity with activity of the reaction remaining above 100 % for the duration of the observations. Both phosphorylated and unphosphorylated short G-substrate however showed higher phosphatase activity than the uninhibited reaction for the first 45 min after which PP1 activity in the presence of the unphosphorylated short protein dipped to below 30 % within 10 min and remained at approximately that level for the duration of the observation. These observations indicate that although phosphorylated G-substrate effectively inhibits total brain PP1 activity, the unphosphorylated full length protein and both phosphorylated and unphosphorylated short G-substrate either have no effect on or enhance total activity of PP1 in the brain.

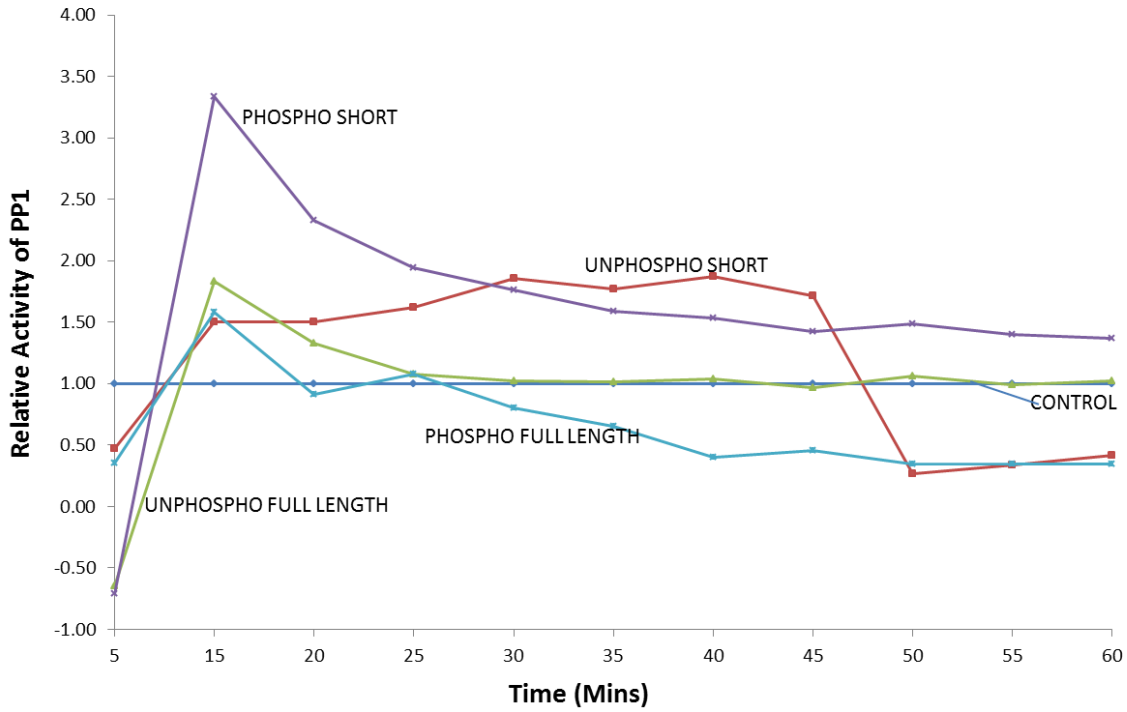

Figure 4.1: Dephosphorylation of pNPP by Rat Brain PP1 in the presence of G-substrate Variants.

Relative activity was determined by expressing enzyme activity in the inhibited reaction as a percentage of activity in the uninhibited reaction (control). In each reaction, 10 μM of the appropriate G-substrate form was used.

4.1.2 Inhibition of Rat Brain PP2A Activity

Both short and full length G-substrate, when unphosphorylated, did not seem to adversely affect the activity of total brain PP2A (Figure 4.2), with activity in the presence of both variants remaining above the level of the uninhibited reaction for the duration of the observation. When phosphorylated, however, both variants of G-substrate markedly reduced the activity of the brain PP2A, with the phosphorylated short protein reducing activity further (below 60 %) than the phosphorylated full length protein, which reduced total brain PP2A activity to about 90 % of the uninhibited reaction.

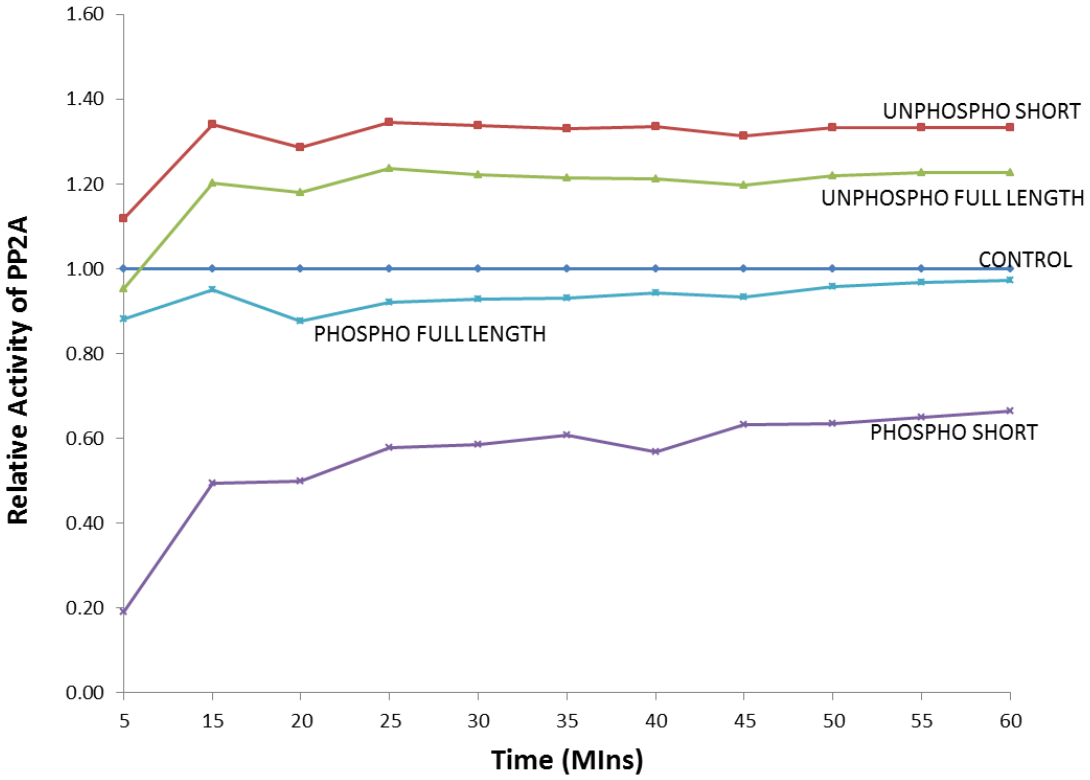

Figure 4.2: Dephosphorylation of pNPP by Rat Brain PP2A in the presence of G-substrate Variants.

Relative activity was determined by expressing enzyme activity in the inhibited reaction as a percentage of activity in the uninhibited reaction (control). In each reaction, 10 μM of the appropriate G-substrate form was used.

4.2 Inhibition of Phosphatase Activity of Rat Cerebellar and Cerebral Extracts

Since both the PP1 and PP2A holoenzymes consist of several subunits which have been determined to vary appreciably between the different tissue types, separate extracts of PP1 and PP2A were prepared from the cerebella and cerebra of adult rats and assayed for phosphatase activity in the presence of G-substrate variants.

4.2.1 Inhibition of Cerebellar PP1 Activity

In cerebellar extracts, the presence of all the G-substrate forms resulted in PP1 activity levels (Figure 4.3) falling below 100% for the duration of the observations.

PP1 activity in the presence of the unphosphorylated isoforms seemed to recover more rapidly after approximately 40 mins compared with activity in the presence of the phosphorylated proteins. This recovery suggests that the phosphorylated G-substrate variants are more resistant to factors present in the cerebellar extract that might affect interaction with PP1. Such factors might include proteases, which degrade the proteins and subsequently abolish their effects on PP1 or other regulators of PP1 that might abolish interaction of G-substrate variants with the PP1 holoenzyme. It is also possible that the ability of phosphorylated full length G-substrate to inhibit cerebellar PP1 for a longer period than the phosphorylated short protein is due to differences in their resistance to dephosphorylation by the combination of phospho-protein phosphatases most likely present in the cerebellar extract.

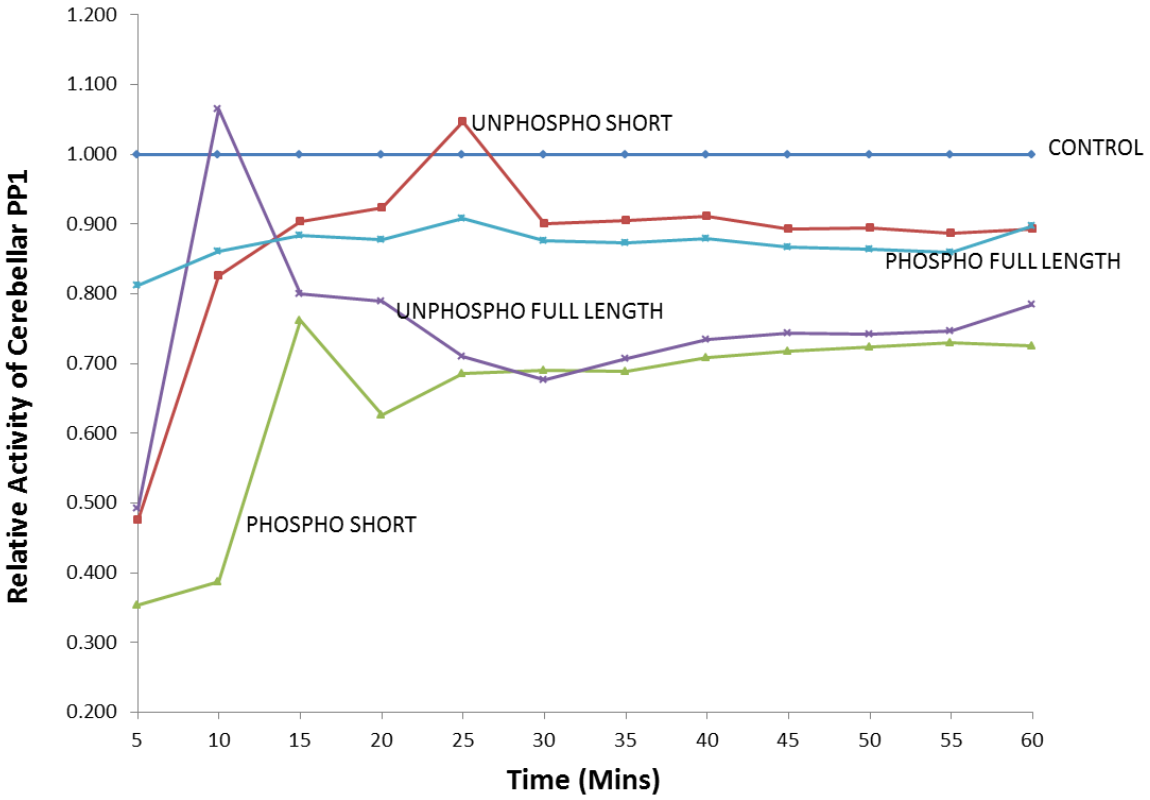

Figure 4.3: Dephosphorylation of pNPP by Cerebellar PP1 in the presence of G-substrate Variants.

Relative activity was determined by expressing enzyme activity in the inhibited reaction as a percentage of activity in the uninhibited reaction (control). In each reaction, 10 µM of the appropriate G-substrate form was used.

In the presence of varying concentrations of the G-substrate isoforms (Figure 4.4), phosphorylated short G-substrate consistently results in lower PP1 activity than the unphosphorylated short protein. Total cerebellar PP1 activity below that observed in uninhibited reactions (representing PP1 inhibition), however, is observed only after the phosphorylated short protein reaches a concentration of 2 µM. PP1 activity remained at 90 % when the phosphorylated short G-substrate concentration was increased to 5 µM, while activity in the presence of unphosphorylated short G-substrate remains consistently above 100 %.

In contrast, the presence of phosphorylated full length G-substrate results in activity levels lower than 100 % for all the concentrations studied, with the greatest inhibition in the presence of 5 µM phosphorylated full length G-substrate.

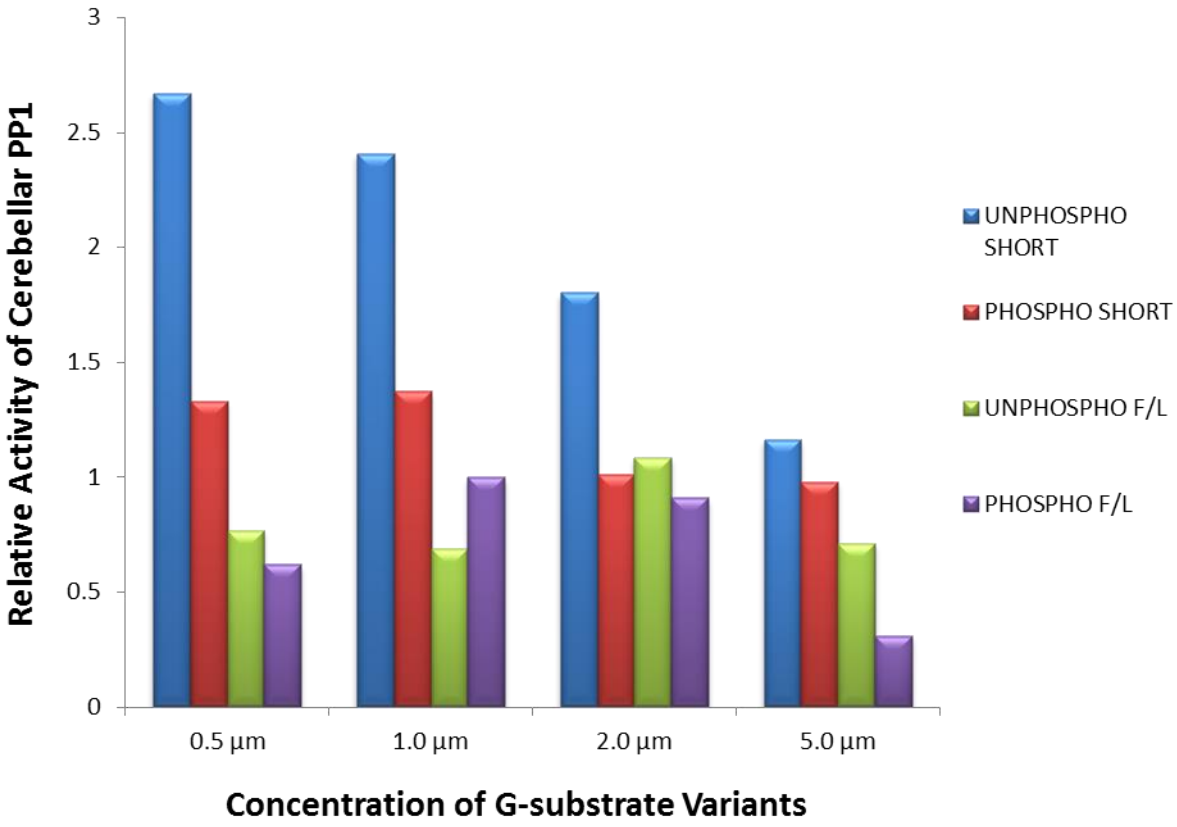

Figure 4.4: Activity of Cerebellar PP1 in the presence of Different G-substrate Concentrations. Relative activity was determined by expressing enzyme activity in the inhibited reaction as a percentage of activity in the uninhibited reaction (control).

4.2.2 Inhibition of Cerebellar PP2A Activity

In the cerebellar extracts, PP2A activity was least affected by unphosphorylated short G-substrate, which reduced phosphatase activity to about 90 % in approximately 15 min (Figure 4.5) The unphosphorylated full length protein and the phosphorylated forms of both variants all reduced PP2A activity to between 60 % and 75 % of the uninhibited reaction from the start of the experiment and reduced PP2A activity was

maintained throughout the observation. Unlike PP1, cerebellar PP2A activity was most affected by phosphorylated short G-substrate, which resulted in an approximately 30 % reduction in phosphatase activity throughout the observation. Both phosphorylated and unphosphorylated full length G-substrate reduced cerebellar PP2A activity to similar levels, with the phosphorylated form maintaining a slightly higher level of phosphatase inhibition than the unphosphorylated form.

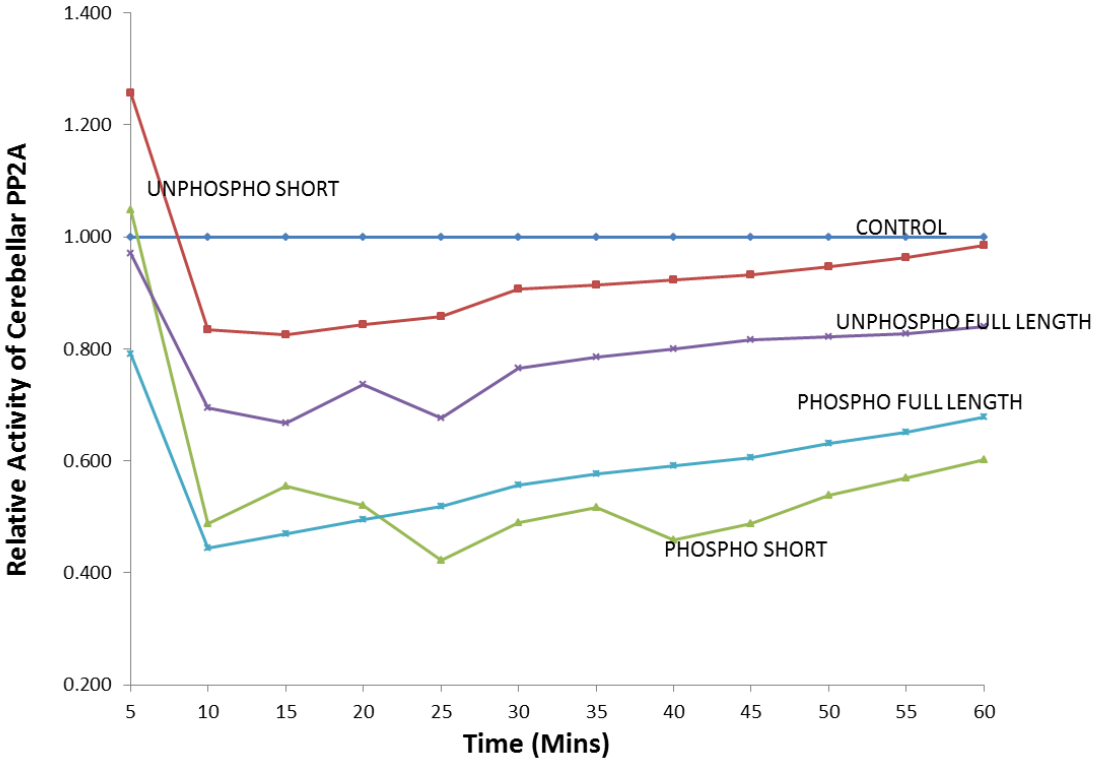

Figure 4.5: Dephosphorylation of pNPP by Cerebellar PP2A in the presence of G-substrate Variants.

Relative activity was determined by expressing enzyme activity in the inhibited reaction as a percentage of activity in the uninhibited reaction (control). In each reaction, 10 µM of the appropriate G-substrate form was used.

The presence of both phosphorylated and unphosphorylated forms of the two G-substrate isoforms resulted in reduced cerebellar PP2A activity across all the protein concentrations studied (Figure 4.6). The greatest inhibition was observed for

phosphorylated short G-substrate, which reduced PP2A activity by approximately 55% at a concentration of 0.5 µM. PP2A activity levels remained largely stable in higher concentrations of G-substrate protein, with both the phosphorylated and phosphorylated forms inhibiting phosphatase activity to approximately the same extent.

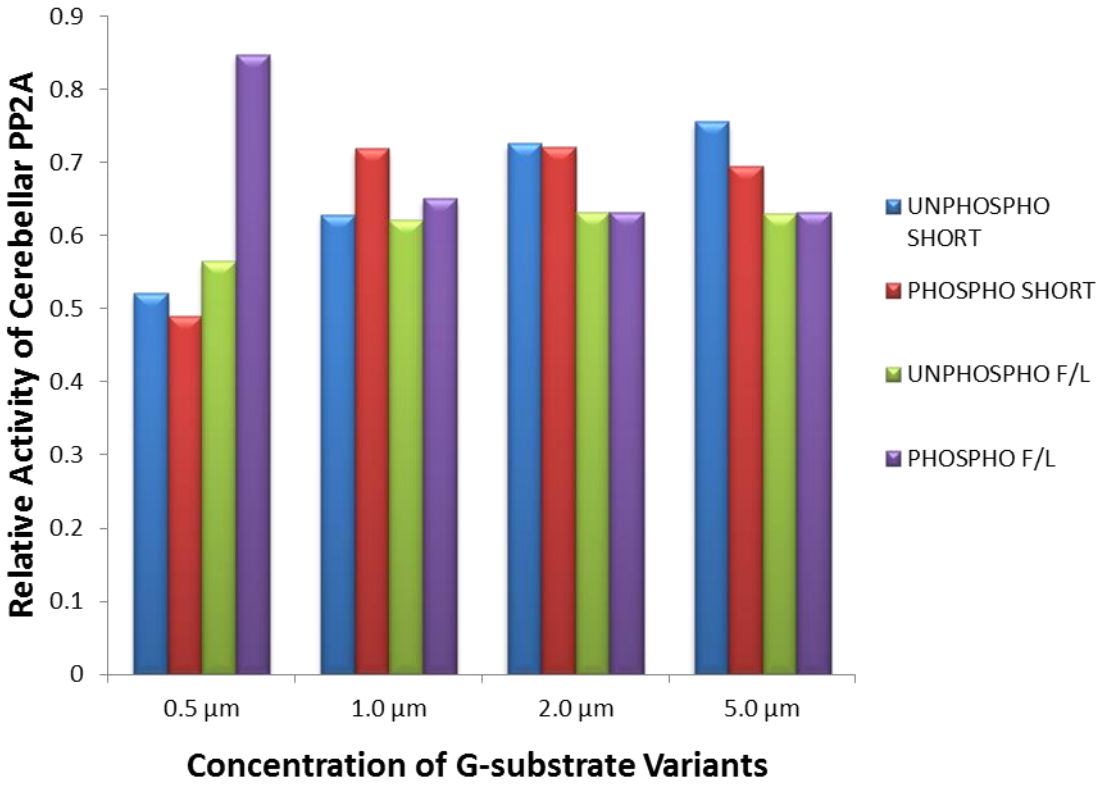

Figure 4.6: Activity of Cerebellar PP2A in the presence of Increasing Concentrations of Unphospho- and Phospho-Short G-substrate.

Relative activity was determined by expressing enzyme activity in the inhibited reaction as a percentage of activity in the uninhibited reaction (control).

4.2.3 Inhibition of Cerebral PP1 Activity

In cerebellar preparations, the greatest inhibition of PP1 activity occurred in the presence of the phosphorylated forms of both isoforms (Figure 4.7), with activity in the presence of both unphosphorylated forms remaining identical throughout the duration of the reaction. For the first 40 mins of the reaction, the presence of the phosphorylated full length protein resulted in slightly more inhibition of cerebellar PP1 activity than was observed for the phosphorylated short protein. After 40 mins, however, both phospho-forms inhibited the phosphatase activity of the cerebellar extract to the same extent.

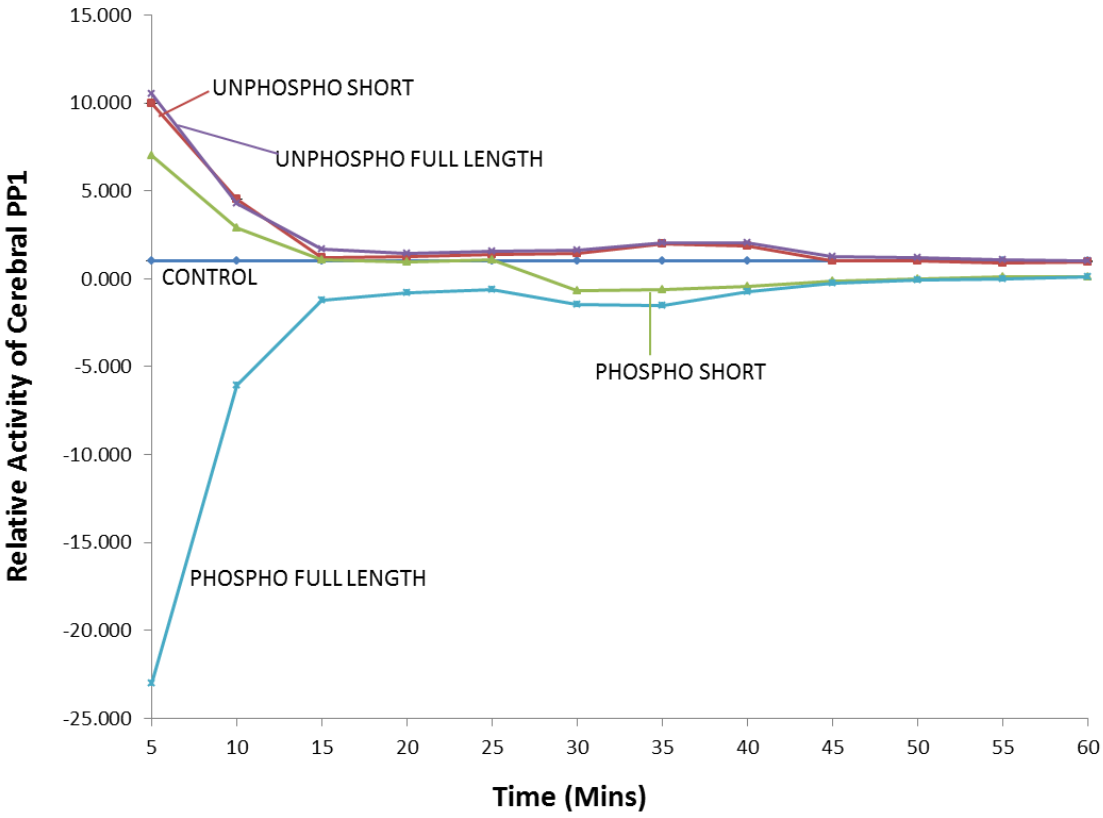

Figure 4.7: Dephosphorylation of pNPP by Cerebral PP1 in the presence of G-substrate Variants.

Relative activity was determined by expressing enzyme activity in the inhibited reaction as a percentage of activity in the uninhibited reaction (control). In each reaction, 10 μM of the appropriate G-substrate form was used.

In cerebral preparations, although both forms reduced PP1 activity, the extent of inhibition in the presence of the unphosphorylated short protein remained constant across all the concentrations tested (Figure 4.8). The phosphorylated short protein only showed a slight increase in inhibition with increasing concentration. The presence of the unphosphorylated full length protein reduced PP1 activity to a greater extent than the phosphorylated protein at concentrations less than 5 μM. Above this, phosphorylated full length G-substrate reduced PP1 activity slightly more than the unphosphorylated protein.

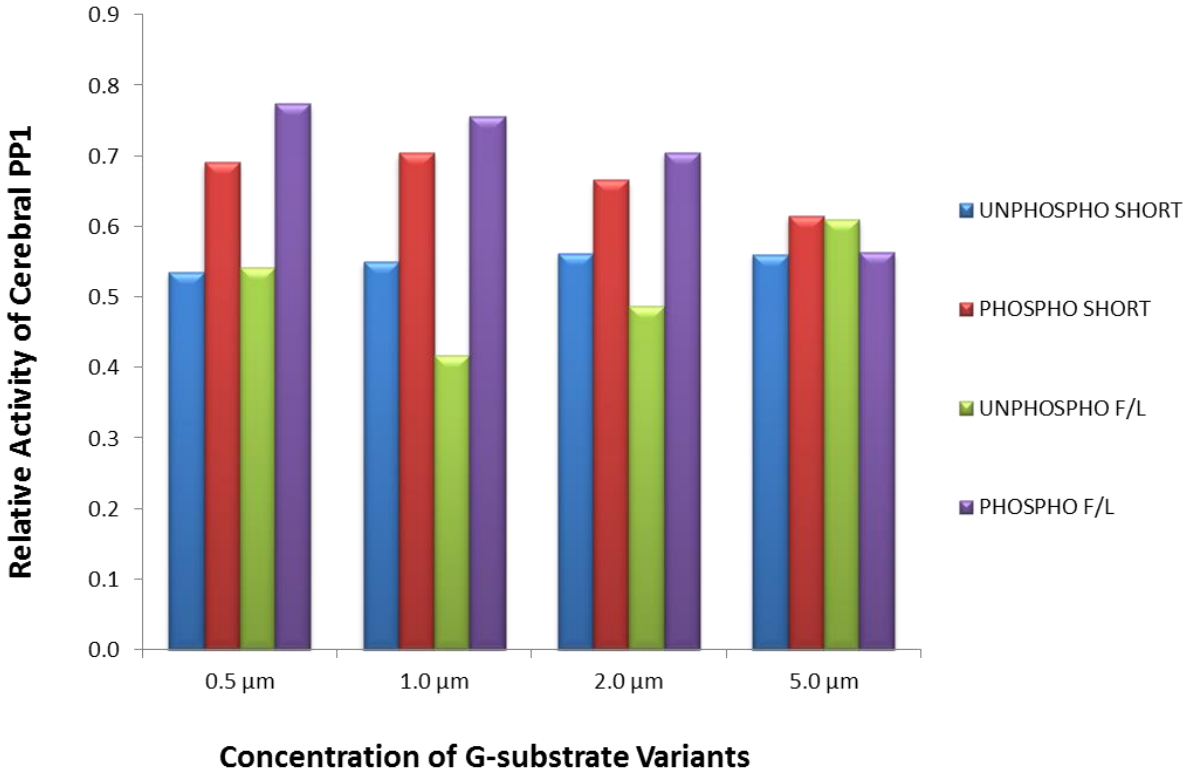

Figure 4.8: Activity of Cerebral PP1 in the presence of Increasing Concentrations of Unphospho- and Phospho- G-substrate.

Relative activity was determined by expressing enzyme activity in the inhibited reaction as a percentage of activity in the uninhibited reaction (control).

4.2.4 Inhibition of Cerebral PP2A Activity

The effect of the G-substrate isoforms on cerebral PP2A was very similar to that observed in the cerebellar preparations, with both phosphorylated forms reducing PP2A activity to a greater extent than the unphosphorylated forms. Unlike the cerebellar PP2A where all the isoforms reduced phosphatase activity, the presence of one form of G-substrate, the unphosphorylated short isoform, resulted in cerebral PP2A activity that was essentially enhanced for the duration of the reaction (Figure 4.9). This variation in the effect of unphosphorylated short G-substrate on PP2A activity in the different areas of the brain might be a hint at the existence of subtle differences in the roles of the various isoforms of G-substrate in different areas of the brain and the possibility that since different PP2A holoenzymes are targeted to different areas by their B-subunits (73), the different G-substrate forms might interact preferentially with different holoenzymes of PP2A in the different areas of the brain.

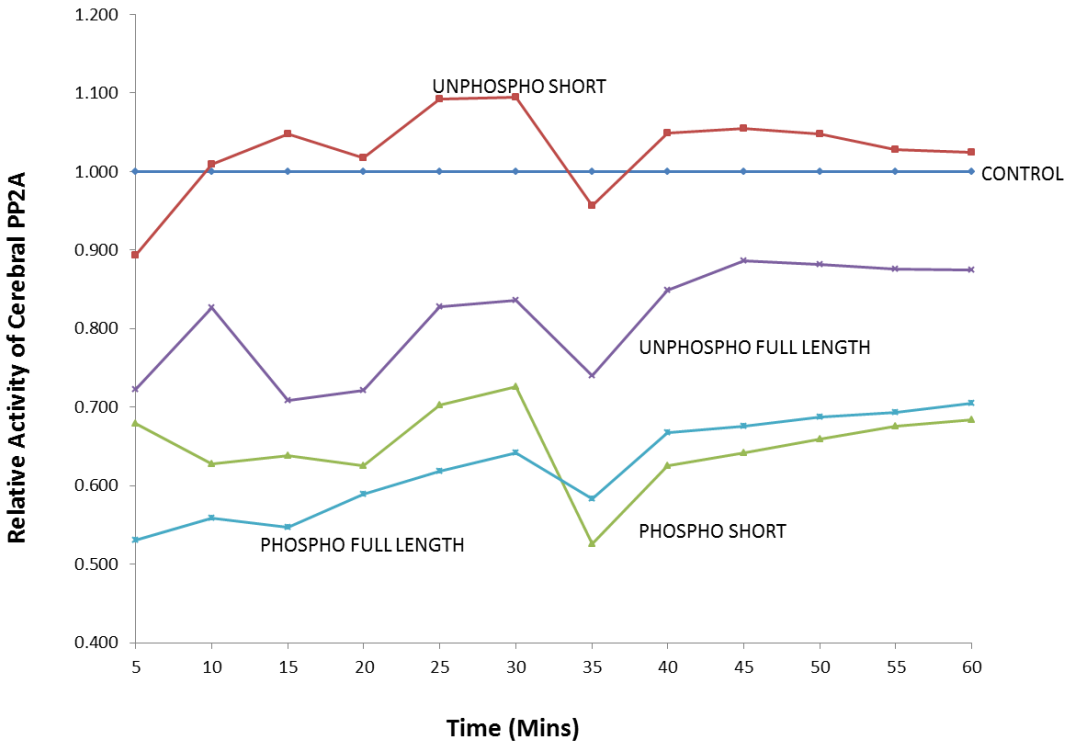

Figure 4.9: Dephosphorylation of pNPP by Cerebral PP2A in the presence of G-substrate Variants.

Relative activity was determined by expressing enzyme activity in the inhibited reaction as a percentage of activity in the uninhibited reaction (control). In each reaction, 10 µM of the appropriate G-substrate form was used.

When varying concentrations of the G-substrate isoforms were studied (Figure 4.10), all forms except the phosphorylated short protein reduced PP2A activity of the cerebral extract to approximately constant levels up to 2 µM after which the phosphorylated short protein produced the most inhibition with the effects of the other forms remaining largely unaltered.

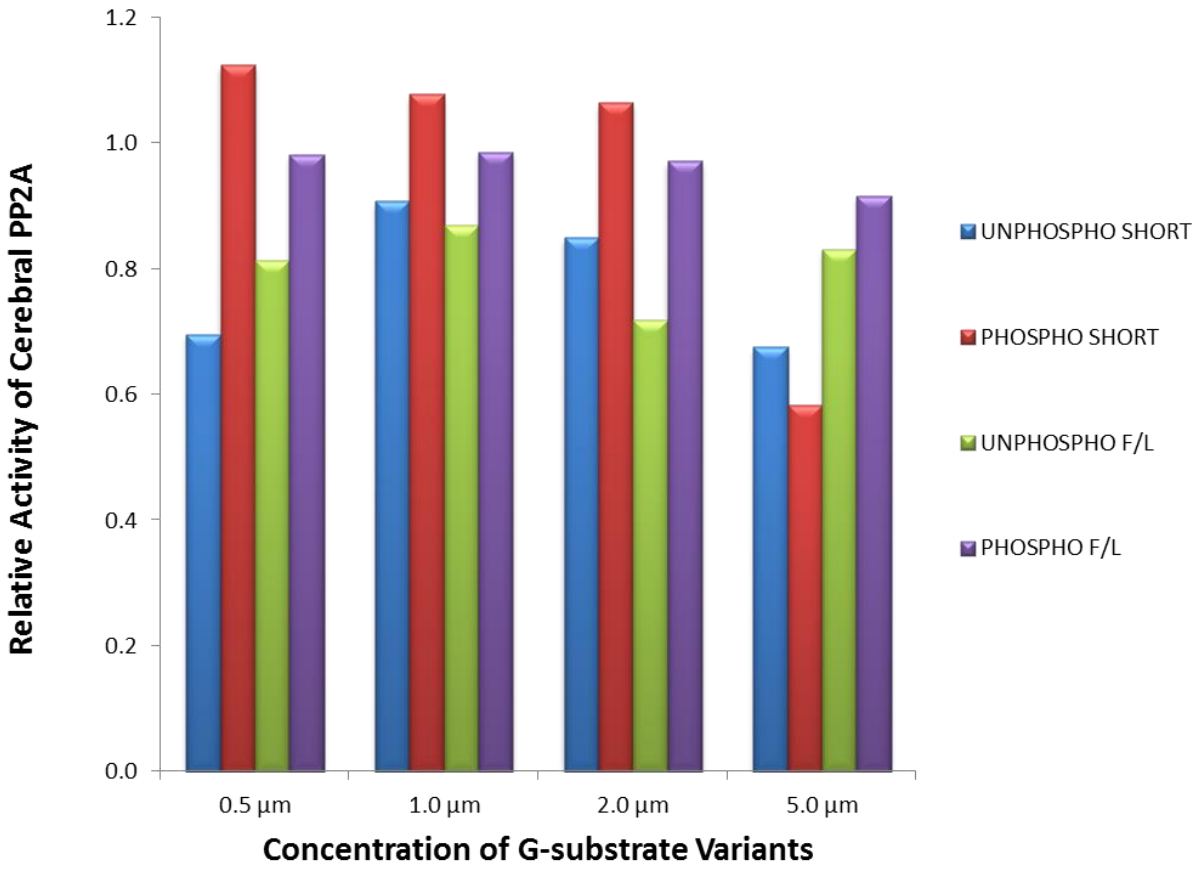

Figure 4.10: Activity of Cerebral PP2A in the presence of Increasing Concentrations of G-substrate.

Relative activity was determined by expressing enzyme activity in the inhibited reaction as a percentage of activity in the uninhibited reaction (control). In each reaction, 10 µM of the appropriate G-substrate form was used.

The activities of PP1 gamma and PP5, kindly provided by Professor Patricia Cohen of the University of Dundee were investigated in the presence of G-substrate. Although G-substrate has been shown to inhibit PP1 purified from mammalian brain, no information on its effect on specific PP1 isoforms is currently available.

4.2.5 Inhibition of PP1 Gamma Activity

The gamma isoform of PP1 is important for cell cycle regulation with experiments showing the selective loading of a pool of PP1γ onto chromatin at anaphase (74). Both phosphorylated and unphosphorylated forms of short G-substrate reduced the activity of PP1γ as can be seen in Figure 4.11. The unphosphorylated short form was, however, the most potent inhibitor of PP1γ activity. The unphosphorylated forms of both G-substrate isoforms reduced PP1γ activity to approximately the same extents, while the presence of the phosphorylated full length protein enhanced PP1γ activity, resulting in phosphatase activity that remained consistently higher than the uninhibited control reaction.

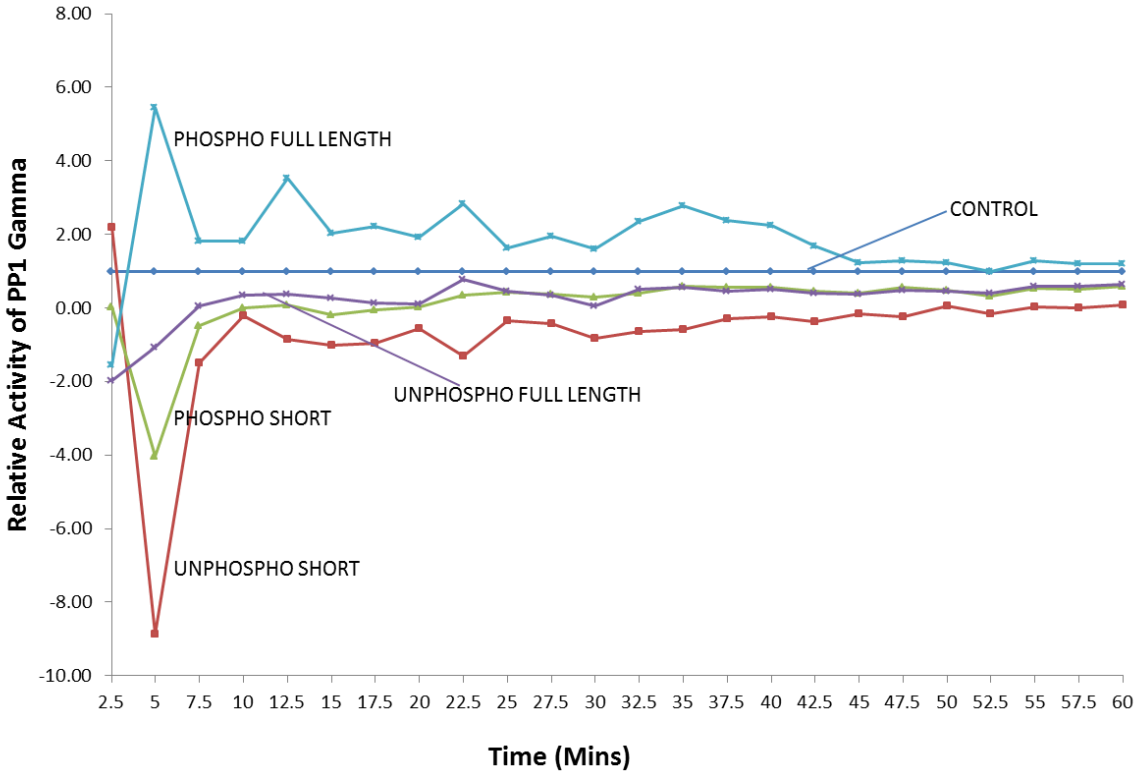

Figure 4.11: Dephosphorylation of pNPP by PP1 Gamma in the presence of G-substrate Variants.

Relative activity was determined by expressing enzyme activity in the inhibited reaction as a percentage of activity in the uninhibited reaction (control). In each reaction, 10 μM of the appropriate G-substrate form was used.

4.2.6 Inhibition of Protein Phosphatase 5 Activity

Protein phosphatase 5 (PP5) is a serine threonine phosphatase, which has been implicated in a wide range of cellular processes including cell cycle arrest, the cellular heat shock response and DNA damage repair via the p53 and ATM/ATR pathways (75).

The small pool of PP5 associated with microtubules has been shown to dephosphorylate abnormally phosphorylated tau protein in the presence of arachidonic acid *in vitro* (76). This observation suggests an important role for PP5 in conditions such as Alzheimer's disease, where it could potentially undo the abnormal tau protein phosphorylation that results in the formation of neurofibrillary tangles.

To explore the possibility that G-substrate affects the activity of other serine/threonine phosphatases, the effect of phosphorylated and unphosphorylated forms of both G-substrate isoforms on PP5 dephosphorylation of pNPP was investigated.

Unphosphorylated forms of both G-substrate isoforms reduced PP5 activity after about 5 mins, while the phosphorylated full length isoform of G-substrate inhibited PP5 activity after 15 mins (Figure 4.12). The phosphorylated short isoform, however, resulted in phosphatase activity that remained very close to the uninhibited control reaction after the first 15 mins, suggesting that phosphorylated short G-substrate has little or no effect on PP5 activity. The unphosphorylated full length protein was found to be the most inhibitory, reducing PP5 activity to less than 70 % after 5 min and maintaining the lowest PP5 activity for the duration of the experiment.

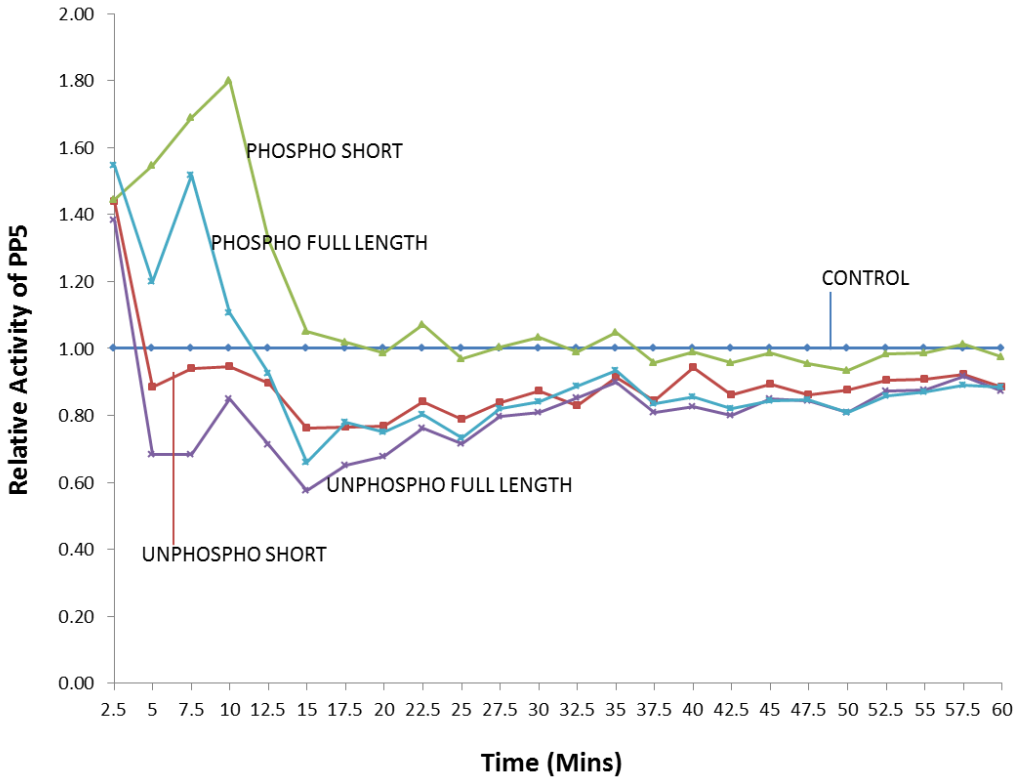

Figure 4.12: Dephosphorylation of pNPP by PP5 in the presence of G-substrate Variants. Relative activity was determined by expressing enzyme activity in the inhibited reaction as a percentage of activity in the uninhibited reaction (control). In each reaction, 10 µM of the appropriate G-substrate form was used.

4.3 Purification of Protein Phosphatases 1 and 2-A from Rat Muscle

In order to investigate the effect of the G-substrate isoforms on PP1 and PP2A catalytic subunits (PP1c and PP2Ac), these were purified from rat skeletal tissue as described in section 2.10 and their activities assayed in the presence of phosphorylated and unphosphorylated forms of both G-substrate isoforms.

Fractions obtained from ion exchange purification, detailed in section 2.10.3 of the 'Materials and Methods' chapter were tested for phosphatase activity. Fractions with the highest activity were pooled and the effects of phosphorylated and unphosphorylated forms of both G-substrate isoforms on the pooled fractions tested using pNPP as a substrate.

.

4.3.1.1 Activity of Purified PP1

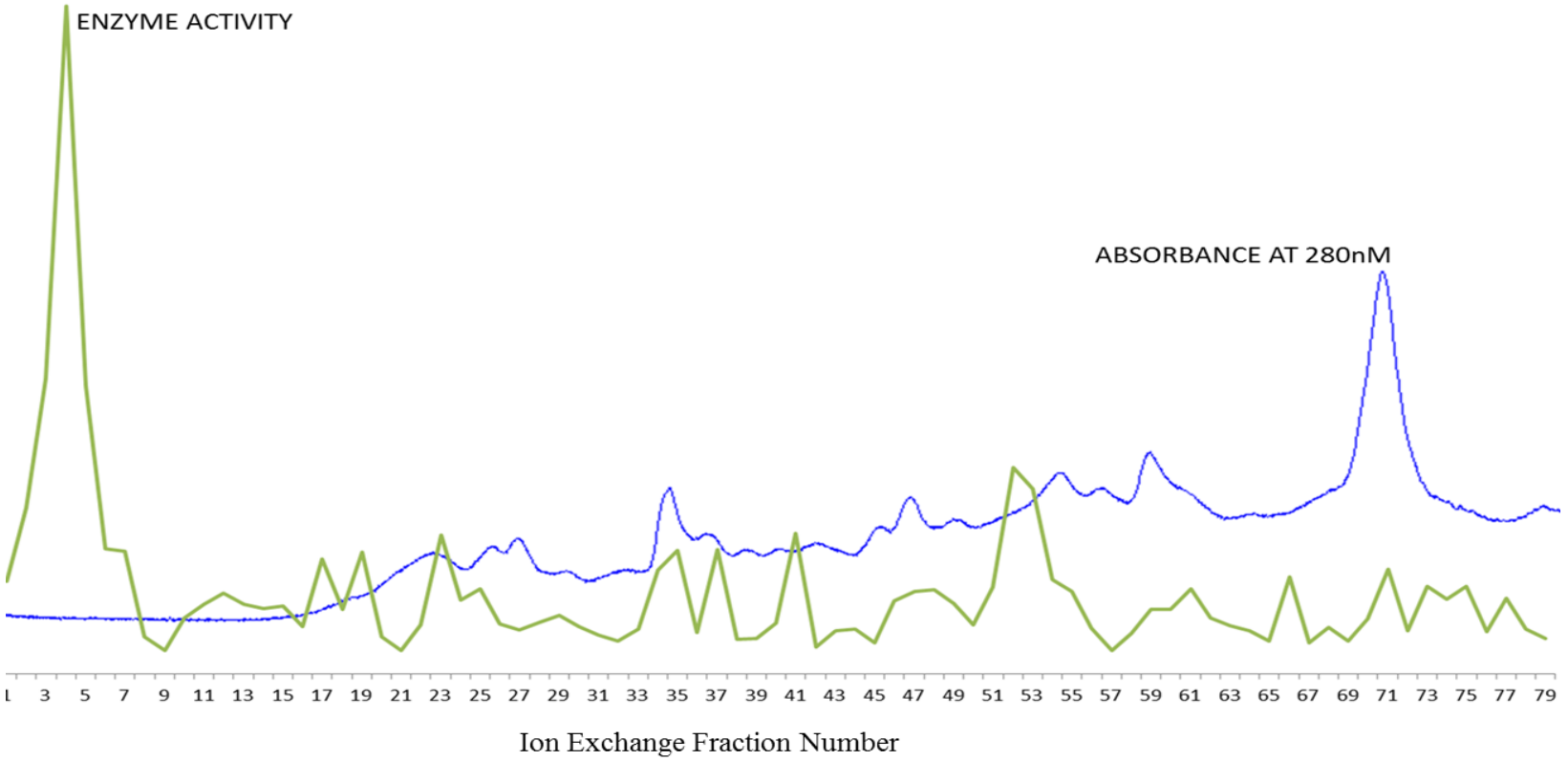

Figure 4.13: Overlay of UV absorbance and enzyme activity traces of PP1c fractions purified from rat skeletal muscle.

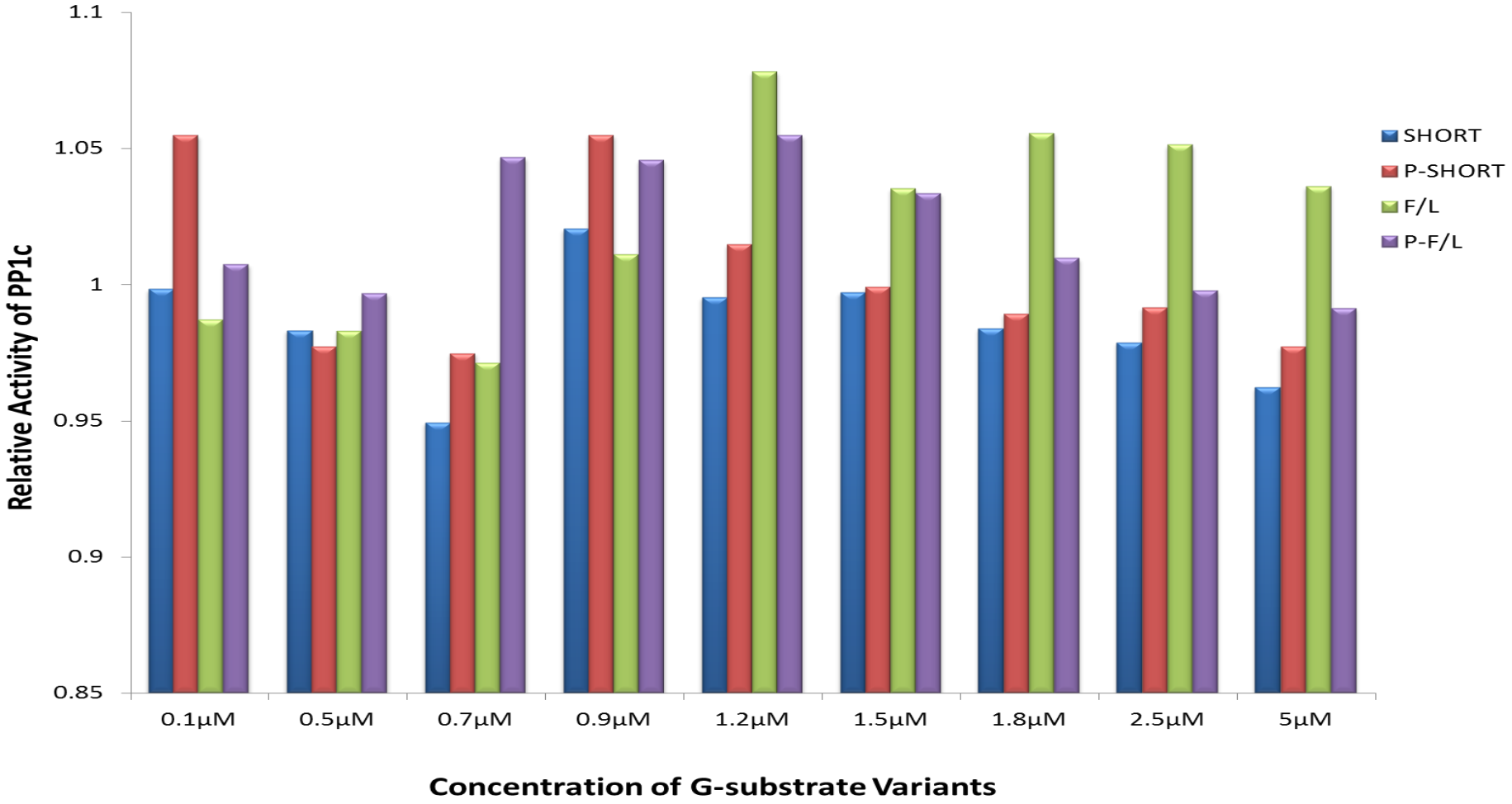

Figure 4.14: Activity of PP1c from Rat Skeletal Muscle on Different Concentrations of G-substrate.

Relative activity was determined by expressing enzyme activity in the inhibited reaction as a percentage of activity in the uninhibited reaction (control).

Phosphatase assay of the catalytic subunit of PP1 (Figure 4.14) showed lower activity in the presence of unphosphorylated short G-substrate than the phosphorylated short isoform, indicating that the unphosphorylated short protein is a better inhibitor of PP1c than the phospho-form of the same isoform. This pattern of PP1c inhibition by short G-substrate remained the same for virtually all the concentrations investigated.

At concentrations lower than 1.2 μM for unphosphorylated full length G-substrate lower PP1c activity was observed than with its phosphorylated form. At concentrations of 1.2 μM and higher, however, as expected, the phosphorylated full length protein shows a greater inhibition of PP1c than the unphosphorylated form suggesting the existence of an apparent threshold of phosphorylated G-substrate concentration required for PP1c inhibition. Both forms of short G-substrate resulted in PP1c activity higher than or about the same as for full length G-substrate at the same concentration. While at concentrations lower than this apparent threshold, both forms of short G-substrate resulted in greater inhibition of PP1c activity than observed for both forms of the full length protein.

These observations suggest the possibility of a concentration dependent activation of G-substrate inhibition of the PP1 catalytic subunit with aberrant effects observed for the phosphorylated and unphosphorylated forms of the two isoforms dependent on whether or not their concentrations exceed the threshold.

Phosphorylated and unphosphorylated forms of both short and full length G-substrate affected the catalytic subunit of PP2A to approximately the same extent across the protein concentrations studied (Figure 4.16: Activity of PP2Ac in the presence of Different Concentrations of G-substrate.). This suggests that, as observed in extracts of whole brain, cerebra and cerebella,-all forms of G-substrate protein are able to inhibit this PP2A.

4.3.1.2 Activity of Purified PP2A

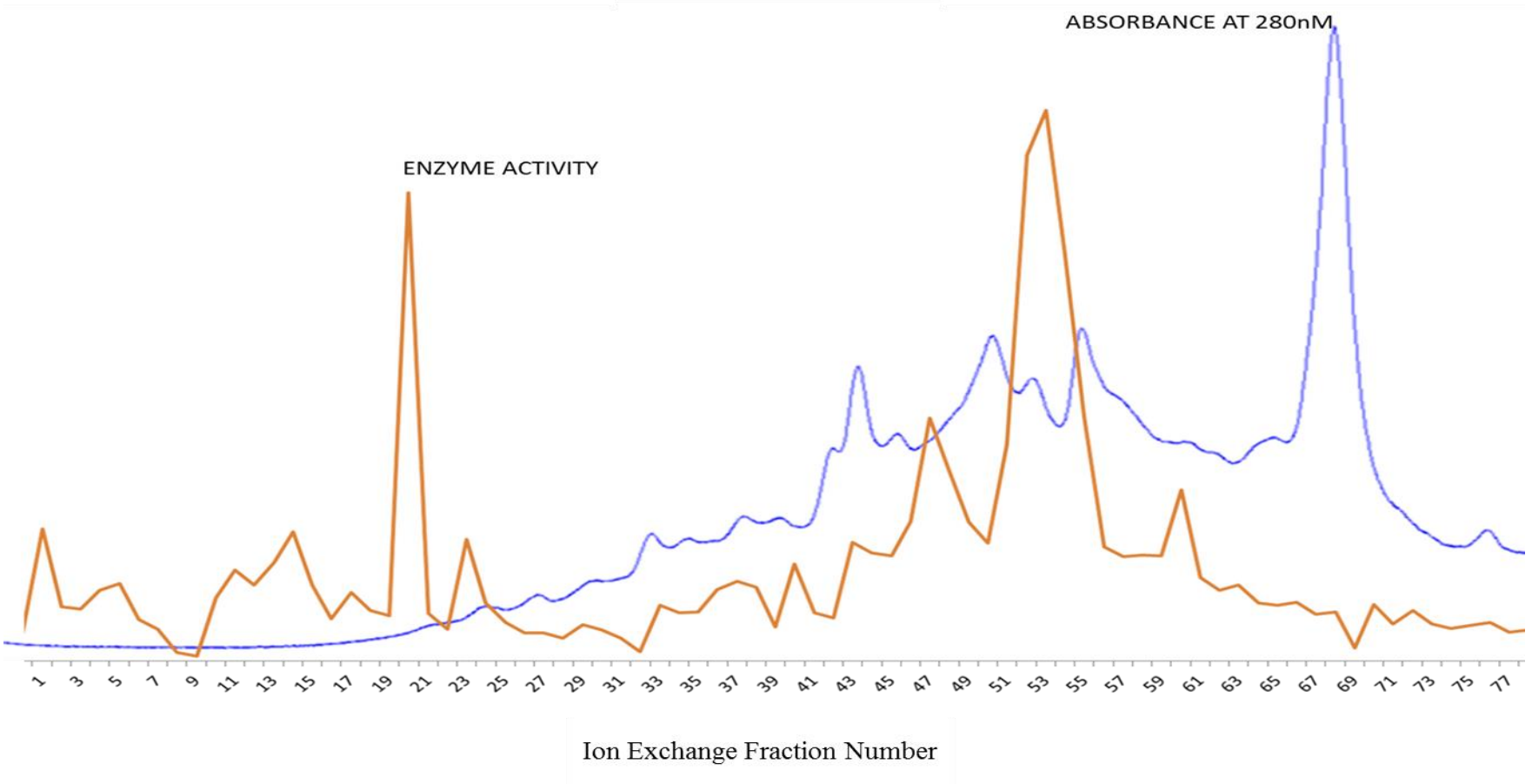

Figure 4.15: Overlay of UV absorbance and enzyme activity traces of PP2Ac fractions purified from rat skeletal muscle

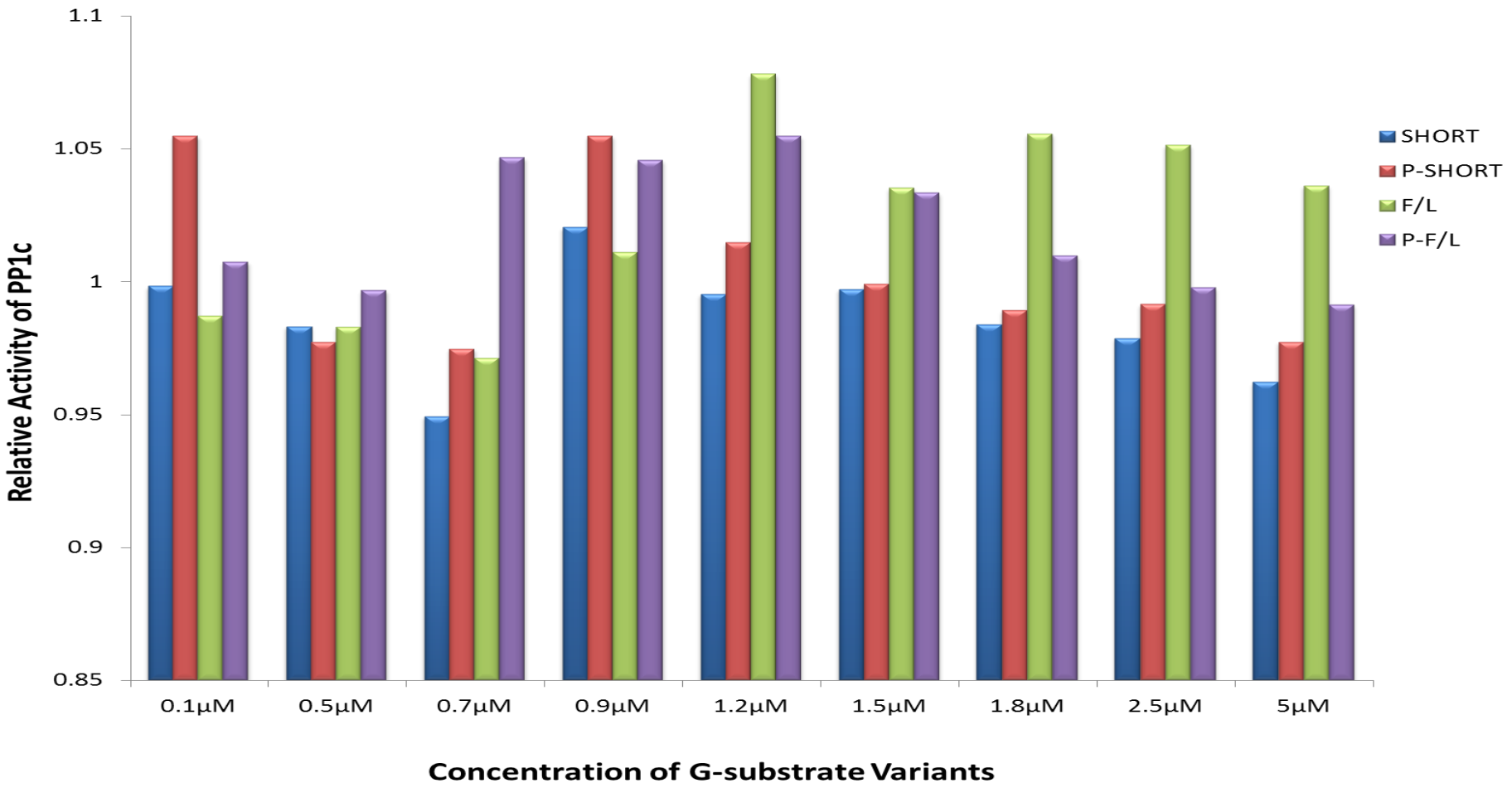

Figure 4.16: Activity of PP2Ac in the presence of Different Concentrations of G-substrate.

Relative activity was determined by expressing enzyme activity in the inhibited reaction as a percentage of activity in the uninhibited reaction (control)

.**Table 4.1: Summary of Effects of G-substrate variants on the Activities of different forms of PP1 and PP2A.**

The effect of the G-substrate variants on activities of the phosphatases have been represented with stars (*), with **** indicating the greatest inhibition of phosphatase activity and * indicating the lowest inhibition of phosphatase activity.

	RAT BRAIN PP1	RAT BRAIN PP2A	CEREBELLAR PP1	CEREBELLAR PP2A	CEREBRAL PP1	CEREBRAL PP2A	PP1 GAMMA	PP5
UNPHOSPHO-SHORT	**	*	*	*	**	*	****	***
PHOSPHO – SHORT	*	****	****	****	***	***	***	*
UNPHOSPHO-FULL LENGTH	***	**	***	**	**	**	***	****
PHOSPHO – FULL LENGTH	****	***	**	***	****	****	*	**

4.4 Discussion

Table 4.1 summarizes the effects of the different variants of G-substrate on the different phosphatases studied. The two variants of human G-substrate affected PP1 and PP2A in brain extracts to different extents. The phosphorylated short G-substrate isoform was the most effective at inhibiting both PP1 and PP2A from rat cerebella, while the phosphorylated full length protein inhibited both PP1 and PP2A from rat cerebra most effectively.

Where the activities of these phosphatases in whole brain extracts were studied, the phosphorylated full length G-substrate protein was most effective at inhibiting PP1, while the presence of the phosphorylated short G-substrate isoform produced the greatest reduction in activity of whole brain PP2A.

The phosphorylated forms of both isoforms of G-substrate protein affected the activities of PP1 and PP2A in the different brain regions to greater extents than their unphosphorylated forms, confirming observations by other researchers that G-

substrate becomes a potent inhibitor of protein phosphatases when phosphorylated (8,9). It is possible, however, that the phosphorylation of G-substrate is not necessary for the regulation of other phosphatases since experiments with PP5 showed the unphosphorylated full length G-substrate protein showing the greatest inhibition, followed by the unphosphorylated short isoform, with the phosphorylated short isoform especially showing very little effect on PP5 activity.

The observation that the different isoforms of G-substrate affect the activities of PP1 and PP2A in different areas of the brain to different extents suggests a specialization of the G-substrate variants for the regulation of PP1 and PP2A activities in different brain areas, with the phosphorylated full length protein regulating PP1 and PP2A more effectively in the cerebrum and the phosphorylated short G-substrate isoform regulating the same phosphatases more effective in the cerebellum.

It must be noted, however, that in assaying brain PP1 and PP2A, no discrimination is made between the different holoenzymes of PP1 and PP2A, which localize to different brain areas (see sections 1.1.5.1 and 1.1.5.2) and as a result, the observed effects of the G-substrate isoforms on the phosphatase activities of these preparations may be a combination of the effects of the G-substrate isoforms on the different PP1 and PP2A holoenzymes present in the brain.

Observations that both phosphorylated and unphosphorylated forms of the two G-substrate isoforms reduce cerebellar PP2A activity even at low concentrations suggest that PP2A regulation is an important function of G-substrate in the cerebellum, where it is most abundant. Such regulation of cerebellar PP2A, which is an important phospho-tau phosphatase, provides a possible link between G-substrate activity and Alzheimer’s disease via tau protein hyperphosphorylation.

Chapter 5: G-substrate Structure

Obtaining structural information is vital to the study of any protein as structure and function are inextricably linked such that the loss of structure often results in a loss of protein function, ultimately leading to the destruction of the protein by dedicated cellular processes. Structural information is also essential in drug design and might also assist in the development of inhibitors to protect against a proteins less desirable effects.

G-substrate has been linked to the protection of A9 dopaminergic neurons from Parkinson's disease toxins and information on its structure will assist in the identification of any other proteins it might interact with in performing this function, leading to a better understanding of the process and a possible remedy for the devastation of dopaminergic cells caused by Parkinson's disease.

Previous attempts by other members of the Aitken research group to solve the crystal structure of G-substrate were unsuccessful as extensive crystal screens set up did not yield any crystals from which the structure of the protein could be elucidated. The inability to obtain crystals of G-substrate led to the decision in this project to study G-substrate structure in solution.

5.1 Analytical Ultracentrifugation of G-substrate

To determine the conformation of G-substrate in solution, analytical ultracentrifugation was performed in conjunction with Dr Olwyn Byron of Glasgow University. Sedimentation velocity (SV) and sedimentation equilibrium (SE) experiments were employed to determine the size distribution and self-association characteristics of full length G-substrate protein. Results obtained indicate that the native state of G-substrate is a monomer (Figure 5.1). Since short G-substrate only differs from the full length protein by the loss of a 51 amino acid section, it can be inferred that short G-substrate also exists as a monomer.

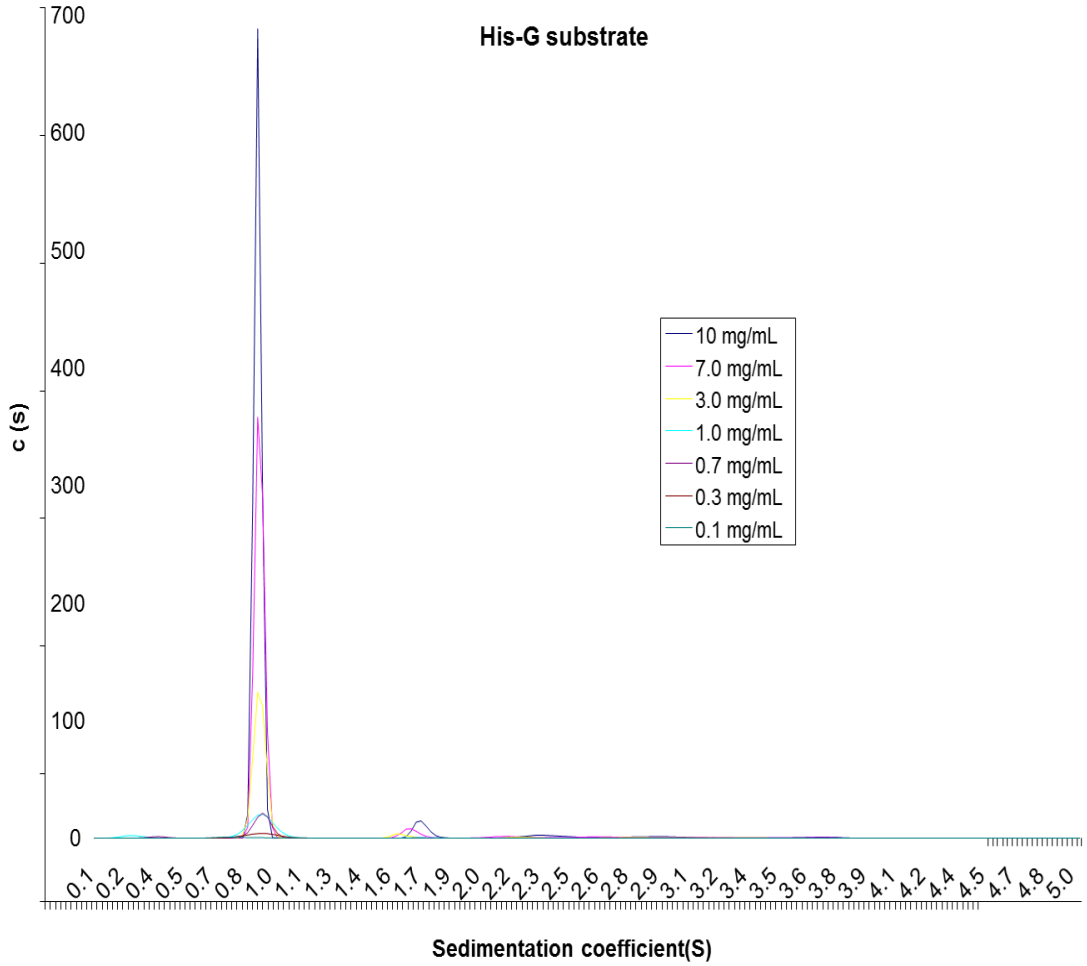

Figure 5.1: Sedimentation velocity analysis of G-substrate.
C (s) distributions were derived from SEDFIT using SV interference data collected over a range of sample concentrations.

5.2 In-silico Structure Prediction

5.2.1 Secondary structure

Online structural prediction software (www.predictprotein.org) was used to investigate the most likely structures of the G-substrate variants from their amino acid sequences. Results obtained indicate that both variants of G-substrate exist as largely unstructured proteins. A summary of the proportion of each secondary structure type possessed by each G-substrate variant is presented in Table 5.1 below.

Short G-substrate was predicted to be slightly more structured than the full length protein, possessing about 10 % less loop structure. For both variants, however, predictions for the recombinant protein suggested a structure less compact than that predicted for the native proteins. Figure5.2 shows a representation of the predicted secondary structures for the two variants and Figure 5.3 and Figure 5.4 present the predicted structures for the native and recombinant proteins for each variant side by side for comparison.

Table 5.1: Percent of secondary structure types present in G-substrate variants as predicted by online software at predictprotein.org

SECONDARY STRUCTURE	PERCENTAGE SECONDARY STRUCTURE PREDICTED			
	FULL LENGTH G-SUBSTRATE	RECOMBINANT FULL LENGTH G-SUBSTRATE	SHORT G-SUBSTRATE	RECOMBINANT SHORT G-SUBSTRATE
HELIX	12.90	8.95	21.15	10.42
STRAND	1.29	2.11	2.88	4.17
LOOP	85.81	88.94	75.96	85.42

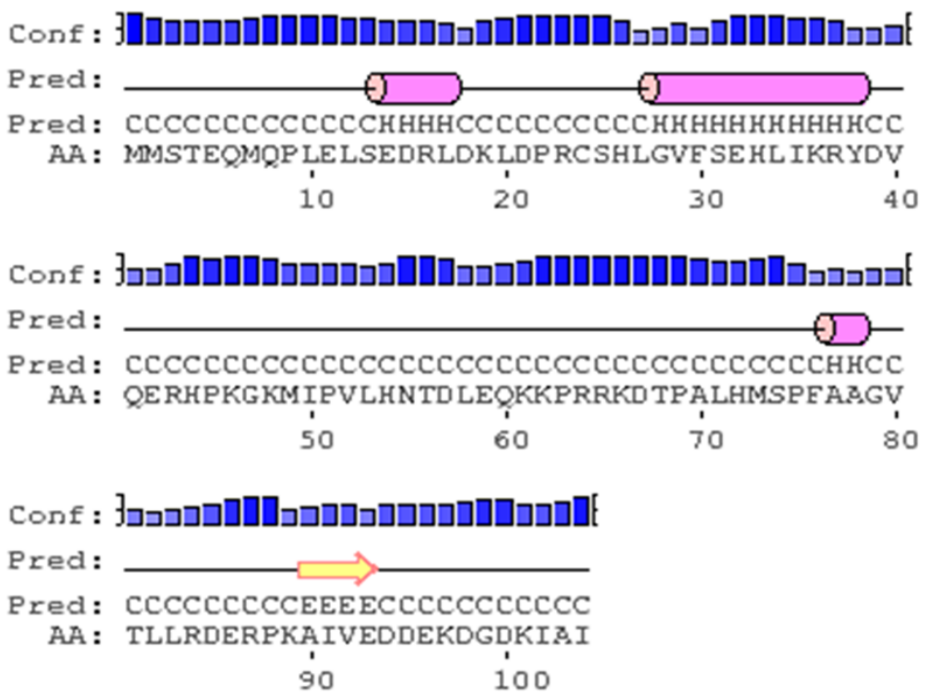

A. Short G-substrate

B. Full Length G-substrate

Figure5.2: Secondary Structure Prediction for G-substrate variants from the PSIPRED Protein Structure Prediction Server (http://bioinf.cs.ucl.ac.uk/psipred)

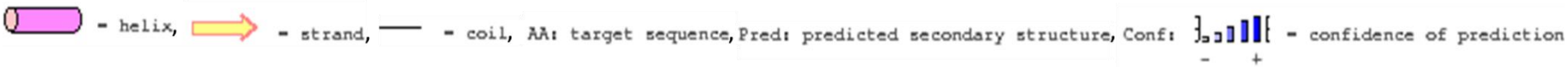

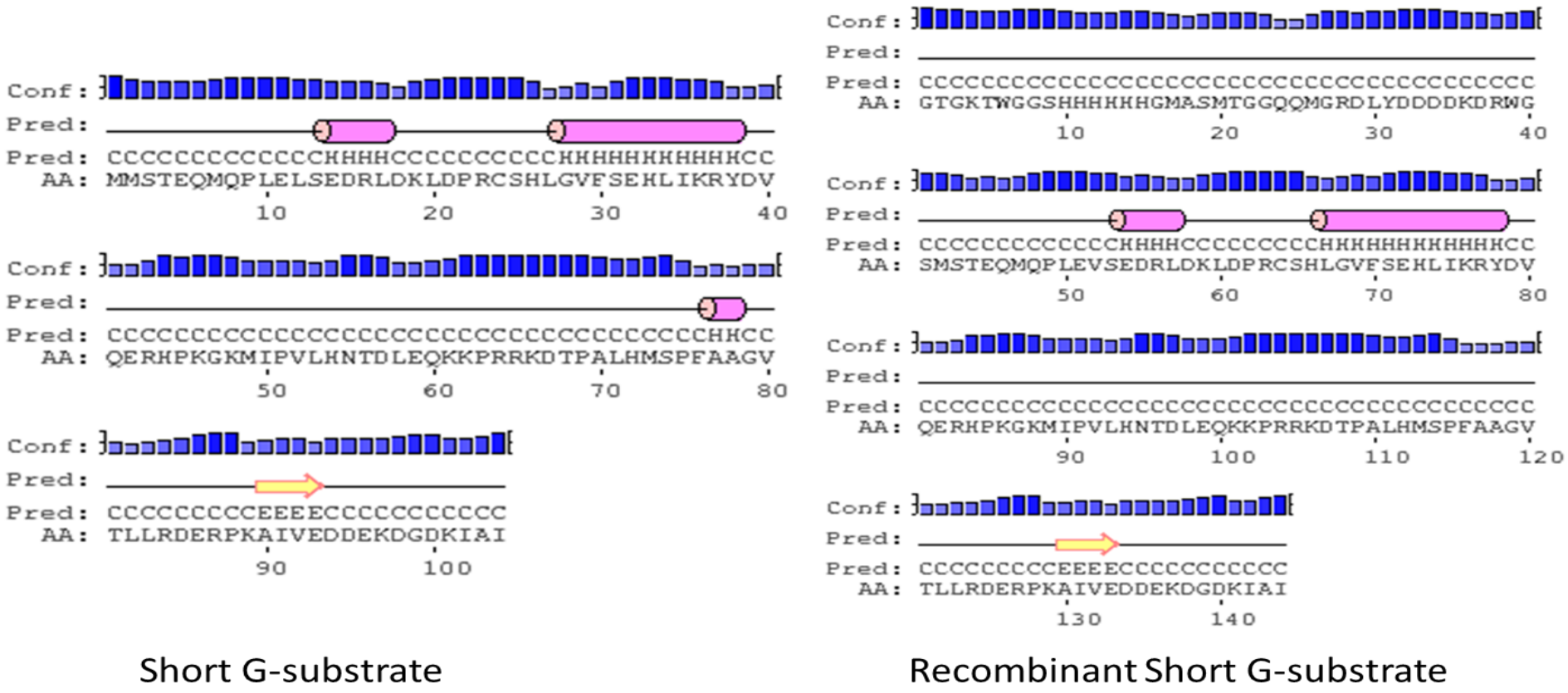

Figure 5.3: Secondary Structure Prediction for native and recombinant short G-substrate variants from the PSIPRED Protein Structure Prediction Server

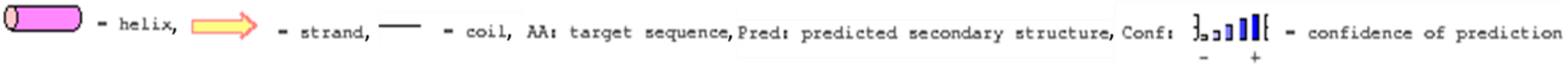

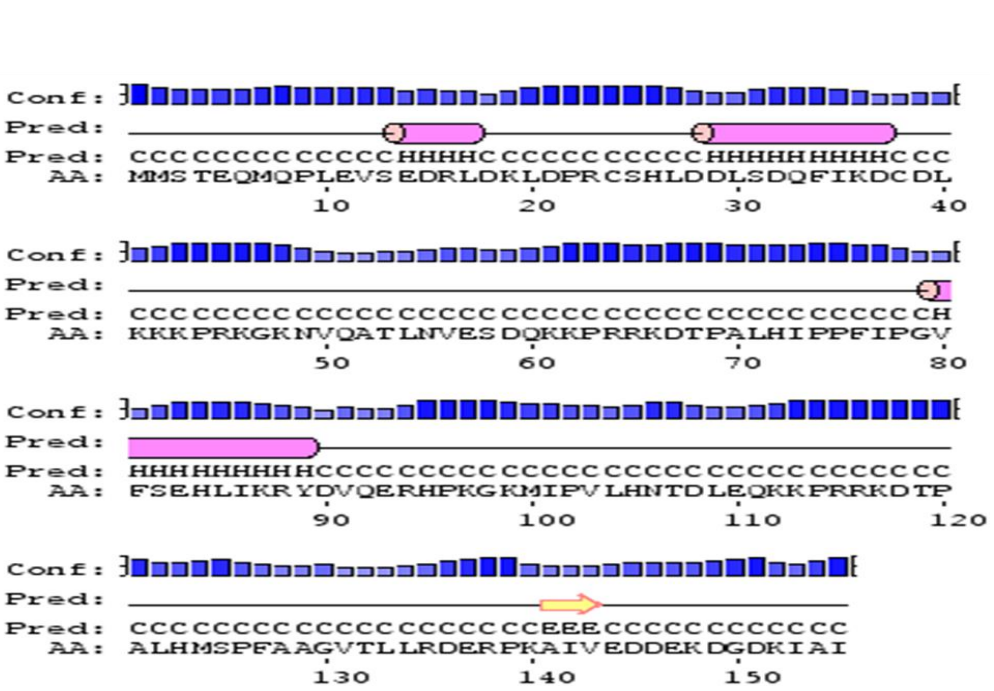

Full Length G-substrate

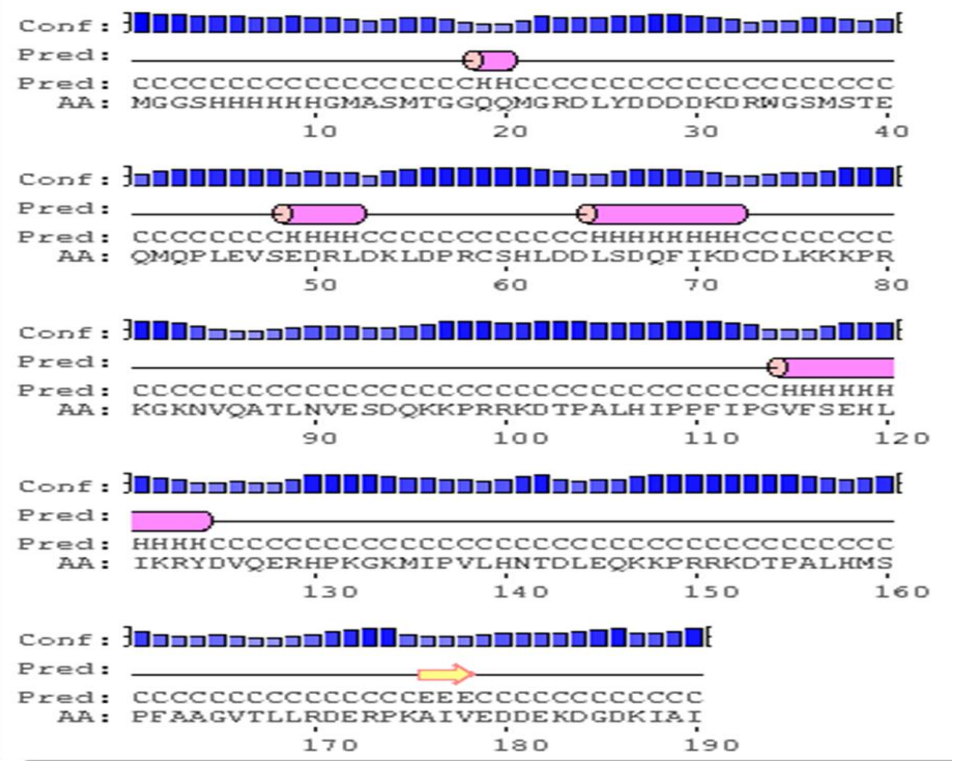

Recombinant Full Length G-substrate

Figure 5.4: Secondary Structure Prediction for native and recombinant full length G-substrate from the PSIPRED Protein Structure Prediction Server

5.2.2 Non-Regular Secondary Structure

NOn-Regular Secondary Structure predictor (NORSp) software available at www.predictprotein.org was used to investigate the presence of disordered regions in the G-substrate protein variants. The software predicted vast regions lacking regular secondary structure for the recombinant forms of both full length and short G-substrate. The prediction also showed the native full length protein to be entirely disorded from residue 33 to 155 but interestingly, despite possessing 104 amino acids completely identical to the full length protein, short G-substrate was predicted to possess no disordered regions at all by the NORS software. Another protein, DARPP-32, which also potently inhibits protein phosphatase 1 when phosphorylated on a threonine residue, was predicted to be entirely disordered by the same software. This large extent of disorder in the protein structure might explain our lack of success in obtaining crystals for G-substrate.

5.3 Circular Dichroism

Two dimensional structures of the G-substrate variants were further investigated by Circular Dichroism (CD) spectroscopy. Using the CDSSTR and CONTIN analysis methods full length G-substrate was found to exist in solution as 9.9 % helix, 16.6 % strand, 14.5 % turns and 59.0 % unordered structure (Figure 5.6), while short G-substrate was found to exist as 8.6 % helix, 17.3 % strand, 14.4 % turns and 59.6 % unordered structure(Figure 5.5). Phosphorylation was shown to significantly alter the structures of both isoforms of G-substrate. As shown in Figure 5.7, the phospho-forms of the proteins possessed considerably reduced levels of ellipticity, implying that upon phosphorylation, both G-substrate variants lose a substantial degree of secondary structure, becoming less compactly folded and more disordered.

Full length G-substrate is known to tolerate temperatures up to 90 °C and the extent to investigate whether short G-substrate is also able to withstand high temperatures cd spectra were acquired for both variants at 85°C followed by acquisition at 25°C. In both cases, the significant loss of secondary structure observed at 85°C was almost entirely recovered upon cooling to 25°C, indicating that short G-substrate is equally tolerant of high temperatures.

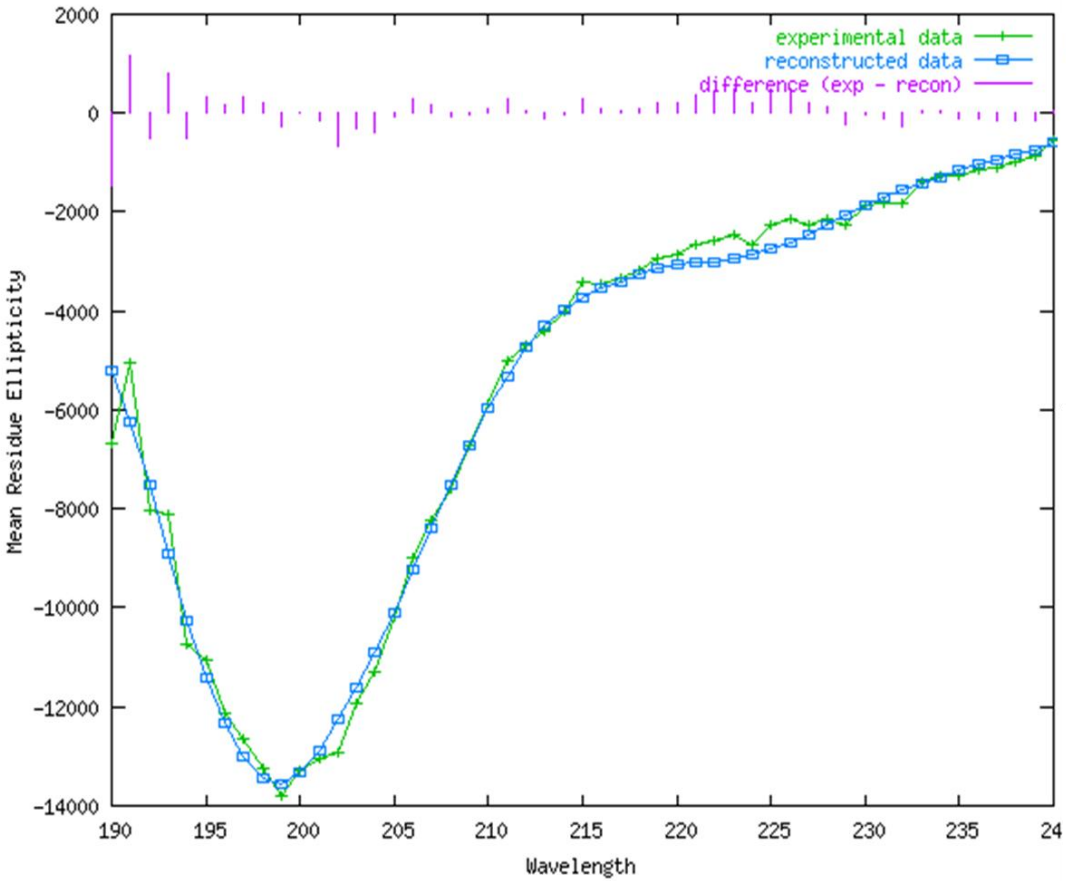

Provencher & Glockner Method: Reference set 7

NRMSD:0.055

Helix segments per 100 residues: 0.887

Strand segments per 100 residues: 3.163

Ave helix length per segment: 5.426

Ave strand length per segment: 5.262

Result	Helix1	Helix2	Strand1	Strand2	Turns	Unordered	Total
1	0.016	0.070	0.104	0.069	0.144	0.596	0.999

Figure 5.5: Representative Deconvolution for Short G-substrate

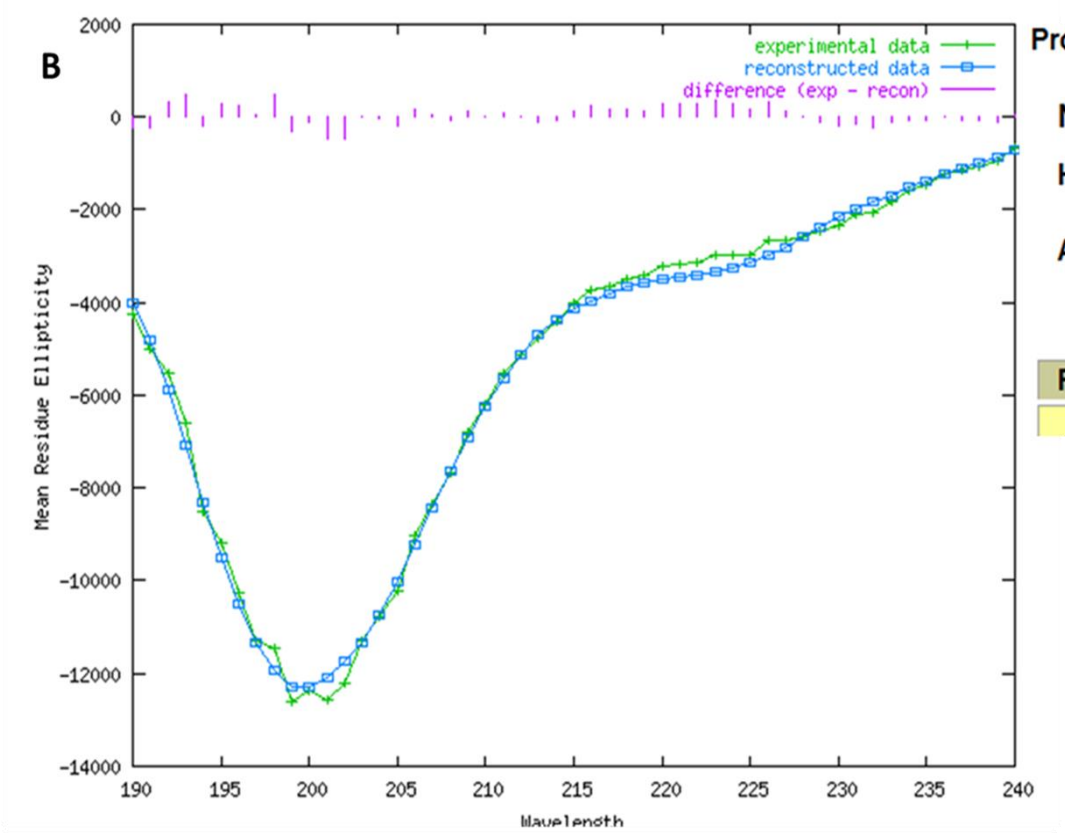

Provencher & Glockner Method: Reference set 7

NRMSD:0.033

Helix segments per 100 residues: 1.032

Strand segments per 100 residues: 3.205

Ave helix length per segment: 6.072

Ave strand length per segment: 5.299

Result	Helix1	Helix2	Strand1	Strand2	Turns	Unordered	Total
1	0.027	0.072	0.099	0.067	0.145	0.590	1

Figure 5.6: Representative Deconvolution for Full Length G-substrate

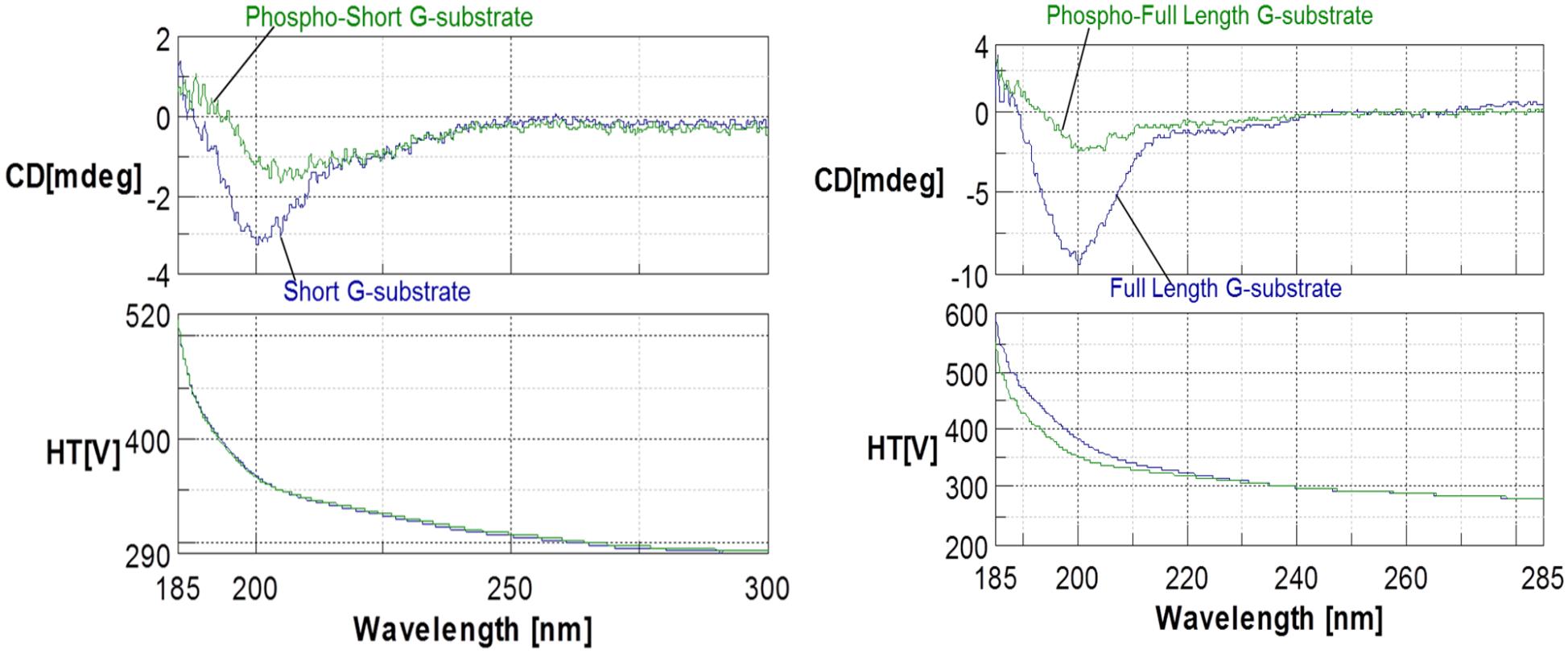

Figure 5.7: Overlays of CD spectra showing differences in ellipticity between unphosphorylated and phosphorylated G-substrate variants

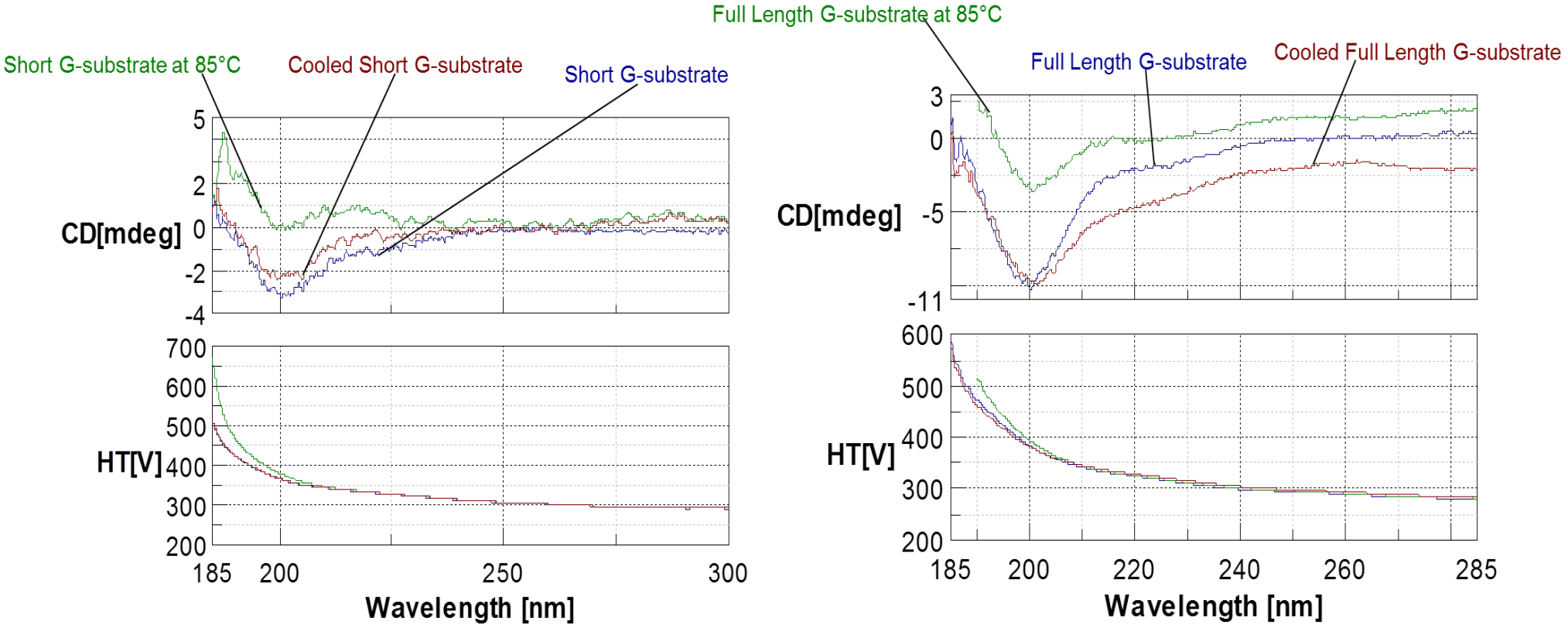

Figure 5.8: Overlays of CD spectra showing differences in ellipticity between G-substrate protein samples at different temperatures

5.4 Nuclear Magnetic Resonance Spectroscopy

Nuclear Magnetic Resonance (NMR) spectroscopy was employed to further investigate the structure of the G-substrate variants and possibly obtain a solution to their three dimensional structures. One dimensional proton spectra obtained for both variants were very similar (Figure 5.9), indicating that in solution, their structures were very much alike. As very little structural information can be obtained from 1D data due to its complexity, NOESY spectra, which map the correlations between protons in a molecule providing more useful structural information, were acquired to further investigate structure.

Data obtained from NOESY experiments showed the presence of very few cross peaks, representing protons which are very close together in the amino acid sequence and those brought close as a result of interactions due to tertiary structure. This suggests that in general, both variants of G-substrate possess very little structure. At the same intensity, full length G-substrate showed slightly more cross peaks than short G-substrate (Figure 5.10), suggesting that the structure of full length G-substrate in solution is slightly more compact than that of short G-substrate.

Comparison of NOESY spectra obtained from phosphorylated forms of the G-substrate variants with spectra from unphosphorylated samples (Figure 5.11) showed a difference in the population of cross peaks which indicated that upon phosphorylation, fewer interactions occurred between the nuclei, corresponding to a reduction in compact structure of the proteins upon phosphorylation.

Batches of the G-substrate variants labelled with the heavier Nitrogen-15 isotope were produced to make possible the assignment of specific amino acids to the peaks obtained from the NMR experiments. This assignment, which would ultimately lead to a solution structure for G-substrate, could not be pursued further due to unforeseen logistical issues.

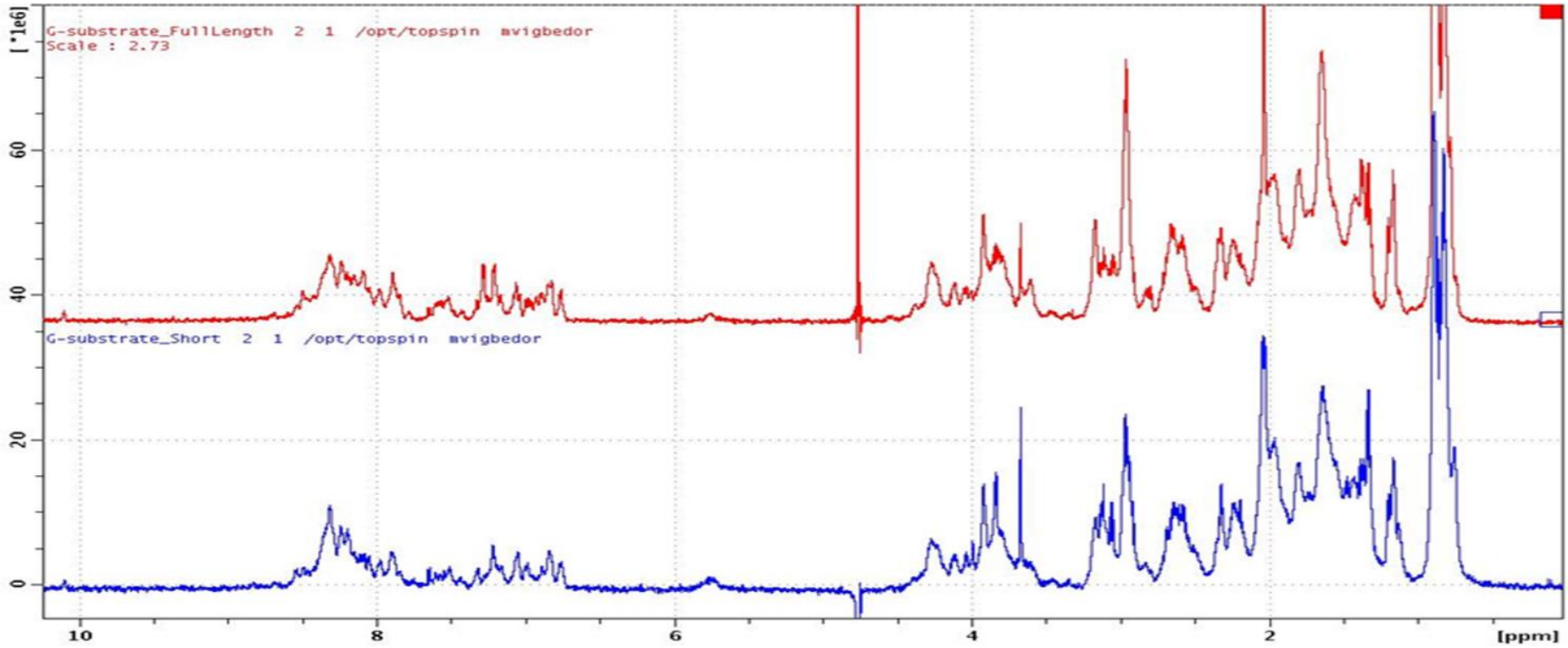

Figure 5.9: Overlay of 1D NMR spectra for full length (red) and short (blue) G-substrate

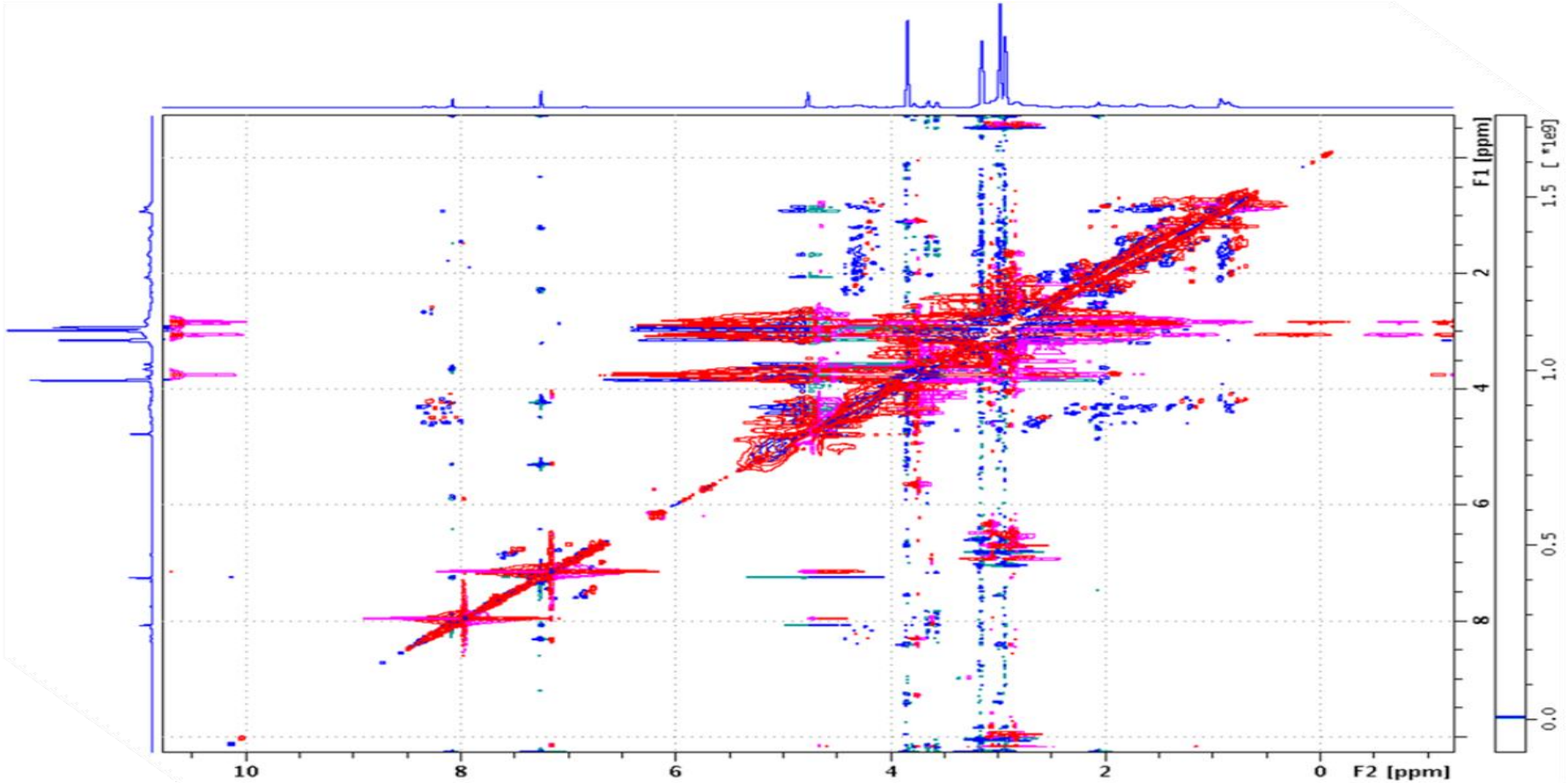

Figure 5.10: Overlay of NOESY contour plots for full length (blue) and short (red) G-substrate

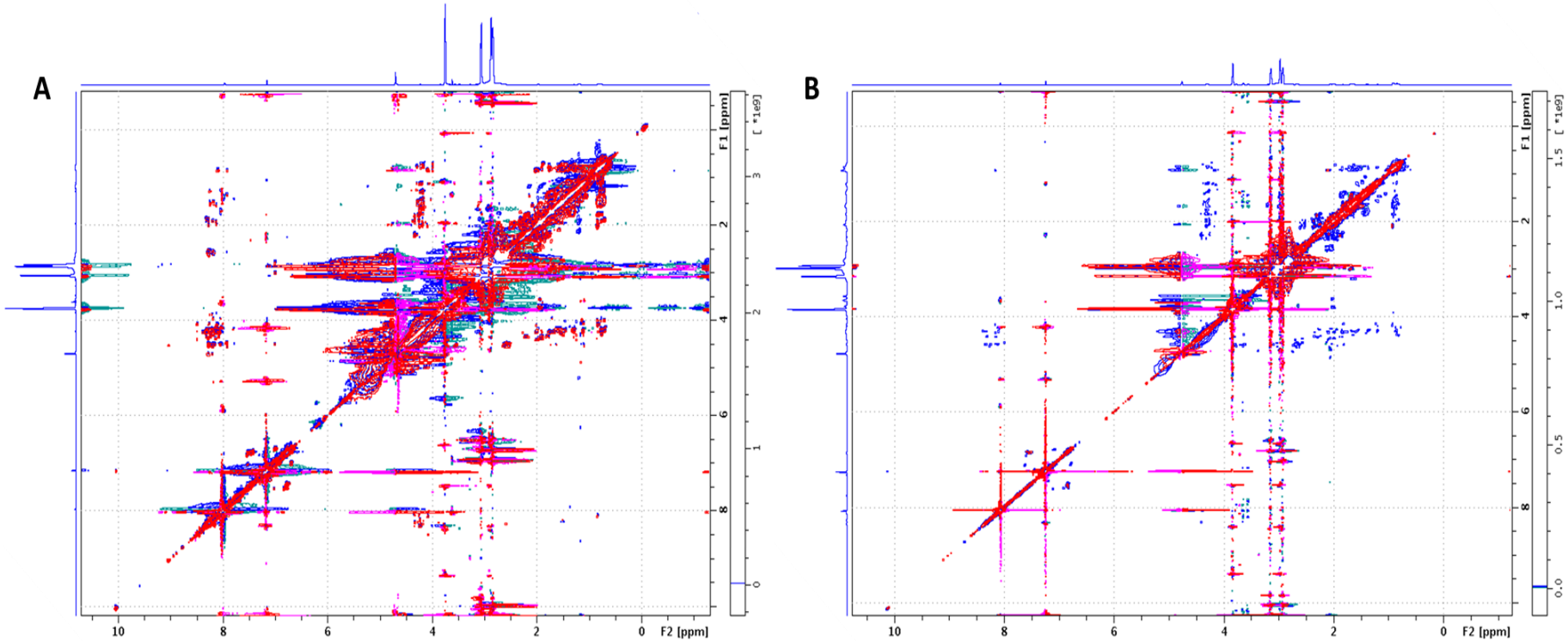

Figure 5.11: Overlays of NOESY contour plots for unphosphorylated (blue) and phosphorylated (red) samples of short (A) and full length (B) G-substrate

5.5 Discussion

Data obtained from CD and NMR agreed to a large extent with predictions (1) that both variants of G-substrate are largely unstructured, indicating that the prediction that short G-substrate possessed no non regular structure at all was erroneous, possibly brought about by the inability of the software to adequately predict interactions between the amino acids in solution, which may not be entirely obvious from the amino acid sequence alone. The portion of full length G-substrate missing from the short variant is proline rich, with 6 residues in a 51 amino acid section. This presented the possibility that the short G-substrate isoform would be more compactly folded than the full length protein due to the fact that the presence of proline disrupts secondary structure including α helixes and β sheets, leading mainly to the formation of loops and turns. Results however revealed that the full length protein was slightly more compact in structure than the short variant.

G-substrate is not dissimilar to other phosphatase inhibitors in terms of its existence as a predominantly disordered protein. Inhibitor 1 and DARPP-32 are both potent inhibitors of protein phosphatase 1 that, like G-substrate, require phosphorylation on a threonine residue for activation of their phosphatase inhibitory activities, and are both predominantly unstructured (77). The existence of some structural similarity among these proteins is highlighted in Figure 5.12, which shows an alignment of the amino acid residues surrounding the threonine residues important for phosphatase inhibitory activation in G-substrate, Inhibitor-1 and DARPP-32. The alignment also reveals that for all three proteins the phosphorylateable threonines are mainly surrounded by basic and small, hydrophobic amino acids.

The nuclear inhibitor of protein phosphatase 1, NIPP1, has also been shown to possess an intrinsically disordered PP1-binding domain (37). This evidence suggests that structural disorder may be vital to their function as protein phosphatase 1 inhibitors. The observation that G-substrate becomes even more disordered upon phosphorylation, a requirement for its phosphatase inhibition activity, is interesting and suggests an important role for structural disorder in the mechanism of protein phosphatase 1 inhibition.

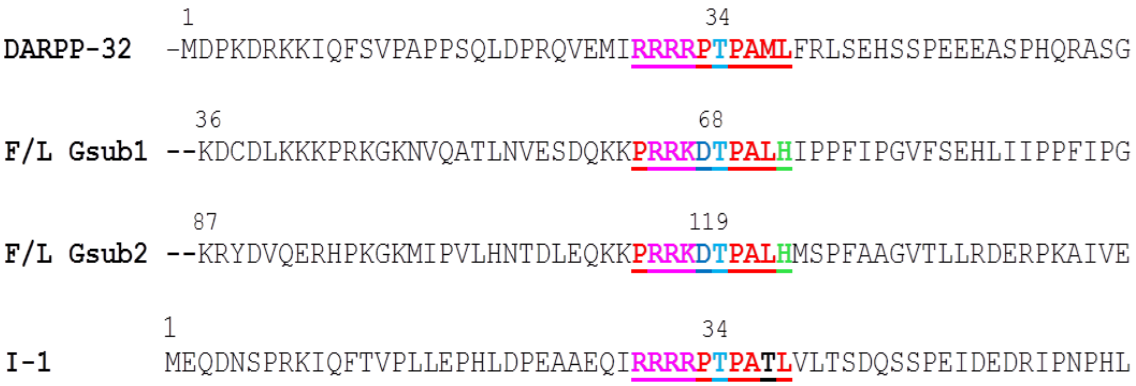

Figure 5.12: Alignment of partial amino acid sequences for DARPP-32, G-substrate and Inhibitor-1 (I-1).
The amino acid sequences surrounding the two phosphorylation sites in full length G-substrate are denoted F/L Gsub1 and F/L Gsub1. Threonine residues phosphorylated to activate PP1 inhibitory activity are coloured blue. Basic amino acids are magenta and small, hydrophobic amino acids in red.

The proteins discussed above and other inhibitors of PP1, although largely unstructured, have been found to fold upon binding to PP1. It would be interesting, therefore, to determine what conformation G-substrate assumes upon interaction with PP1 and PP2A. It would also be interesting to determine whether G-substrate gains any structure during the brief interaction with cGK that results in its phosphorylation *in vivo*. Since our results have shown that G-substrate becomes even more unstructured after phosphorylation, this would provide interesting insight into the extent of structural flexibility G-substrate possesses.

Chapter 6: G-substrate Interacting Proteins

The role of phosphorylated G-substrate as a potent inhibitor of protein phosphatases is well documented (9,21). It is however unclear exactly what mechanisms are employed in performing this function and what other roles G-substrate plays in addition to phosphatase inhibition. Protein pull-downs from rat brain were employed to investigate G-substrate interacting proteins and provide valuable clues for the detection of its associated proteins *in vivo*.

Pull-downs were performed according to the protocol described in 'Materials and methods' section 2.12. Figure 6.1shows the image of a typical gel obtained from rat brain pull down experiments.

In order to avoid chemical interaction of the rat brain proteins with excess reactive sites on the magnetic beads, BSA (in the case of tosylactivated beads) and ethanolamine (in the case of amine beads) were used to block excess active sites after beads were incubated with G-substrate and before incubation with rat brain extract.

Control experiments were performed by binding either BSA or ethanolamine to the relevant magnetic beads in the absence of G-substrate and carrying out the rat brain protein interaction steps identical to those employed for the G-substrate-bound beads (see section 2.12). Protein hits obtained for the G-substrate forms investigated were not reported if they were obtained for the control experiments as well.

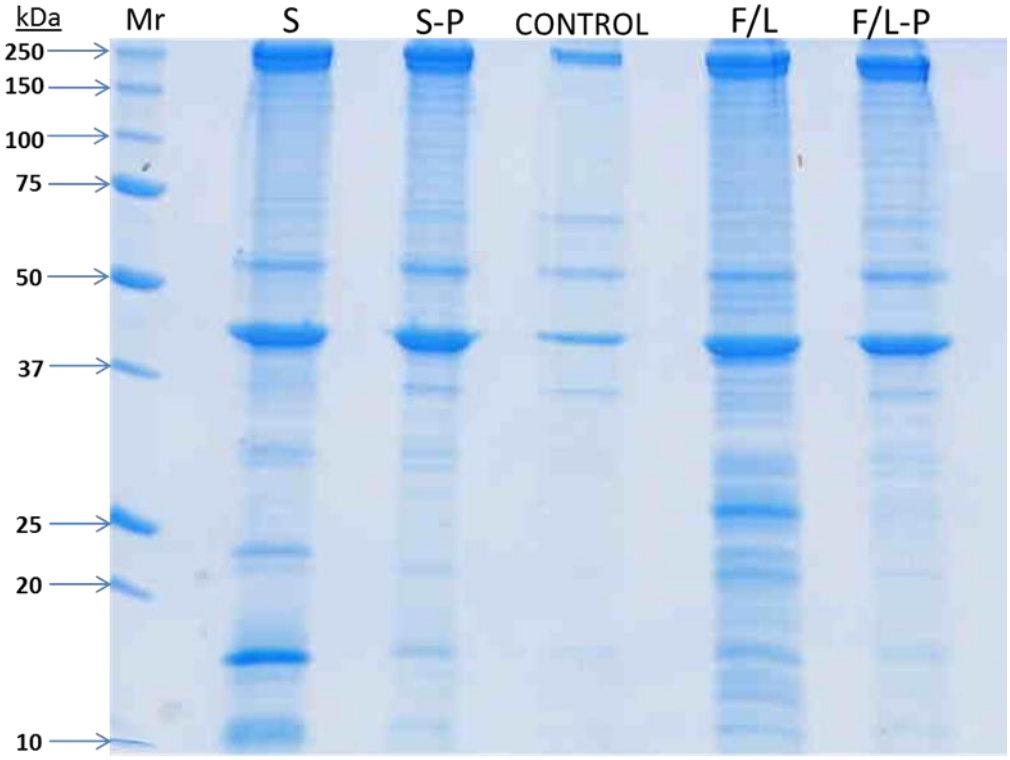

Figure 6.1: SDS-PAGE of proteins pulled down by the different forms of G-substrate protein; S=short, S-P=phospho-short, F/L=full length and P-F/L=phospho-full length.

Protein hits obtained with the Mascot software (www.matrixscience.com) from peptides obtained from MALDI-tof mass spectroscopy are reported in Table 6.1. Reported proteins had MOWSE scores classified as 'significant' with $p<0.05$, representing a less than 5 % chance that the observed match was a random event. The MOWSE score is a probability-based algorithm, which expresses the probability of protein matches being authentic as -10*log10 (absolute probability of the match) based on the peptide masses observed and the size of the identified protein.

Table 6.1: Rat brain proteins pulled down by different forms of G-substrate.

Molecular weight values shown under the different forms of G-substrate indicate the molecular weights at which the proteins were identified in the G-substrate pull down gels.

PROTEIN	UNIPROT ACCESSION	PHOSPHO PEPTIDE	FULL LENGTH G-SUBSTRATE	PHOSPHO - FULL LENGTH G-SUBSTRATE	SHORT G-SUBSTRATE	PHOSPHO - SHORT G-SUBSTRATE	COMMENTS (FUNCTION, SUBCELLULAR LOCATION, TISSUE-SPECIFIC EXPRESSION, ETC.)
CYTOSKELETAL/STRUCTURAL PROTEINS							
FORMIN-LIKE PROTEIN 2 (123.3kDa)	Q96PY5	-	**58kDa**	-	-	-	REGULATION OF CELL MORPHOLOGY AND CYTOSKELETAL ORGANIZATION. REQUIRED IN CORTICAL ACTIN FILAMENT DYNAMICS.
NEBULIN-RELATED ANCHORING PROTEIN ISOFORM C (195.8kDa)	Q80XB4	**175kDa**	**175kDa**	-	-	-	INVOLVED IN ANCHORING THE TERMINAL ACTIN FILAMENTS IN THE MYOFIBRIL TO THE MEMBRANE AND IN TRANSMITTING TENSION FROM THE MYOFIBRILS TO THE EXTRACELLULAR MATRIX NOT DETECTED IN BRAIN.
NUCLEAR MITOTIC APPARATUS PROTEIN 1 (238.2kDa)	Q14980	-	**25kDa**	-	-	-	MAY BE A STRUCTURAL COMPONENT OF THE NUCLEUS.
TITIN / CONNECTIN (3.816MDa)	Q8WZ42	-	**80kDa**	-	-	-	KEY COMPONENT IN THE ASSEMBLY AND FUNCTIONING OF VERTEBRATE STRIATED MUSCLES. PHOSPHORYLATED UPON DNA DAMAGE, PROBABLY BY ATM OR ATR.
MICROTUBULE-ASSOCIATED SER/THR PROTEIN KINASE 4 (284.3kDa)	O15021	**36kDa**	**36kDa**	-	-	-	PHOSPHORYLATED UPON DNA DAMAGE, PROBABLY BY ATM OR ATR.
DREBRIN/DEVELOPMENTALLY-REGULATED BRAIN PROTEIN (77.4kDa)	Q07266	-	**130kDa**	-	**130kDa**	-	BINDS F-ACTIN. DREBRINS MIGHT PLAY A ROLE IN CELL MIGRATION, EXTENSION OF NEURONAL PROCESSES AND PLASTICITY OF DENDRITES.

PROTEIN	UNIPROT ACCESSION	PHOSPHO PEPTIDE	FULL LENGTH G-SUBSTRATE	PHOSPHO - FULL LENGTH G-SUBSTRATE	SHORT G-SUBSTRATE	PHOSPHO - SHORT G-SUBSTRATE	COMMENTS (FUNCTION, SUBCELLULAR LOCATION, TISSUE-SPECIFIC EXPRESSION, ETC.)
NON-MUSCLE MYOSIN 9 AND NON-MUSCLE MYOSIN 10 (226.5kDa AND 229.0kDa)	P35579 P35580	-	**180kDa**	**180kDa**	-	**180kDa**	CELLULAR MYOSIN THAT APPEARS TO PLAY A ROLE IN CYTOKINESIS, CELL SHAPE, AND SPECIALIZED FUNCTIONS SUCH AS SECRETION AND CAPPING.
METAVINCULIN/VINCULIN (123.7kDa)	P18206	-	**46kDa**	-	-	-	ACTIN FILAMENT (F-ACTIN)-BINDING PROTEIN INVOLVED IN CELL-MATRIX ADHESION AND CELL-CELL ADHESION. MUSCLE SPECIFIC.
ACTIN-BINDING Z-DISK PROTEIN (NEBULETTE) (116.4kDa)	O76041	**7kDa**	-	-	-	-	BINDS TO ACTIN AND PLAYS AN IMPORTANT ROLE IN THE ASSEMBLY OF THE Z-DISK. ISOFORM 2 MIGHT PLAY A ROLE IN THE ASSEMBLY OF FOCAL ADHESION.
CONTACTIN-1 (113.3kDa)	Q12860	**100kDa**	**100kDa**	-	-	-	MEDIATES CELL SURFACE INTERACTIONS DURING NERVOUS SYSTEM DEVELOPMENT.
CYTOSPIN-A (124.6kDa)	Q69YQ0	**7kDa**	**18kDa**	-	-	-	INVOLVED IN CYTOKINESIS AND SPINDLE ORGANIZATION. MAY INTERACT WITH BOTH MICROTUBULES AND ACTIN CYTOSKELETON.
TROPOMYOSIN ALPHA-3 CHAIN (32.8kDa)	P06753	-	-	-	**33kDa**	-	BINDS TO ACTIN FILAMENTS IN MUSCLE AND NON-MUSCLE CELLS.
DYNAMIN-1 (97.4kDa)	Q05193	-	-	-	-	**88kDa**	MICROTUBULE-ASSOCIATED FORCE-PRODUCING PROTEIN INVOLVED IN PRODUCING MICROTUBULE BUNDLES AND ABLE TO BIND AND HYDROLYZE GTP.
PRELAMIN A/C (74.3kDa)	P48679	-	-	-	-	**180kDa**	LAMINS ARE COMPONENTS OF THE NUCLEAR LAMINA.
NON-MUSCLE (L) CALDESMON (60.5kDa)	Q62736	-	-	**120kDa**	-	-	ACTIN- AND MYOSIN-BINDING PROTEIN IMPLICATED IN THE REGULATION OF ACTOMYOSIN INTERACTIONS IN SMOOTH MUSCLE AND NONMUSCLE CELLS INVOLVED IN SCHWANN CELL MIGRATION DURING PERIPHERAL NERVE REGENERATION.
SARCOLEMMAL MEMBRANE-ASSOCIATED PROTEIN (96.9kDa)	Q3URD3	-	**17kDa**	-	-	-	EXPRESSED IN PROLIFERATING MYOBLASTS AND DIFFERENTIATED MYOTUBES. EXPRESSED IN MYOBLASTS, CARDIAC AND SKELETAL MUSCLES.HOMODIMER WHICH INTERACTS WITH MYOSIN.
FILAMIN-A-INTERACTING PROTEIN 1 (137.7kDa)	Q8K4T4	-	-	-	-	**29kDa**	BY ACTING THROUGH A FILAMIN-A/F-ACTIN AXIS, CONTROLS THE START OF NEOCORTICAL CELL MIGRATION FROM THE VENTRICULAR ZONE. MAY BE ABLE TO INDUCE DEGRADATION OF FILAMIN A. EXPRESSED IN MUSCLE.

PROTEIN	UNIPROT ACCESSION	PHOSPHO PEPTIDE	FULL LENGTH G-SUBSTRATE	PHOSPHO - FULL LENGTH G-SUBSTRATE	SHORT G-SUBSTRATE	PHOSPHO - SHORT G-SUBSTRATE	COMMENTS (FUNCTION, SUBCELLULAR LOCATION, TISSUE-SPECIFIC EXPRESSION, ETC.)
CELL CYCLE PROTEINS							
CENTROSOMAL PROTEIN OF 112 kDa (112.7kDa)	Q8N8E3	**30kDa**	-	-	-	-	-
PUTATIVE UNCHARACTERISED PROTEIN Haus6 (61.7kDa)	Q8CB73	**15kDa**	-	-	-	-	CONTRIBUTES TO MITOTIC SPINDLE ASSEMBLY, MAINTENANCE OF CENTROSOME INTEGRITY AND COMPLETION OF CYTOKINESIS AS PART OF THE HAUS AUGMIN-LIKE COMPLEX.
SYNAPTONEMAL COMPLEX PROTEIN 1 (114.2kDa)	Q15431	**65kDa**	**62kDa**	-	-	-	MAJOR COMPONENT OF TRANSVERSE FILAMENTS OF SYNAPTONEMAL COMPLEXES, FORMED BETWEEN HOMOLOGOUS CHROMOSOMES DURING MEIOTIC PROPHASE.
HEAT SHOCK PROTEIN HSP 90-BETA (83.3kDa)	P08238	-	**100kDa**	-	-	-	MOLECULAR CHAPERONE THAT PROMOTES THE MATURATION, STRUCTURAL MAINTENANCE AND PROPER REGULATION OF SPECIFIC TARGET PROTEINS INVOLVED FOR INSTANCE IN CELL CYCLE CONTROL AND SIGNAL TRANSDUCTION.
METABOLIC ENZYMES							
ACYL-CoA DEHYDROGENASE FAMILY MEMBER 10 (118.8kDa)	Q6JQN1	-	**109kDa**	-	-	-	ACYL-COA DEHYDROGENASE ONLY ACTIVE WITH R- AND S-2-METHYL-C15-COA.
GLYCERALDEHYDE-3-PHOSPHATE DEHYDROGENASE (36.1kDa)	P04406	-	**44kDa**	-	-	-	HAS BOTH GLYCERALDEHYDE-3-PHOSPHATE DEHYDROGENASE AND NITROSYLASE ACTIVITIES, THEREBY PLAYING A ROLE IN GLYCOLYSIS AND NUCLEAR FUNCTIONS, RESPECTIVELY.
PYRUVATE DEHYDROGENASE E1 COMPONENT SUBUNIT BETA (38.9kDa)	P49432	-	**39kDa**	-	-	-	THE PYRUVATE DEHYDROGENASE COMPLEX CATALYZES THE OVERALL CONVERSION OF PYRUVATE TO ACETYL-COA AND CO2.
ALDEHYDE DEHYDROGENASE FAMILY 1 MEMBER L1 (98.8kDa)	O75891	-	**39.6kDa**	-	-	-	IDENTIFIED AS AN UNDEREXPRESSED BIOMARKER OF TUMOUR AGGRESSIVENESS IN ASTROCYTIC TUMOURS.

PROTEIN	UNIPROT ACCESSION	PHOSPHO PEPTIDE	FULL LENGTH G-SUBSTRATE	PHOSPHO - FULL LENGTH G-SUBSTRATE	SHORT G-SUBSTRATE	PHOSPHO - SHORT G-SUBSTRATE	COMMENTS (FUNCTION, SUBCELLULAR LOCATION, TISSUE-SPECIFIC EXPRESSION, ETC.)
2-METHOXY-6-POLYPRENYL-1,4-BENZOQUINOL METHYLASE (37.3kDa)	Q4G064	-	**200kDa**	-	-	-	INVOLVED IN COFACTOR BIOSYNTHESIS; UBIQUINONE BIOSYNTHESIS.
TRANSCRIPTIONAL/TRANSLATIONAL PROTEINS							
FAR UPSTREAM ELEMENT-BINDING PROTEIN 2 (73.1kDa)	Q92945	-	**75kDa**	-	-	-	PART OF A COMPLEX INVOLVED IN PRE-mRNA DOWNSTREAM CONTROL SEQUENCE (DCS).
POLY [ADP-RIBOSE] POLYMERASE 14 (202.8kDa)	Q460N5	-	**58kDa**	-	-	-	ENHANCES STAT6-DEPENDENT TRANSCRIPTION.
ZINC FINGER PROTEIN 445 (118.9kDa)	P59923	-	**23kDa**	-	-	-	MAY BE INVOLVED IN TRANSCRIPTIONAL REGULATION.
PIF1 DNA HELICASE ISOFORM BETA (69.8kDa)	Q9H611	-	**42kDa**	-	-	-	DNA-DEPENDENT ATPASE AND DNA HELICASE INHIBITING TELOMERASE ACTIVITY BY UNWINDING DNA/RNA DUPLEX FORMED BY TELOMERASE RNA AND TELOMERIC DNA IN A 5' TO 3' POLARITY.
DNA REPAIR PROTEIN SWI5 HOMOLOGUE (10.3kDa)	Q63ZV7	-	-	-	-	**125kDa**	COMPONENT OF THE SWI5-SFR1 COMPLEX, A COMPLEX REQUIRED FOR DOUBLE-STRAND BREAK REPAIR VIA HOMOLOGOUS RECOMBINATION.
EUKARYOTIC TRANSLATION INITIATION FACTOR 4 GAMMA (175.4kDa)	Q04637	**30kDa**	-	-	-	-	PROBABLE COMPONENT OF PROTEIN COMPLEX EIF4F, INVOLVED IN RECOGNITION OF mRNA CAP, ATP-DEPENDENT UNWINDING OF 5'-TERMINAL SECONDARY STRUCTURE AND mRNA RECRUITMENT TO RIBOSOME. THOUGHT TO BE A FUNCTIONAL HOMOLOGUE OF EIF4G1.
THIOREDOXIN DOMAIN-CONTAINING PROTEIN 8 (14.5kDa)	Q69AB2	-	**25kDa**	-	-	-	MAY BE REQUIRED FOR POST-TRANSLATIONAL MODIFICATION OF PROTEINS REQUIRED FOR ACROSOMAL BIOGENESIS.
NUCLEOLAR RNA HELICASE 2 (85.9kDa)	Q3B8Q1	-	**200kDa**	**200kDa**	-	-	CAN UNWIND DOUBLE-STRANDED RNA (HELICASE) AND CAN FOLD OR INTRODUCE A SECONDARY STRUCTURE TO A SINGLE-STRANDED RNA (FOLDASE). FUNCTIONS AS COFACTOR FOR JUN-ACTIVATED TRANSCRIPTION

PROTEIN	UNIPROT ACCESSION	PHOSPHO PEPTIDE	FULL LENGTH G-SUBSTRATE	PHOSPHO - FULL LENGTH G-SUBSTRATE	SHORT G-SUBSTRATE	PHOSPHO - SHORT G-SUBSTRATE	COMMENTS (FUNCTION, SUBCELLULAR LOCATION, TISSUE-SPECIFIC EXPRESSION, ETC.)
ZINC FINGER CCCH DOMAIN-CONTAINING PROTEIN 13 (196.6kDa)	Q5T200	**20kDa**	-	-	-	-	PHOSPHORYLATED UPON DNA DAMAGE, PROBABLY BY ATM OR ATR.
60S RIBOSOMAL PROTEIN L15 (24.1kDa)	P61314	-	**24kDa**	-	-	-	-
HETEROGENEOUS NUCLEAR RIBONUCLEOPROTEIN Q (59.7kDa)	Q7TP47	-	-	-	-	**63kDa**	HETEROGENOUS NUCLEAR RIBONUCLEOPROTEIN (HNRNP) IMPLICATED IN mRNA PROCESSING MECHANISMS.
HISTONE H1OO(OOCYTE-SPECIFIC HISTONE H1) (35.8kDa)	Q8IZA3	**52kDa**	-	-	-	-	MAY PLAY A KEY ROLE IN THE CONTROL OF GENE EXPRESSION DURING OOGENESIS AND EARLY EMBRYOGENESIS, PRESUMABLY THROUGH THE PERTURBATION OF CHROMATIN STRUCTURE.
HUNTINGTIN-INTERACTING PROTEIN 1(HIP-1) (116.2kDa)	O00291	-	**46kDa**	-	-	-	INVOLVED IN REGULATING AMPA RECEPTOR TRAFFICKING IN THE CENTRAL NERVOUS SYSTEM IN AN NMDA-DEPENDENT MANNER. ENHANCES ANDROGEN RECEPTOR (AR)-MEDIATED TRANSCRIPTION.
NUCLEOSOME ASSEMBLY PROTEIN 1-LIKE 1 (45.4kDa)	P55209	**50kDa**	-	-	-	-	MAY BE INVOLVED IN MODULATING CHROMATIN FORMATION AND CONTRIBUTE TO REGULATION OF CELL PROLIFERATION.
ENDOCYTOSIS/VESICLE – RELATED PROTEINS							
VESICLE-FUSING ATPase (82.7kDa)	Q9QUL6	-	-	**150kDa**	-	-	REQUIRED FOR VESICLE-MEDIATED TRANSPORT. CATALYZES THE FUSION OF TRANSPORT VESICLES WITHIN THE GOLGI CISTERNAE.
CYTOPLASMIC DYNEIN I HEAVY CHAIN (532.4kDa)	Q14204	-	**80kDa**	-	-	-	ACTS AS A MOTOR FOR THE INTRACELLULAR RETROGRADE MOTILITY OF VESICLES AND ORGANELLES ALONG MICROTUBULES. DEFECTS IN DYNC1H1 ARE THE CAUSE OF SPINAL MUSCULAR ATROPHY, LOWER EXTREMITY, AUTOSOMAL DOMINANT (SMALED) AND CHARCOT-MARIE-TOOTH DISEASE TYPE 2O (CMT2O).
CYTOPLASMIC DYNEIN 2 HEAVY CHAIN (492.6kDa)	Q8NCM8	-	**58kDa**	-	-	-	MOTOR FOR INTRAFLAGELLAR RETROGRADE TRANSPORT. DEFECTS IN DYNC2H1 ARE THE CAUSE OF ASPHYXIATING THORACIC DYSTROPHY TYPE 3 (ATD3) AND SHORT RIB-POLYDACTYLY SYNDROME TYPE 3 (SRPS3).

PROTEIN	UNIPROT ACCESSION	PHOSPHO PEPTIDE	FULL LENGTH G-SUBSTRATE	PHOSPHO - FULL LENGTH G-SUBSTRATE	SHORT G-SUBSTRATE	PHOSPHO - SHORT G-SUBSTRATE	COMMENTS (FUNCTION, SUBCELLULAR LOCATION, TISSUE-SPECIFIC EXPRESSION, ETC.)
SYNTAXIN-BINDING PROTEIN 1 (67.5kDa)	O08599	-	-	-	**68kDa**	-	REGULATION OF SYNAPTIC VESICLE DOCKING AND FUSION, POSSIBLY THROUGH INTERACTION WITH GTP-BINDING PROTEINS. ESSENTIAL FOR NEUROTRANSMISSION AND BINDS SYNTAXIN, A COMPONENT OF THE SYNAPTIC VESICLE FUSION MACHINERY.
KINESIN-LIKE PROTEIN KIF1C (122.9kDa)	O43896	-	**25kDa**	-	-	-	MOTOR REQUIRED FOR THE RETROGRADE TRANSPORT OF GOLGI VESICLES TO THE ENDOPLASMIC RETICULUM. HAS A MICROTUBULE PLUS END-DIRECTED MOTILITY.
BREFELDIN A-INHIBITED GUANINE NUCLEOTIDE-EXCHANGE PROTEIN 2 (202.0kDa)	Q9Y6D5	-	**46kDa**	-	-	-	PROMOTES GUANINE-NUCLEOTIDE EXCHANGE ON ARF1, ARF5 AND ARF6. PROMOTES THE ACTIVATION OF ARF1/ARF5/ARF6 THROUGH REPLACEMENT OF GDP WITH GTP. DEFECTS IN ARFGEF2 ARE THE CAUSE OF AUTOSOMAL RECESSIVE PERIVENTRICULAR NODULAR HETEROTOPIA TYPE 2 (PVNH2).
GTP RELATED PROTEINS							
G-PROTEIN-REGULATED INDUCER OF NEURITE OUTGROWTH 1 (GRIN_1) (102.3kDa)	Q7Z2K8	**7kDa**	**42kDa**	-	-	-	MAY BE INVOLVED IN NEURITE OUTGROWTH. WIDELY EXPRESSED IN THE CENTRAL NERVOUS SYSTEM, WITH HIGHEST LEVELS IN SPINAL CORD.
FYVE, RhoGEF and PH DOMAIN-CONTAINING PROTEIN 2 (74.9kDa)	Q7Z6J4	-	**28kDa**	-	-	-	ACTIVATES CDC42, A MEMBER OF THE RAS-LIKE FAMILY OF RHO- AND RAC PROTEINS, BY EXCHANGING BOUND GDP FOR FREE GTP. PLAYS A ROLE IN REGULATING THE ACTIN CYTOSKELETON AND CELL SHAPE.
GRIP1-ASSOCIATED PROTEIN 1 (96.1kDa)	Q9JHZ4	-	-	**170kDa**	-	-	INTERACTS WITH GRIP1, GRIP2 AND AMPA RECEPTORS. PROTEOLYTICALLY CLEAVED BY CASPASE-3.
RAB GTPASE-BINDING EFFECTOR PROTEIN 1 (99.4kDa)	O35550	-	**25kDa**	-	-	-	RAB EFFECTOR PROTEIN ACTING AS LINKER BETWEEN GAMMA-ADAPTIN, RAB4A AND RAB5A. PROTEOLYTIC CLEAVAGE BY CASPASES IN APOPTOTIC CELLS CAUSES LOSS OF ENDOSOME FUSION ACTIVITY.

PROTEIN	UNIPROT ACCESSION	PHOSPHO PEPTIDE	FULL LENGTH G-SUBSTRATE	PHOSPHO - FULL LENGTH G-SUBSTRATE	SHORT G-SUBSTRATE	PHOSPHO - SHORT G-SUBSTRATE	COMMENTS (FUNCTION, SUBCELLULAR LOCATION, TISSUE-SPECIFIC EXPRESSION, ETC.)
KINASES/PHOSPHATASES AND RELATED PROTEINS							
DUAL SPECIFICITY SERINE/THREONINE AND TYROSINE PROTEIN KINASE (105.2kDa)	Q6XUX3	**28kDa**	-	-	-	-	MAY INDUCE BOTH CASPASE-DEPENDENT APOPTOSIS AND CASPASE-INDEPENDENT CELL DEATH. DETECTED IN SEVERAL TUMOUR CELL LINES.
PROTEIN KINASE C EPSILON TYPE (83.5kDa)	P09216	-	-	**100kDa**	-	-	REGULATION OF MULTIPLE CELLULAR PROCESSES LINKED TO CYTOSKELETAL PROTEINS. NEURON GROWTH AND ION CHANNEL REGULATION. INVOLVED IN IMMUNE RESPONSE, CANCER CELL INVASION REGULATION OF APOPTOSIS AND WOUND HEALING.
ACYLPHOSPHATASE 2 (11kDa)	P00820	-	-	-	-	**98kDa**	PHYSIOLOGICAL ROLE NOT YET CLEAR.
PROTEIN CIP2A (102.2kDa)	Q8TCG1	**17kDa**	-	-	-	-	ONCOPROTEIN THAT INHIBITS PP2A AND STABILIZES MYC IN HUMAN MALIGNANCIES. PROMOTES ANCHORAGE-INDEPENDENT CELL GROWTH AND TUMOUR FORMATION.
MITOGEN ACTIVATED PROTEIN KINASE KINASE KINASE 3 (70.9kDa)	Q99759	-	**80kDa**	-	-	-	MEDIATES ACTIVATION OF THE NF-KAPPA-B, AP1 AND DDIT3 TRANSCRIPTIONAL REGULATORS. (ACTIVATED BY PHOSPHORYLATION ON THR-530).
UBIQUITIN RELATED PROTEINS							
UBIQUITIN CARBOXYL-TERMINAL HYDROLASE 25 (122.2kDa)	Q9UHP3	-	**28kDa**	-	-	-	FUNCTIONS TO PROCESS NEWLY SYNTHESIZED UBIQUITIN, TO RECYCLE UBIQUITIN MOLECULES OR TO EDIT POLYUBIQUITIN CHAINS AND PREVENTS PROTEASOMAL DEGRADATION OF SUBSTRATES.
E3 SUMO-PROTEIN LIGASE RanBP2 (358.2kDa)	P49792	-	**25kDa**	-	-	-	E3 SUMO-PROTEIN LIGASE WHICH FACILITATES SUMO1 AND SUMO2 CONJUGATION BY UBE2I. SPECIFIC DOCKING SITE FOR THE NUCLEAR EXPORT FACTOR EXPORTIN-1. INTERACTS WITH PARK2

PROTEIN	UNIPROT ACCESSION	PHOSPHO PEPTIDE	FULL LENGTH G-SUBSTRATE	PHOSPHO - FULL LENGTH G-SUBSTRATE	SHORT G-SUBSTRATE	PHOSPHO - SHORT G-SUBSTRATE	COMMENTS (FUNCTION, SUBCELLULAR LOCATION, TISSUE-SPECIFIC EXPRESSION, ETC.)
ION TRANSPORT AND SIGNALLING PROTEINS							
INOSITOL-1,4,5 TRIPHOSPHATE RECEPTOR, TYPE 1 (308.6kDa)	G5E9P1	-	**80kDa**	-	-	-	INTRACELLULAR CHANNEL THAT MEDIATES CALCIUM RELEASE FROM THE ENDOPLASMIC RETICULUM FOLLOWING STIMULATION BY INOSITOL 1,4,5-TRISPHOSPHATE. DEFECTS CAUSE SPINOCEREBELLAR ATAXIA 15.
BARDET-BIEDL SYNDROME 15 PROTEIN (85.1kDa)	O95876	-	**40kDa**	-	-	-	PROBABLE EFFECTOR OF THE PLANAR CELL POLARITY SIGNALLING PATHWAY WHICH REGULATES THE SEPTIN CYTOSKELETON IN BOTH CILIOGENESIS AND COLLECTIVE CELL MOVEMENTS DEFECTS IN THIS PROTEIN ARE THE CAUSE OF BARDET-BIEDL SYNDROME TYPE 15 (BBS15).
EPHRIN TYPE-A RECEPTOR 7 (112kDa)	P54759	-	**36kDa**	-	-	-	RECEPTOR TYROSINE KINASE WHICH BINDS PROMISCUOUSLY GPI-ANCHORED EPHRIN-A FAMILY LIGANDS RESIDING ON ADJACENT CELLS, LEADING TO CONTACT-DEPENDENT BIDIRECTIONAL SIGNALLING INTO NEIGHBOURING CELLS.
MISCELLANEOUS PROTEINS							
COILED-COIL DOMAIN CONTAINING PROTEIN 66 (109.4kDA)	A2RUB6	**17kDa**	-	-	-	-	-
TRANSGELIN-3 (NEURONAL PROTEIN 22) (22.5kDa)	P37805	-	-	-	-	**22.5kDa**	MEMBER OF THE CALPONIN PROTEIN FAMILY. INVOLVED IN THE REGULATION OF NEURITE GROWTH. INTERACTS WITH F-ACTIN.
LINE-1 TYPE TRANSPOSASE DOMAIN-CONTAINING PROTEIN 1 (88.2kDa)	Q587J6	**48kDa**	-	-	-	-	-
FGFR1 ONCOGENE PARTNER 2 HOMOLOGUE (29.4kDa)	Q6TA25	-	-	-	-	**240kDa**	MAY BE INVOLVED IN WOUND HEALING PATHWAY UNDERLYING THE FAVOURABLE EARLY WOUND CLOSURE CHARACTERISTICS OF ORAL MUCOSA.

PROTEIN	UNIPROT ACCESSION	PHOSPHO PEPTIDE	FULL LENGTH G-SUBSTRATE	PHOSPHO - FULL LENGTH G-SUBSTRATE	SHORT G-SUBSTRATE	PHOSPHO - SHORT G-SUBSTRATE	COMMENTS (FUNCTION, SUBCELLULAR LOCATION, TISSUE-SPECIFIC EXPRESSION, ETC.)
PARK7/PROTEIN DJ-1 (19.9kDa)	Q99497	-	-	-	**80kDa**	-	FUNCTIONS AS A CYSTEINE PROTEASE UPON CLEAVAGE OF A C-TERMINAL PEPTIDE. PROTECTS CELLS AGAINST OXIDATIVE STRESS AND CELL DEATH.

6.1 Proteins interacting with the G-substrate Isoforms

Proteins interacting with phosphorylated and un-phosphorylated G-substrate isoforms 1 (full-length) and 2 (short) as well as the G-substrate phospho-peptide (section 6.1.3) were investigated using pull-down assays and interacting proteins identified by MALDI-tof mass spectrometry. The proteins have, for the most part, MOWSE scores considered 'significant' within a 5% error although interesting associations with proteins whose scores were considered 'non-significant' are also mentioned. Molecular weights of some of the proteins corresponded to the appropriate sizes on the polyacrylamide gels used although in most cases bands at lower molecular weights, which most likely represent fragments of the identified proteins, were encountered. In a few cases proteins identified using the Mascot software were of molecular masses lower than the molecular weights at which their corresponding bands ran on the pull-down gels. One possible reason for such observations is the fact that some proteins, like G-substrate, run anomalously on SDS-PAGE. Each protein has been assigned a functional group in the table above based on its most significant function or associated pathway although a number of the proteins fall into more than one of the categories shown. Based on the identity of proteins pulled down, G-substrate is potentially involved in processes including apoptosis, the maintenance of the cytoskeleton/cell structure, cell cycle control, regulation of transcription and translation, endocytosis and cellular metabolism.

6.1.1 G-substrate Isoform 1

In addition to providing the largest proportion of putative interacting proteins, full-length G-substrate was the only form of the protein that pulled down proteins involved in metabolism, ion-transport and signalling. From the results only three proteins were pulled down by both full length and short G-substrate – the 77kDa developmentally-regulated brain protein (Drebrin) and non-muscle myosins 9 and 10. The cellular myosin is thought to play a role in secretion and capping as well as cytokinesis and the maintenance of cell shape while the F-actin-binding drebrin is implicated in dendritic plasticity, cell migration and the extension of neural processes. Interestingly, full-length, short G-substrate and the phosphopeptide all

pulled down distinct actin-binding proteins as well, suggesting *in vivo* interactions with actin for both isoforms of G-substrate, both phosphorylated and unphosphorylated.

6.1.2 G-substrate Isoform 2

Compared with full length G-substrate, short G-substrate pulled down fewer proteins, perhaps due to the fact that the full length protein is much more abundant than the short isoform. The main unique interactions observed for short G-substrate were with proteins associated with the cytoskeleton and cellular structure including the motor protein dynamin and the F-actin-binding alpha-3 chain of tropomyosin.

6.1.3 Proteins Interacting with G-substrate Phosphopeptide

In order to adequately investigate interactions involving phosphorylated G-substrate isoforms, which potentially directly involve the phosphorylation motif, pull-downs were performed with the G-substrate phosphopeptide CDQKKPRRKD[pT]PAL-amide (where pT is a phosphorylated threonine), coupled to magnetic beads. The phosphopeptide was coupled to the magnetic beads at its N-terminus (using the cysteine residue) in order to avoid masking the phosphorylated threonine residue. Proteins pulled down uniquely by the peptide were involved in the maintenance of centrosome integrity and completion of cytokinesis, mRNA cap recognition and mRNA recruitment to the ribosome. The DUSTY protein kinase, whose role in programmed cell death is discussed below, was also pulled down by the peptide, suggesting roles in cytokinesis, translation and apoptosis for both forms of phosphorylated G-substrate.

6.2 Discussion

A number of proteins pulled down possess similar domains and / or are implicated in a common cellular process. A few of these interesting associations are discussed in the following paragraphs.

6.2.1 Intracellular Vesicle Transport

The possibility of an interaction between G-substrate and the IP_3 receptor, which is located on the endoplasmic reticulum of the Purkinje cells, may be further supported by the observation that interactions seem to exist between G-substrate and other proteins involved in intracellular vesicle transport, possibly involving the endoplasmic reticulum. Full length G-substrate pulled down the vesicle-fusing ATPase, which is required for transport mediated by vesicles and is also a catalyst for the fusion of transport vesicles inside the cisternae. A number of proteins involved in vesicle activity were also pulled down by full length G-substrate. These included the kinesin-like protein KIF1C and the heavy chains of cytoplasmic dyneins 1 and 2, all of which function primarily as motors for vesicle motility. Defects in the heavy chain of cytoplasmic dynein 1 have been associated with dominant spinal muscular atrophy (78) as well as severe intellectual disability and defects in neuronal migration (79) Defects in the heavy chain of cytoplasmic dynein 2, which is important for the generation and maintenance of cilia (80) is associated with asphyxiating thoracic dystrophy type 3 (ATD3) and short rib-polydactyly syndrome type 3 (SRPS3). Mutations in both dynein and kinesin proteins have been shown to result in a reduction of the Sonic hedgehog (Shh) signalling pathway, which is important for the growth and patterning of brain structures during development (81) The Shh pathway has also been found to play an essential role in neurite outgrowth, a process in which contactin-1 and GRIN-1 (both pulled down by both full length G-substrate and the G-substrate peptide) are involved.

6.2.2 Cerebellar Long Term Depression

Cerebellar long-term depression (LTD) is thought to be the cellular mechanism for cerebellar motor learning (51) and involves a reduction in the efficacy of neuronal synapses over time. It has been suggested that G-substrate plays a role in the regulation of LTD induction in Purkinje cells as part of the NO/cGMP/PKG pathway (10). Evidence from several experiments also suggest that the IP_3/Ca^{2+} pathway is responsible for LTD (82,83) although the details remain largely unresolved. The fact that the opening of the IP_3 receptor and the induction of LTD require a similar set of input signals may provide further insight into the process - the opening of the IP_3 receptor channel depends on the simultaneous presence of IP_3 and calcium, while the induction of LTD requires the detection of a near simultaneous arrival of synaptic inputs from the climbing fibres (resulting in the generation of a calcium signal) and the parallel fibres (activation of metabotropic receptors to produce IP_3) by the Purkinje neuron (84). The observation that the G-substrate phosphopeptide pulled down the IP_3 receptor provides further support for the involvement of these two proteins in LTD. Interestingly, the most abundant expression of G-substrate is in cerebellar Purkinje cells, which places it at the right location for participation in this process. The observation that the IP_3 receptor was pulled down by the G-substrate peptide suggests that interaction with the IP_3 receptor in humans could be with the phospho-forms of either full length or short G-substrate or even both isoforms since both isoforms possess the same phosphorylation motif with the only difference being that full length G-substrate possesses two while short G-substrate possesses one. The absence of interaction with the same receptor in pull-downs performed with the phospho- forms of both isoforms might be due to the fact that analyses with the peptide were performed to ensure the orientation of the phosphopeptide such that it was completely unobstructed and available for interaction while the possibility exists that although of identical structure, the phosphorylation motifs in the intact proteins might have been less available for interaction.

6.2.3 Inositol Triphosphate Signalling

G-substrate has been implicated in several diseases including hypercholesterolemia (28) and Parkinson's disease (PD) because it is possibly involved in a number of pathways that are important in maintaining proper cellular function. It has been known for several years that G-substrate is part of the NO-sGC-cGMP-PKG pathway but results showing a possible interaction of full length G-substrate with IP_3R1 suggests an additional role in the IP_3 pathway, which is important for the maintenance of calcium homeostasis and has been linked to several diseases including spinocerebellar ataxia type 1 (SCA 1), Huntington's disease and Alzheimer's. The role of calcium signalling in Alzheimer's disease (AD) (85) is reinforced by the fact that mutations in the genes for presenilins 1 and 2 and in the amyloid precursor protein (APP) gene, all resulting in abnormal signalling in the endoplasmic reticulum, have been strongly linked to familial AD. In addition, the use of calcium channel blockers in the treatment of AD has resulted in some success (86). One important role of the IP_3 signalling pathway is the activation of PKC, a serine threonine kinase whose activation can involve both DAG and the increase in intracellular Ca^{2+} stimulated by the binding of IP_3 to its receptor (Figure 6.2). PKC can also be activated by limited proteolysis with calpain to produce a smaller component, which is enzymatically active completely independently of Ca^{2+}, phospholipid or DAG. Membrane-bound PKC is thought to be more susceptible to this proteolysis than soluble PKC (87). Interestingly, G-substrate is also proteolytically cleaved by calpain and it has been suggested that the calpain-mediated degradation of G-substrate represents an important mechanism contributing to NMDA-induced amacrine cell death (88). Interaction of G-substrate with IP_3R1 is of great interest because both proteins have been found to show altered expression in SCA1 transgenic mouse models with G-substrate mRNA being significantly down regulated (64).

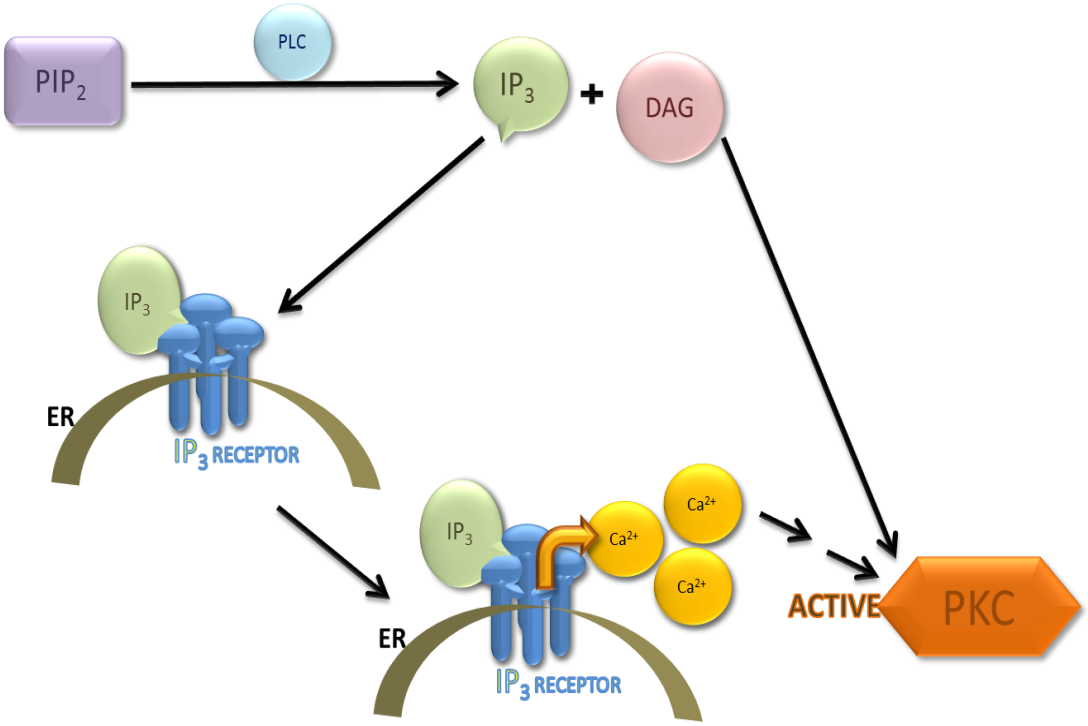

Figure 6.2: Protein kinase C regulation.

PIP_2= phosphatidylinositol-4,5-bisphosphate, PLC=phospholipase C, IP_3=inositol triphosphate, DAG=diacyl glycerol, ER=endoplasmic reticulum, PKC=protein kinase C.

Interaction of G-substrate with proteins located on or associated with the endoplasmic reticulum (in this case IP_3R1) is supported by the observation that G-substrate contains a possible endoplasmic reticulum membrane retention signal – a 'KKXX-like' motif represented by the sequence DKIA in the C-terminal region and one of two peroxisomal targeting signals (PTS2) within the sequence --- KLDPRCSHL--- located near its N-terminal region. Both of these putative localization signals occur outside the section missing from the short protein. This implies that the possibility of interaction with the endoplasmic reticulum and peroxisomes exists for both isoforms of human G-substrate. Peroxisomes are derived from the endoplasmic reticulum and function mainly in the oxidation of long chain fatty acids in humans (89). The observation that G-substrate interacts with glyceraldehyde-3-phosphate dehydrogenase, another protein associated with peroxisomes, further strengthens the argument for association of G-substrate with peroxisomes.

6.2.4 The Pleckstrin Homology Domain

The production of the phosphatidylinositols (PtdIns) PtdIns-3,4,5-trisphosphate and PtdIns-3,4-bisphosphate leads to the recruitment of proteins containing the pleckstrin homology domain to the plasma membrane. The pleckstrin homology (PH) domain is an approximately 100 amino acid domain that occurs in a wide range of proteins involved in cytoskeletal structure and intracellular signalling. The domain has been found in over 40 proteins including protein kinases, phospholipases, guanine nucleotide exchange factors and cytoskeletal proteins. Although the function of this domain is not known for sure, it has been suggested that it could include binding to lipids, phosphorylated serine/threonine residues and the β/ψ subunits of heterotrimeric G-proteins.

The G-substrate protein pull-downs resulted in the identification of three proteins involved with/or possessing the PH domain. Considering information about putative binding partners, dynamin, which was pulled down by phospho-short G-substrate, could possibly be interacting with the phosphorylated threonine residue of G-substrate via its PH domain. Since full length G-substrate protein possesses two such phosphorylated threonine residues within similar phosphorylation motifs, it is possible that the phosphorylated full length protein might also interact with dynamin. The absence of identified interactions of the full length protein with dynamin could be a result of the interaction preferring the presence of only one phospho-threonine residue (as seen in phospho-short G-substrate). Full length G-substrate pulled down the Ras-like family member protein FYVE, RhoGEF and PH domain containing protein 4 (Protein 4) and the kinesin-like protein KIF1C, which functions in the retrograde transport of golgi vesicles to the endoplasmic reticulum. Protein 4 is thought to activate cell division control protein 42 (CDC42), a member of the Ras-like family of Rho- and Rac proteins, by exchanging bound GDP for free GTP and also activate the stress-activated protein kinase JNK1 (JNK1) via CDC42. Protein 4 also binds to phosphatidylinositols (PtdIns) (PtdIns-4,5-bisphosphate, PtdIns-3,4,5-trisphosphate, PtdIns-5-monophosphate, PtdIns-4-monophosphate and PtdIns-3-monophosphate).

6.2.5 Apoptosis

Eight proteins involved in the apoptotic process or cleaved by caspases were pulled down by G-substrate; five of them, glyceraldehyde-3-phosphate dehydrogenase (GAPDH), Rab GTPase effector protein 1 (Rabatin), heat shock protein HSP 90-beta (HSP 90-B), E3 sumo-protein ligase RanBP2 and Huntingtin-interacting protein 1 (HIP-1), were pulled down by full length G-substrate. Protein kinase C epsilon (PKCε) and grip1-associated protein 1 (GRAP-1) were both pulled down by phosphorylated full length G-substrate and the dual serine/threonine tyrosine protein kinase (DUSTY protein kinase) was pulled down by the G-substrate phospho-peptide. These three proteins can, therefore, be said to interact with phosphorylated (full length) G-substrate with DUSTY protein kinase possibly interacting with the phosphorylation motif. Five of these proteins have been described as caspase substrates; Rabatin and GRAP-1 are cleaved by caspase-3 and GAPDH and HSP 90-B by caspase-6. RanBP2 has been shown to possess a putative caspase cleavage site using proteomic methods (90). HIP-1, via its caspase-dependent death effector domain, is involved in the induction of apoptosis (91) while DUSTY protein kinase plays a part in the induction of both caspase-dependent and caspase-independent apoptosis. Zha and co-workers (92) showed that the overexpression of the protein in Hek 293 cells induced DNA fragmentation, which is considered a hallmark of caspase-dependent apoptosis. The absence of inhibition of DUSTY protein kinase induced cell death morphology in the presence of the pan-caspase inhibitor VAD-fmk led the researchers to suggest the involvement of DUSTY protein kinase in a second caspase-independent apoptotic pathway.

In addition to being a substrate for caspase-6 during apoptosis, GAPDH, when S-nitrosylated in response to oxidative stress forms a complex with Siah-1, an E3 ubiquitin ligase. This SNO-GAPDH : Siah1 complex is subsequently translocated to the nucleus where it induces apoptosis by the ubiquitination and degradation of nuclear proteins in a process independent of GAPDH glycolytic activity (93).

PKCε has been shown to inhibit caspases-8 and -9, which contribute substantially to the induction of proteolytic cascades essential for the effective execution of apoptosis in cells marked for death. Jabůrek and co-workers (94) confirmed the co-localization of PKCε and the ATP-sensitive mitochondrial channel mitoK_{ATP} on the mitochondrial inner membrane and

described a functional association between the two proteins reportedly present in rat liver, heart and brain. The pull-down of PKCε by phosphorylated G-substrate is particularly interesting because the NO/sGC/cGMP/PKG pathway (described in 6.2.3) has been shown to influence the opening of mitoK_{ATP} on the mitochondrial inner membrane, leading to swelling of the mitochondrial matrix and the generation of reactive oxygen species. The detection of PKCε as a possible interacting partner of phosphorylated G-substrate suggests involvement of phospho-G-substrate in the signal transduction process that regulates the opening of the mitoK_{ATP} channel. The observation that PP2A, known to be effectively inhibited by phospho-G-substrate reverses the PKCε-dependent opening of mitoKATP (95) strengthens the possibility of G-substrate involvement in this process. This may provide more insight into the mechanism by which G-substrate overexpression works to protect A9 DA cells from PD toxins, since oxidative stress is a major hallmark of PD. Deficiency in the cysteine protease DJ-1, also known as PARK7, has been shown to sensitize dopaminergic neurons to stress-mediated apoptosis in hereditary Parkinson's disease. DJ-1 was detected in pull-downs performed with short G-substrate. Western blot analysis using antibodies specific for DJ-1 was performed on G-substrate pull-downs to further investigate DJ-1 association with G-substrate (Figure 6.3). DJ-1 was identified in the rat brain pull-downs with phosphorylated short G-substrate and unphosphorylated full length G-substrate rat brain pull-downs. Although a fainter band was obtained around the same molecular weight for the control pull-downs, the absence of interaction with the other forms of G-substrate and the fact that interaction was observed between G-substrate and DJ-1 *in vitro* suggested that the observed interaction was worthy of further study.

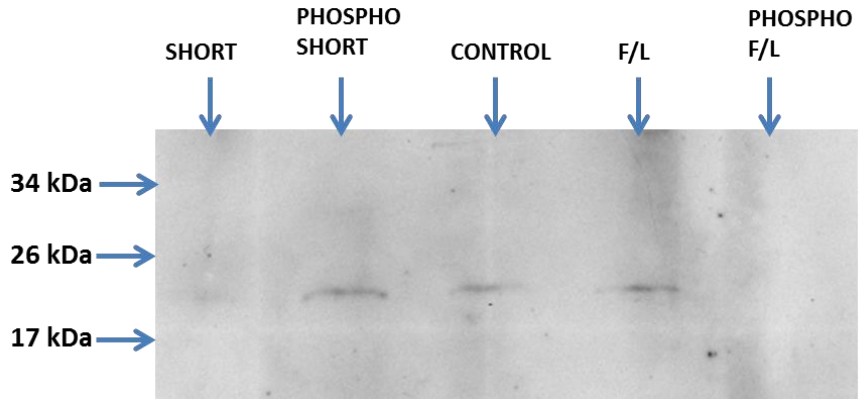

Figure 6.3: Western blot image showing rat brain pull-downs obtained for different forms of G-substrate protein probed with an antibody raised against DJ-1.

The possibility of interaction between G-substrate and DJ-1 is very intriguing since both of these proteins have been linked with neuroprotection in PD. Since DJ-1 has been linked with reactive oxygen species (ROS) damage (96). The pull-down by G-substrate of the IP_3R1 protein, which is localized in the MIM and plays a role in the control of ROS metabolism among other things hints at the tantalizing possibility of exploiting a possible interaction between G-substrate and DJ-1 in the development of interventions for treatment for PD and similar neurodegenerative conditions.

6.3 Cancer/Tumour Growth

Work by Rodriguez and co-workers identified the aldehyde dehydrogenase family 1 member, ALDH1L1, as an under expressed biomarker of tumour aggressiveness in astrocytic tumours (97). ALDH1L1, which was pulled down by full length G-substrate, is involved in folate metabolism and catalyses the conversion of 10-formyltetrahydrofolate (10-FTHF) to tetrahydrofolate. ALDH1L1 is thought to play a regulatory role in cell proliferation (98) and expression of ALDH1L1 in neural tubes correlates with a reduction of cellular proliferation.

Full length G-substrate also pulled down Huntingtin-interacting protein 1 (HIP-1), which is involved in regulating AMPA receptor trafficking in the central nervous system in an NMDA-

dependent manner. In addition to determining the severity of Huntington's disease by its interaction with Huntingtin protein, Hip-1 is up-regulated in prostate and colon cancers.

Work by Jianbin Peng and co-workers using tumour cell lines found DUSTY protein kinase, which was pulled down in this study by the G-substrate peptide, downregulated in tumours of breast, ovary, lung and pancreas (99).

The G-substrate peptide also pulled down the "cancerous inhibitor of PP2A" (CIP2A). CIP2A interacts directly with the oncogenic transcription factor c-Myc and inhibits PP2A-mediated MYC dephosphorylation and proteolytic degradation (42). CIP2A is also known to promote anchorage independent cell growth and *in vivo* tumour formation (100). The fact that CIP2A was pulled down by phosphopeptide, which represents the form of G-substrate involved in PP2A, is interesting and might provide clues for the mechanism of phosphatase inhibition by phospho G-substrate.

DJ-1/Park7 expression is significantly increased in cancer compared to normal tissue and its overexpression has been observed in many cancers including breast, lung, pancreatic, ovarian, and prostate (101). DJ-1 is a negative regulator of the tumour suppressor, PTEN which functions as a dual specificity protein and lipid phosphatase (102). PTEN shows a substrate preference for inositides of PtdIns(3,4,5)P3 > PtdIns(3,4)P2 > PtdIns3P > Ins(1,3,4,5)P4 and its lipid phosphatase activity is thought to be critical for its function as a tumour suppressor (103).

6.4 G-substrate Interactome

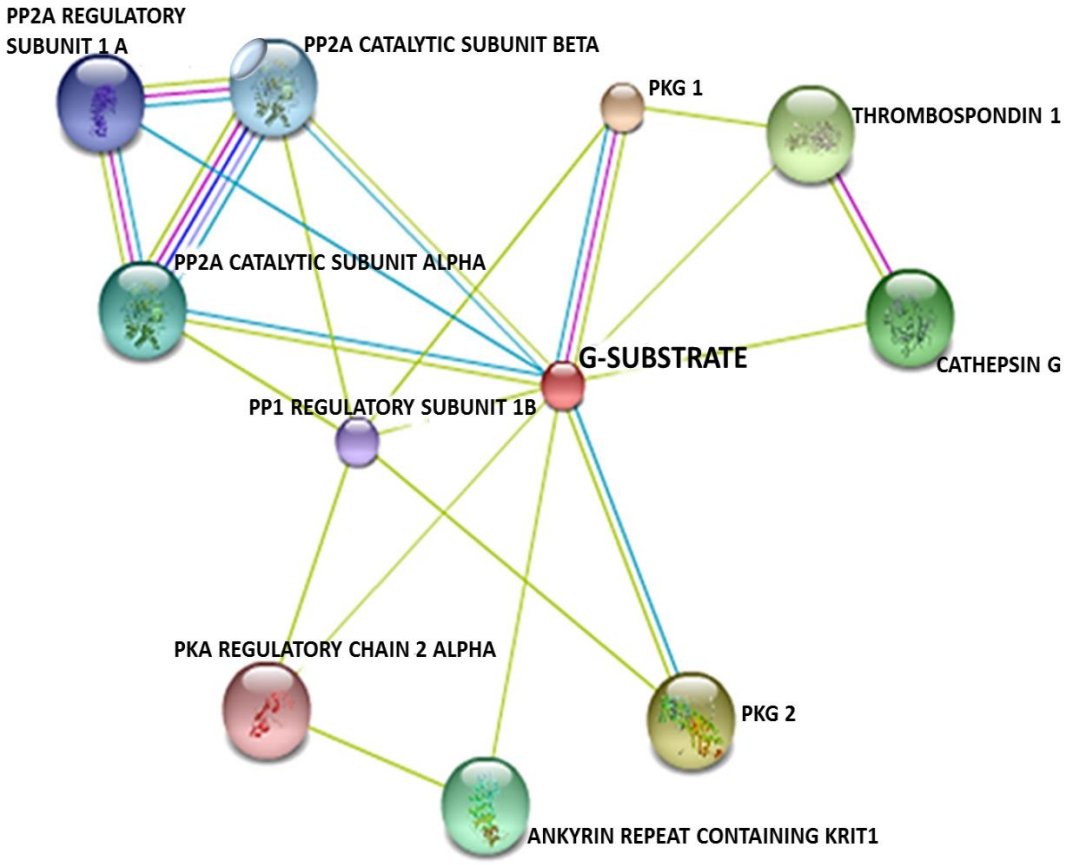

Figure 6.4: G-substrate 'interactome' modified from "string" (string-db.org)

A search using the online tool 'string' (http://string-db.org/), which attempts to bring together all known interactions for a query protein, yielded an 'interactome' (Figure 6.4) for G-substrate protein, which contained associations with catalytic and regulatory subunits of PP2A and a regulatory subunit of PP1. Interactions were also shown for PKA and PKG. It is worth noting that although isoform 1 has been shown as the documented interacting partner for G-substrate, PKG2 is the brain specific isoform of this kinase. Interactions are also reported for thrombospondin 1, cathepsin G and the ankyrin repeat containing protein KRIT1, whose gene is located on the same chromosome (chromosome 7) as G-substrate and plays an important role in the maintenance of intracellular ROS homeostasis and apoptosis.

Based on the cellular processes discussed above, Figure 6.5 summarises the novel interactions observed for G-substrate protein in this study.

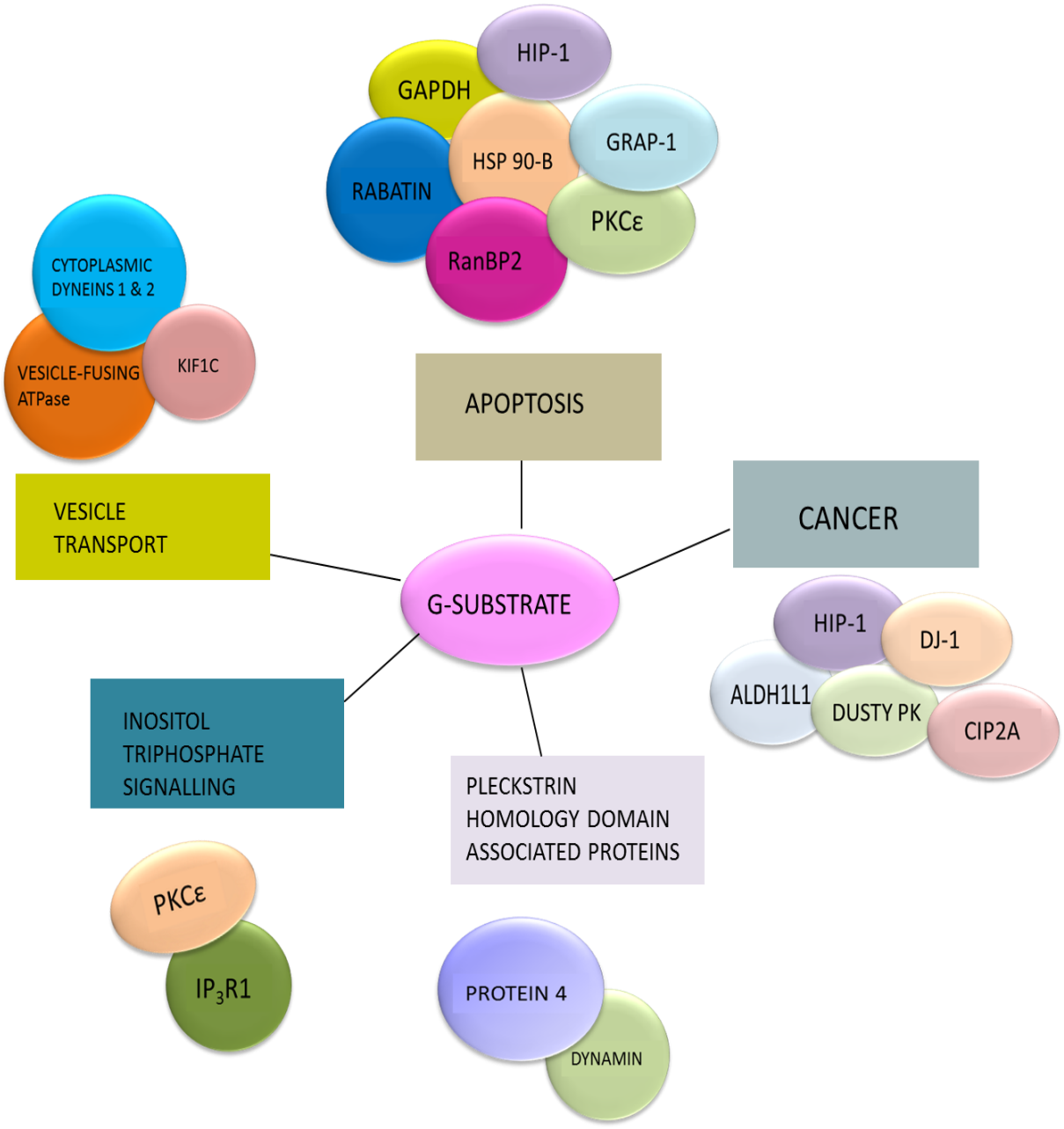

Figure 6.5: Summary diagram showing some novel G-substrate interacting proteins and the processes with which they are involved.

Processes/pathways are represented by rectangles and proteins by circles or ellipses. (See **Table 6.1** for abbreviations).

The use of in-gel tryptic digestion of SDS-PAGE bands followed by mass spectrometry resulted in successful identification of proteins pulled down by G-substrate. In some cases confirmation of protein identity was achieved using western blotting with antibodies specific to the protein of interest.

It is possible in some instances that the protein pulled down might be interacting with G-substrate indirectly, if it is a direct interacting partner of another protein. In this case reciprocal pull-downs, which involve pulling down proteins from a similar sample of rat brain extract with the identified protein followed by western blot analysis of the pull-down proteins with antibodies specific to the original protein, would possibly confirm the interaction in vivo of the two proteins.

Nevertheless, even if some of the proteins listed in Table 6.1are indirect partners of the various G-substrate constructs, their identification indicates potential functional involvement in a protein complex (Figure 6.5).

The Mascot software used to analyse the data obtained from MALDI-tof mass spectrometry was able to identify instances where more than one protein was present in a single band and classified these as mixtures. Where logistically possible, the use of 2D SDS-PAGE to separate interacting proteins obtained from pull-down experiments would result in the separation of proteins with similar molecular weights on the gel and potentially result in more accurate identification of the proteins pulled down.

In addition to the methods used in this work, protein-protein interactions can be observed in vivo by fusing the proteins of interest to fluorescent proteins including the green fluorescent protein (GFP) and its colour variant mutants and co-transforming these proteins into cell lines. The interactions of the proteins of interest can then be observed using fluorescence resonance energy transfers (FRET). This method, in addition to allowing the observation of protein interactions, also makes it possible to determine the subcellular localizations of such interactions and thereby shed more light on the protein's functions in vivo.

The criteria for deciding whether such protein interactions are authentic are reviewed in Mackay et al (104). The article also critically reviews the methodology and table 1 in the

review has an overview of detection limits. The authors suggest that the "gold standard" criterion for reliability in the Molecular Interactions Database (MINT; http://mint.bio.uniroma2.it/mint/) is the existence of co-immunoprecipitation data, which presumes the availability of antibodies specific for all the identified proteins. This is disputed by the curators of "Mint" who suggest that confidence should be built on the integration of all evidence from several experimental approaches (105)

In another article commenting on the Mackay et al review, Welch (106) states that "it must be borne in mind that the protein-interaction mapping for a given cell-type – even when obtained under the most reliable of experimental conditions – represents a relative and variable thing. As trite as it might be to say, the interactome (like all 'omes' downstream from the genome) is a dynamic entity, the structure-and-function of which is constantly subject to intra- and extra-cellular physiological influences. Pre-genomic systems biology has made it all too evident that the interactome is an observationally 'fuzzy', yet seductively attractive, object of curiosity."

The notion of "fuzziness" is also discussed by Tompa and Fuxreiter (107) who found "significant structural disorder or polymorphism" in protein-protein interactions. The presence of dynamism in the composition and interaction of protein complexes most likely confers adaptability, versatility and reversibility on protein-protein interactions. Discoveries such as this call for a revision of the methods currently used in the study of such interactions and the inferences that can be drawn from the results of such studies.

The interactions observed in this study represent a first step following which several other methods can be applied to shed more light on the interactions and cellular functions of G-substrate.

Chapter 7: G-substrate, DJ-1 and Tanganil

The human PARK7/DJ-1 gene is located on chromosome 1 and encodes a 189 amino acid protein, which is ubiquitously expressed (108)and particularly abundant in cerebral tissues (109). DJ-1 belongs to the ThiJ/PfpI family whose members contain a conserved domain and are involved in a wide range of molecular processes including regulation of RNA-protein interaction, proteolysis and chaperoning. DJ-1 has been linked to a number of physiological processes including sperm fertilization (110) regulation of RNA-protein interaction (111) and oxidative stress response (112-114).

7.1 DJ-1 in Parkinson's disease

The 10-15 % of PD cases that are not sporadic have been associated with a variety of loss-of-function mutations in genes including α-synuclein, parkin, PINK1, dardarin /leucine-rich repeat kinase 2 (LRRK2) and DJ-1/PARK7.

DJ-1 is associated with several important neuroprotective roles including transcriptional modulation, oxidative stress sensing and guarding of mitochondrial function. DJ-1 is also involved in apoptosis inhibition by suppressing apoptosis signalling kinase 1 (ASK1) and death protein Daxx while simultaneously supporting the pro survival Akt pathway. In addition, DJ-1 has been found to function as a molecular chaperone to prevent heat-induced aggregation of α-synuclein (SNCA). Although these are diverse roles, they have the net result of opposing apoptosis associated with oxidative stress as is found in PD. Although oxidative stress alone can lead to neuronal death, it also triggers mitochondrial dysfunction and impairment of the ubiquitin-proteasome system, which further aggravates nigral pathology (115). Because of the tight interconnection of these factors, initiation of one inevitably recruits the others to participate in events that ultimately result in situations similar to the pathogenesis of PD. The fact that defects in the gene encoding DJ-1 have been identified as the cause of autosomal recessive juvenile early-onset Parkinson disease 7 underscores the importance of functional DJ-1 to cell survival. Although Parkinsonism caused by this mutation is very rare, DJ-1 is the second most frequent identifiable genetic causes of PD, after parkin/PARK2 (116).

Neurons of the substantia nigra pars compacta (SNc) are the cells most affected by PD and particularly susceptible to oxidative stress as a result of a higher basal oxidative stress resulting from 'mitochondrial flickering'. 'Mitochondrial flickering' refers to a phenomenon involving the transient spontaneous depolarization of mitochondria. This phenomenon induces oxidative stress because the Ca^{2+} ions which enter during depolarization are removed using ATP generated by oxidative phosphorylation in the mitochondria. The high basal oxidative stress endured by the SNc neurons explains their particular sensitivity to hikes in oxidative stress due to conditions like PD. A role in sensing and protecting neurons from reactive oxygen species (ROS) will undoubtedly make active, functional DJ-1 indispensable to these neurons. In addition, DJ-1's prospective role in assisting protein refolding will ensure that any unfolded/misfolded proteins resulting from such cellular stress which may aggregate and stimulate neuronal pathology would be refolded, extending the lives of these neurons.

7.2 DJ-1 Structure

X-ray crystallography revealed that DJ-1consists of eight α-helices and eleven β-sheets and adopts a flavodoxin-like Rossmann fold. DJ-1 possesses structural homology to the bacterial PfpI/PH1704 proteases (117) with an additional α helix at the C- terminus of the protein, which projects away from the remainder of the structure and prohibits access to the active site binding pocket Investigations using size exclusion chromatography and dynamic light scattering showed that DJ-1 exists mainly as a dimer (Sun-Joo Lee et. al., 2003) with two DJ-1 monomers making extensive contacts covering about 35 % of the molecular surface of each molecule. The dimeric interactions in DJ-1 were found between the α1, α 7, and α 8 helices and the β4 strand from each monomer, with the interactions between the β4 strands forming an inter-molecular short sheet (Figure 7.1). A putative active site has been identified near the dimer interface, and the residues Cys-106, His-126, and Glu-18 may play important roles in catalysis by this protein.

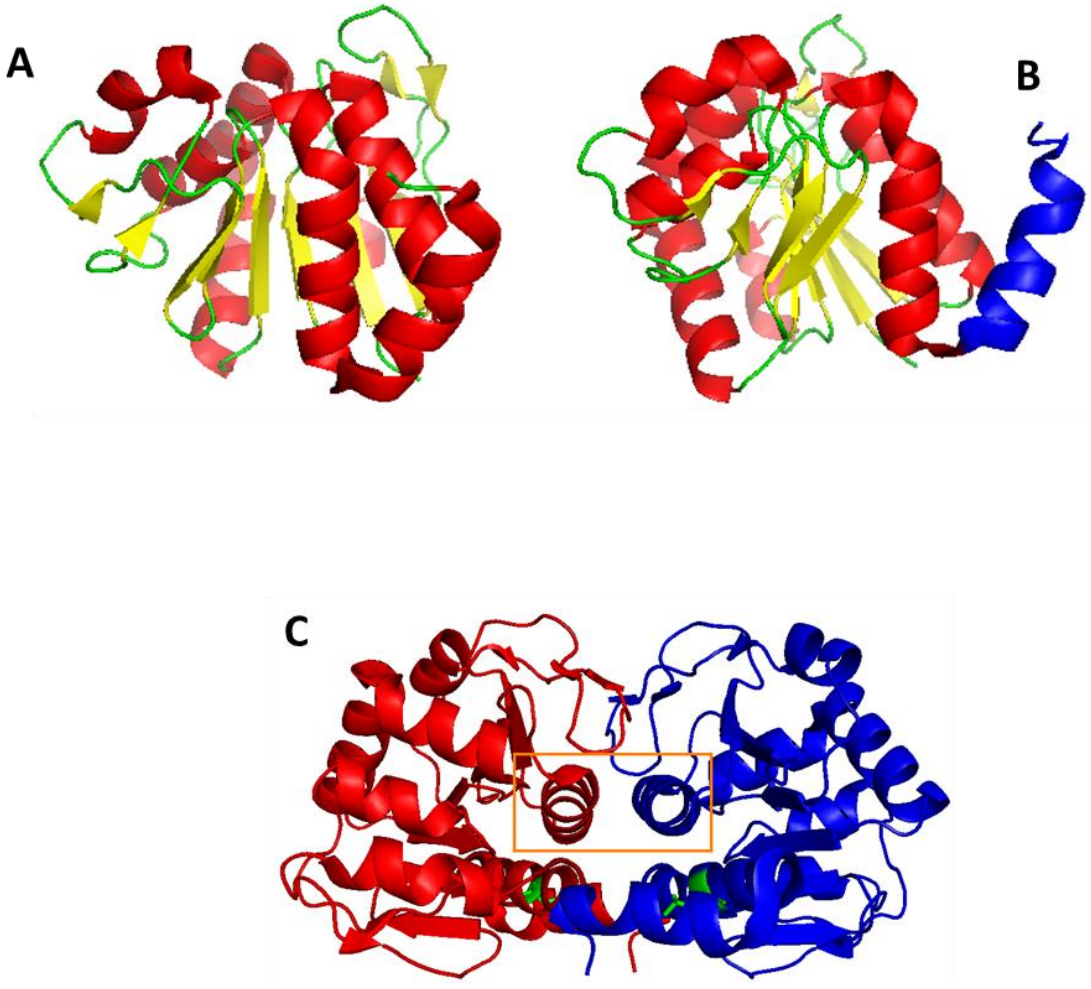

Figure 7.1: Ribbon structure of DJ-1

A: DJ-1 monomer - α-helices are in red; β-sheets in yellow; loops in green**. B:** DJ-1 monomer with C-terminal helix 8, which is cleaved to produce biologically active DJ-1, in blue (PDB accession: 1P5F). **C**: Dimer of wild type DJ-1 with monomers in red and blue. L166 is in green on both monomers and close to the putative dimer interface enclosed in orange rectangle.

The leucine residue at position 166 has been found to be vital for DJ-1 dimerisation (116). This residue is highly conserved among DJ-1 homologues, suggesting that dimerisation is central to the biological function(s) of this protein. A point mutation that replaces the leucine residue at position 166 with proline has been shown to predispose patients in consanguineous Italian families to early onset Parkinsonism (116) L166P is a loss of function mutation which

is likely due to the proline residue disrupting the structure of helix 7, within which L166 is located, leading to misfolding and subsequent loss of protein activity. Several groups have predicted that the protein dysfunction results from failure of L166P DJ-1 to form homodimers or heterodimers with wild-type DJ-1, however Baulac and coworkers (118) showed that L166P mutants still form homodimers in vitro albeit with reduced efficiency and have a higher tendency of forming oligomers of higher molecular weight than wild-type DJ-1.

7.3 DJ-1 as a Cysteine Protease

Observations that DJ-1 possessed a putative catalytic diad, made up of Cys-106 and His-126 which could function in a manner similar to the Cys-His-Glu/Asp catalytic triad characteristic of well-characterised aspartate proteases led to proposals that DJ-1 might function as a protease. Olzmann and coworkers (119) demonstrated DJ-1 protease activity using a highly sensitive, fluorescence-based protease assay, which led to the conclusion that DJ-1 possesses a weak intrinsic protease activity that required activation, a view shared by Chen and coworkers (101), who proved that 15 amino acids of the C-terminal helix, α8, of DJ-1 are cleaved to convert the zymogen into an active protease. Apoptosis assays confirmed that the expression of C-terminally cleaved wild-type DJ-1 in cells results in increased neuroprotection compared to wild-type DJ-1. A likely explanation for this is that α8 obscures substrate access to the active site pocket. The cleavage might also allow the imidazole side chain of His 126 to orient properly to complete a catalytic diad with Cys106. The substrate specificity of DJ-1 has not been determined and the only known potential sites of cleavage are at the peptide bonds: Gly-Pro and Gly-Lys.

In view of the importance of the L166P mutation for dimerization and the requirement of C-terminal helix deletion for DJ-1 protease activity, I cloned and expressed two mutants of DJ-1 for further investigation into the effects of these variants of DJ-1 on its interaction with G-substrate.

Using wild type DJ-1 clones kindly provided by Dr. Mark A. Wilson (University of Nebraska) site-directed mutagenesis of leucine 166 to proline was carried out by PCR with the oligonucleotide primers:

5’ GC AGG CGC AAA CTC GAA GC 3’ and
5’CG CCT GCA ATT GTT GAA GCC C 3’.

A second DJ-1 mutant with site directed mutagenesis of the lysine at position 175 to a stop codon (K175Stop), which mimicks the activated form of DJ-1 by removal of the C-terminal alpha-helix (see section 7.2 above) by PCR using the oligonucleotide primers: 5’ GC CGC CAC CTC CTA GCC 3’ and
5’GCC CTG AAT GGC TAG GAG G 3’.

Functional analysis of the mtuants was carried out in collaboration with three project students: Sylvia Ispasanie (SI), Mun Ching Lee (MCL) and Sean McLaughlin-Stewart (SM-S).

7.4 G-substrate as a DJ-1 substrate

The observed interaction between G-substrate and DJ-1 is intriguing because both of these proteins have been linked to the protection of neuronal cells from toxins. Interestingly, both proteins have links to the pro-survival Akt pathway with DJ-1 promoting Akt phosphorylation upon exposure to oxidative stress (120) and phosphorylated G-substrate potently inhibiting PP2A, an important phospho-Akt phosphatase. Since the phosphorylation of Akt is necessary for its mediation of the pro survival pathway, it is possible that like DJ-1, G-substrate contributes to neuroprotection via the Akt signalling pathway and further investigation into the interaction of these two proteins in the light of this pro-survival pathway could yield vital information that could lead to valuable interventions for conditions such as PD and cancer.

Due to this observation, the ability of DJ-1 to proteolyse both variants of human G-substrate was investigated *in vitro* in association with SI**;** DJ-1 protein activated by trypsin cleavage of its C-terminal tail was found to rapidly degrade both variants of G-substrate, with less rapid proteolysis observed for DJ-1 with an intact C-terminal tail (Figure 7.2).

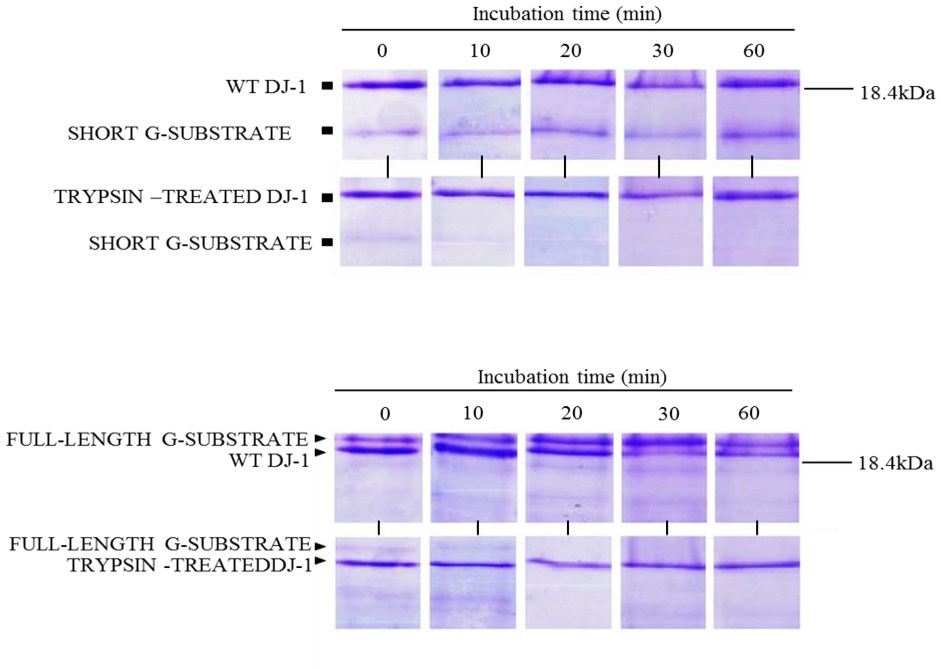

Figure 7.2: Proteolysis of human G-substrate variants by wild type (WT DJ-1) and trypsin treated DJ-1.

Given the importance of dimerization for the activity of DJ-1, the ability of the mutant L166P protein (which is thought to dimerise less well than the wild type protein) to degrade G-substrate was investigated in association SM-S (Figure 7.4). Our results indicate that this mutant has minimal protease activity toward G-substrate possibly due to its inability to adopt the dimeric structure thought to be vital for proteolytic activity.

We also analysed the second mutant, K175Stop, which lacks the 15 amino acid C-terminal section of wild type DJ-1 cleaved in the active protein for proteolytic activity toward G-substrate.

Although this variant displayed the expected constitutive proteolytic activity, this was shown to be significantly less (by approximately 32 %) than activated wild type DJ-1.

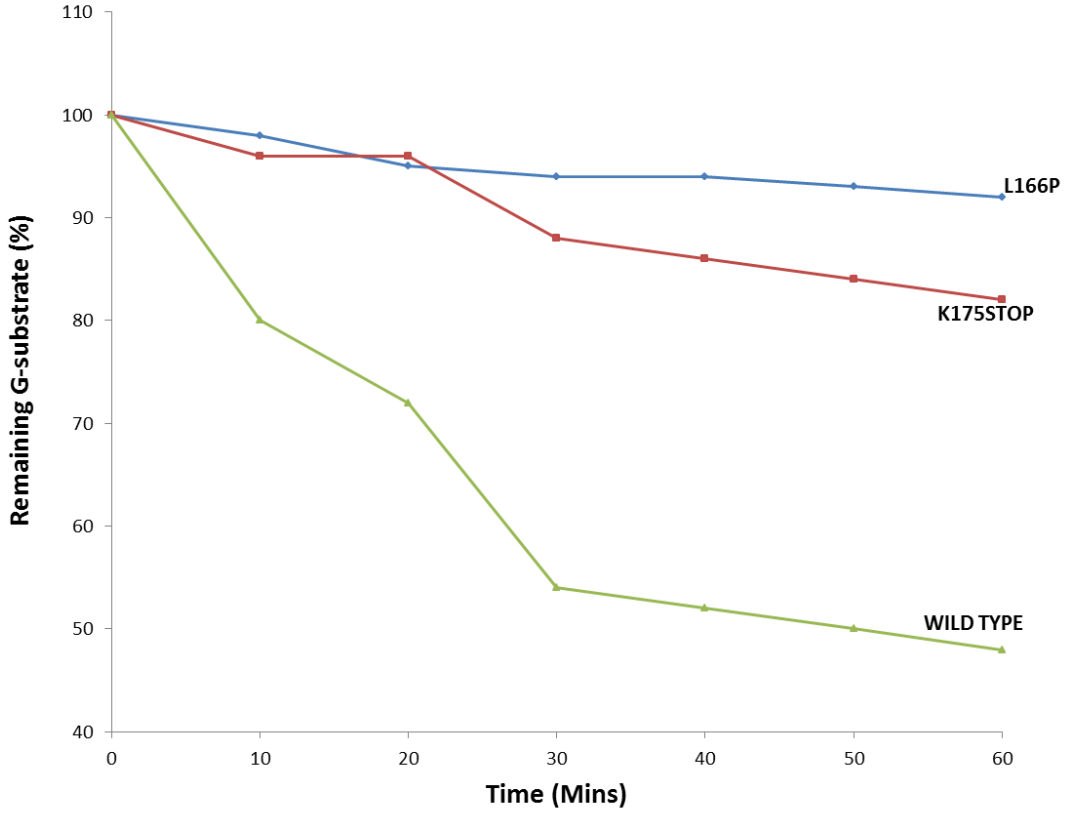

Figure 7.3: Degradation of G-substrate by DJ-1 variants .

7.4.1 Tanganil

In unpublished work carried out in the Aitken laboratory, Tanganil (N-acetyl-DL-Leucine) pulled down DJ-1 from a rat brain preparation. This led to an investigation of its effects on DJ-1 action *in vitro*. Tanganil is a drug widely used to reduce the imbalance and autonomic symptoms associated with acute vertigo (15,121). Despite being used for over 40 years, its mode of action remains poorly understood. In animal models, Tanganil has been shown to accelerate vestibular compensation following unilateral labryrinthectomy (122,123).

Vertigo is a condition of the vestibular system (see section 1.1.2.1) in which the subject experiences an erroneous perception of movement; either a feeling of movement when stationary or a false perception of the environment moving. The symptoms of vertigo are caused by a dysfunction of the vestibular nuclei or the inner ear canal (124).

Vestibular compensation refers to the recovery of oculomotor and postural control after the loss of unilateral vestibular input either partially or completely (Curthoys, 1995). The symptoms observed following damage to unilateral vestibular inputs are characterized by the symptoms of acute vertigo, making the effectiveness of Tanganil at managing both conditions unsurprising. The interaction of the vestibular system is a key link between these two conditions and provides a logical neuronal system upon which the mechanism of Tanganil could be based. The vestibular system has been investigated as the potential target of Tanganil with the drug showing an effect on abnormally polarized medial vestibular neurons (15).

7.4.2 Effect of Tanganil on G-substrate Degradation by DJ-1

The effect of Tanganil on the degradation of G-substrate by DJ-1 was studied in association with SM-S by determining the time taken for DJ-1 to degrade G-substrate in the presence or absence of Tanganil. There was a significant reduction in proteolytic activity of activated wild type DJ-1, by about 30 % in the presence of Tanganil. The L166P variant showed minimal proteolytic activity, which was reduced slightly in the presences of Tanganil. No significant variation in proteolytic activity was observed for the K175Stop mutant in the presence of Tanganil (Figure 7.4).

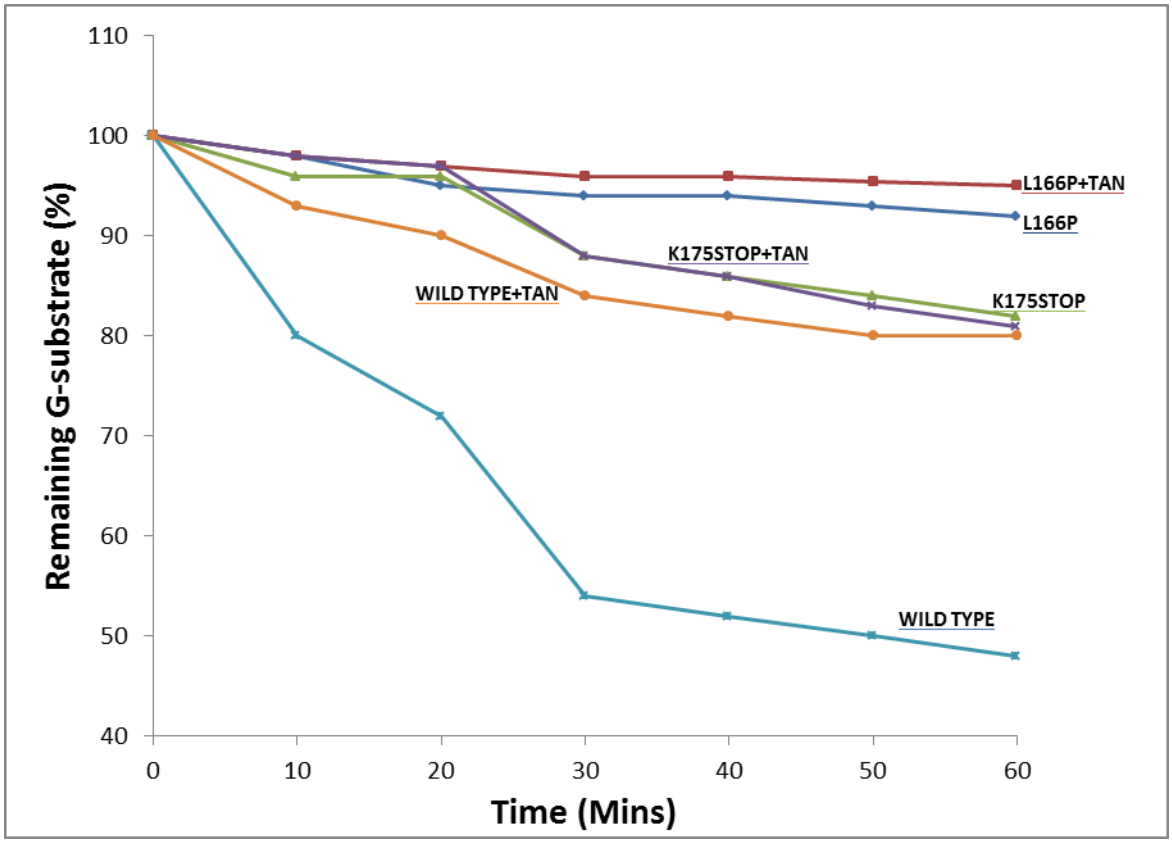

Figure 7.4: Effect of Tanganil on the degradation of G-substrate by DJ-1 variants

7.4.3 Effect of Tanganil on DJ-1 Dimerization

Chemical cross-linking analysis performed in collaboration with MCL and SM-S using the crosslinker Bis [sulfosuccinimidyl] suberate (BS^3) as described in 'Materials and Methods', revealed that Tanganil increases dimeric levels of wild type DJ-1. The level of dimerization of wild type DJ-1 increased by 13 % (Figure 7.5), while dimerization of the L166P variant increased by 12 % - an indication that the presence of the drug affected wild type and L166P DJ-1 to approximately equal extents. In contrast, the extent of dimerization of the K175Stop variant remained unchanged at in the presence of Tanganil.

The observation that Tanganil enhances the dimerization of the disease-causing L166P variant of DJ-1 presents the interesting prospect of exploiting this drug in attempts to resolve the

dimerization issues that are suspected to contribute to the PD pathology brought about by this mutation. This may contribute to the development of interventions for dealing with PD.

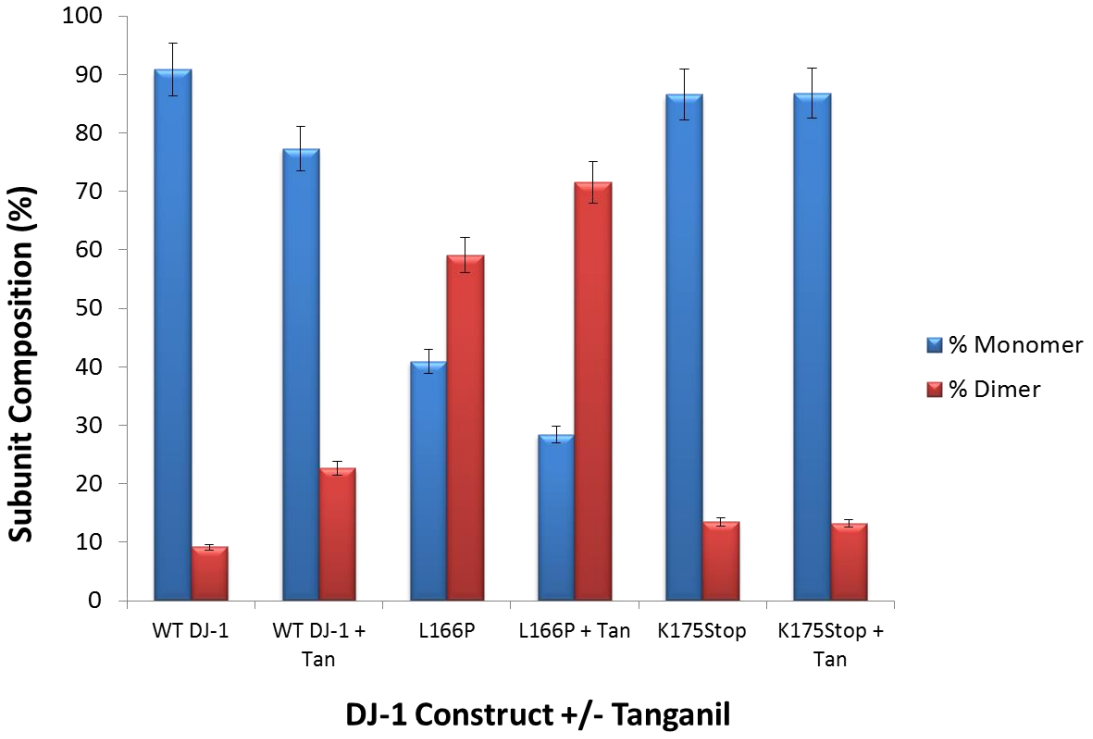

Figure 7.5: Effect of Tanganil on the Dimerization of DJ-1 variants.
Error bars represent the SEM of three replicates.

The potential interaction between DJ-1 and G-substrate via the Akt signalling pathway and our observations that Tanganil contributes to the stability of dimeric DJ-1 and especially dimerization of the disease causing L166P mutant of this protein represents an important line of investigation towards the elucidation of molecular mechanisms that could be exploited in the alleviation of neurodegenerative events in the brain and nervous system.

7.5 Discussion

Recent unpublished work in the Aitken laboratory has shown that N-acetyl-L-leucine is the active ingredient in Tanganil as far as affecting the interaction between DJ-1 and G-substrate is concerned. We have also shown that a number of other acetylated aliphatic L-amino acids including isoleucine, valine, lysine and norleucine also inhibit cleavage of G-substrate by DJ-1.

It is interesting that DJ-1, which is known to protect neurons from neurodegeneration due to oxidative stress successfully cleaves G-substrate, which is also known to be neuroprotective. One possibility is a role of DJ-1 in the regulation of G-substrate forms in the brain; phosphorylation activates the phosphatase inhibitory activity of the G-substrate isoforms and it is important that these phosphatase inhibitors are regulated in order that they do not persist beyond the time frame within which they are required. Recent work in the laboratory (data not shown) has revealed that DJ-1 cleaves phosphorylated G-substrate at a higher rate than the unphosphorylated forms, likely due to cleavage sites being more accessible as a result of the loss of structure in G-substrate that results from phosphorylation (discussed in sections 5.3 and 5.4). This observation and the fact that wild type DJ-1 cleaves G-substrate more effectively than the less abundant mutant DJ-1 forms, further support a role for DJ-1 in the regulation of phosphatase inhibition by G-substrate in the brain.

Observations that the presence of N-acetyl-L-leucine reduces the ability of DJ-1 to cleave G-substrate (Figure 7.4) presents the possibility of selectively controlling the regulatory effect of DJ-1 on the phosphatase inhibitory activities of G-substrate. In cases like Alzheimer's diseases where it is believed that inhibition of PP2A contributes to the hyperphosphorylation of tau protein (125) which results in disease pathology, reducing the amounts of PP2A inhibitors including G-substrate present in the cell by processes such as cleavage of phosphorylated G-substrate by DJ-1 could result in an increase in the amount of PP2A available to dephosphorylate tau and potentially prevent hyperphosphorylation. In other instances where it is desirable to keep PP2A targets phosphorylated, the presence of N-acetyl-L-Leucine might help achieve this purpose by reducing the efficacy of G-substrate cleavage by DJ-1, making more G-substrate available to inhibit phosphatase activity and keep the desired proteins in their phosphorylated states.

Chapter 8: General Discussion and Conclusions

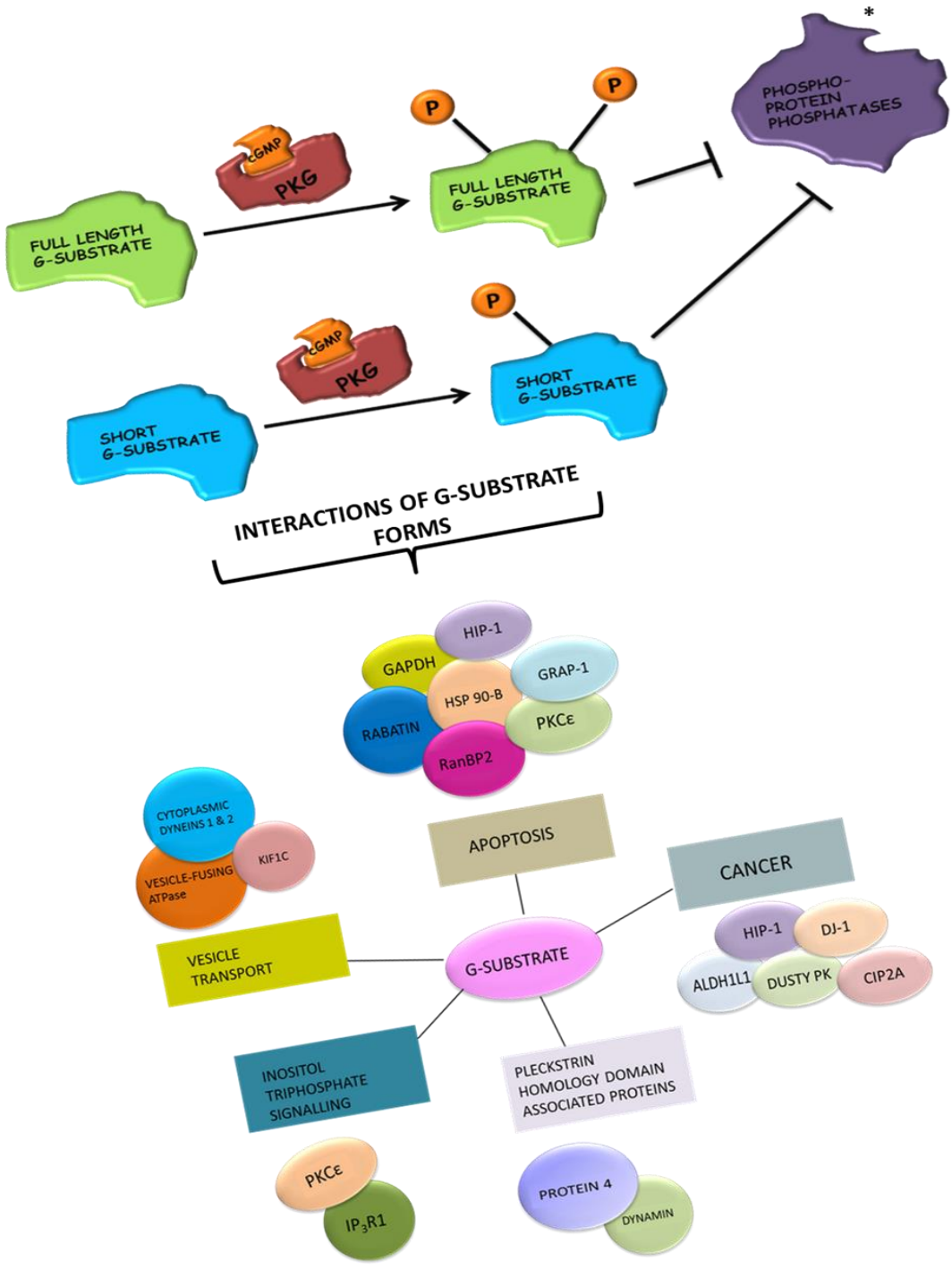

Figure 8.1: Summary of Main G-substrate Activities Discussed in this Work.

*See Table 4.1 for a summary of the effects of different G-substrate forms on the activities of various phosphatases.

8.1 General Discussion

The short isoform of G-substrate was successfully cloned and expressed under conditions similar to those used for the full length protein. Both recombinant proteins were successfully phosphorylated *in vitro* under similar conditions. As expected, phosphorylation of the full length protein required approximately twice as much enzyme as the phosphorylation of short G-substrate to achieve similar rates of phosphorylation due to the short isoform possessing only half as many phosphorylation sites as full length G-substrate.

I hypothesized that the phosphorylated short isoform of G-substrate would inhibit the phosphoprotein phosphatases PP1 and PP2A, both of which are known to be inhibited by the phosphorylated full length protein. This was expected due to the fact that phosphorylation of the threonine residue retained in the short isoform was determined to influence phosphatase inhibition more than the threonine residue absent from the short isoform. These experiments revealed that the short G-substrate isoform does inhibit phosphatase activity at levels similar to those of the full length protein, especially towards PP2A. Given the importance of PP2A in maintaining the balance between phosphorylation and dephosphorylation in cells, the ability of both isoforms to inhibit PP2A activity could be a strategy to ensure that it is possible to differentially regulate PP2A activity within cells using these two G-substrate isoforms.

The activity of PP5 was most affected by the unphosphorylated full length protein, which reduced PP5 activity to approximately 70 % from the start of the experiment. The unphosphorylated short protein was not found to appreciably reduce PP5 activity. After about 30 min, the effect of the phosphorylated full length protein on PP5 was very similar to the effects of the unphosphorylated forms of both isoforms and remained so throughout the time course. This observation suggests that the phosphorylated and unphosphorylated forms of the G-substrate isoforms might affect the different phosphatases they encounter in the cell in distinct ways, with the different forms inhibiting various phosphatases to different extents. As discussed in section 1.1, the various forms of G-substrate probably exist at different times or in distinct parts of the cell. Such a spatio-temporal distribution of the G-substrate forms might necessitate the specialization of the isoforms to regulate the relevant phosphatases effectively.

The analytical ultracentrifugation data agreed with predictions that the G-substrate protein existed as a monomer and formed no observable homodimers or oligomers. NMR spectroscopy results largely confirmed results from CD experiments indicating that in solution, both G-substrate isoforms possessed less than 10 % α helix structure, with the dominant secondary structure for both isoforms being loops and turns. This unstructured nature of G-substrate has been observed in other potent protein inhibitors of protein phosphatase 1, including Inhibitor-1, DARPP-32 and NIPP-1 and may be an indication that a substantial level of structural flexibility is required for optimum inhibition of protein phosphatase 1. Using CD, both G-substrate isoforms were also shown to recover their structures almost entirely after incubation at 85 °C.

Prior to this study, very little information existed on the interaction of G-substrate with proteins apart from cGMP-dependent protein kinase, which phosphorylates G-substrate *in vivo* and protein phosphatases 1 and 2A. In addition, information available on G-substrate almost exclusively referred to the full length isoform, with barely any experimental data available for interactions involving the short isoform.

Results obtained in this study revealed that the full length and short isoforms of G-substrate share interaction with proteins including myosin and the developmentally regulated brain protein drebrin. Since the amino acid sequence of the G-substrate peptide is identical to the phosphorylation motifs in both G-substrate isoforms, interactions with this peptide, most of which involve proteins functioning in the maintenance of cytoskeletal structure, can be attributed to the phosphorylated forms of both isoforms. Most of the unique interactions observed for the short isoform involved proteins associated with the cytoskeleton and cellular structure and included the motor protein dynamin and the F-actin-binding alpha-3 chain of tropomyosin. The full length protein interacted mainly with proteins involved with metabolism, ion transport and signalling.

My results have also highlighted the possibility that G-substrate, through interaction with the IP_3R1 protein, may provide a point of interaction between the cGMP/NO/PKG pathway and the inositol triphosphate pathway.

8.2 Conclusions

Results from this study revealed G-substrate exists as a monomer with both isoforms existing in solution with over 70 % of their secondary structure classified as 'unstructured'. The full length protein however possessed about 1 % more α helix than the short isoform, making it slightly more compact in solution.

Phosphorylated full length protein inhibits PP1 more potently than the other forms of G-substrate under the conditions tested, while all the forms of G-substrate reduce the activity of PP2A to similar extents. In the case of PP5, the unphosphorylated full length protein was the most inhibitory form, while the unphosphorylated short protein had no effect on activity.

The full length G-substrate protein interacted with a larger number of proteins than the short isoform. These proteins were mainly involved in cellular processes including metabolism, ion transport and signalling. The short isoform interacted with relatively few proteins, most of which were involved with the maintenance of cellular structure. The G-substrate peptide, representing phosphorylated forms of both isoforms, interacted with proteins associated with the cell cycle, cellular structure, transcription and translation. G-substrate also interacted with DJ-1, the protein associated with inheritable early onset Parkinson's disease type 7. In vitro experiments revealed that both isoforms of G-substrate were effectively proteolysed by activated DJ-1. The ability of DJ-1 to proteolyse the G-substrate isoforms was adversely affected by Tanganil, a drug used to treat vertigo and whose active form is N-acetyl-L-leucine.

Chapter 9: Further Work

Further investigation into G-substrate interacting proteins, including reciprocal pull-downs and western immunoblotting to confirm the interactions observed will provide much needed information about the role of G-substrate isoforms in the mammalian brain.

The discovery that G-substrate protein is intrinsically disordered explains the lack of success with previous attempts at crystallizing the protein. Given that other inhibitors of PP1 although intrinsically disordered, acquire more structure upon binding to PP1 (discussed in section 5.5), it would be interesting to attempt to co-crystallize G-substrate and PP1 and elucidate the structure of G-substrate from the crystals obtained, since the structure of PP1 is known.

It is also possible, after labelling with appropriate isotopes, to determine the structure of G-substrate in solution, either by itself or bound to one of its interacting partners using nuclear magnetic resonance spectroscopy (NMR). Using this method, it is also possible to study the dynamics of the protein interactions and obtain further information on the mechanism of the interaction. Since interactions between kinases and their substrates are often transient, this would be an interesting way of studying the interaction between G-substrate and its kinase, the cyclic GMP-dependent protein kinase (PKG) since employing a method like crystallization would be potentially challenging due to the fact that kinases do not normally form stable complexes with their substrates.

Further work is currently ongoing in the Aitken laboratory to study the interaction between DJ-1 and G-substrate and the effect of Tanganil on DJ-1.

Chapter 10: References

1. Aswad, D. W., and Greengard, P. (1981) *The Journal of Biological Chemistry* **256**, 3487-3493
2. Endo, S., Suzuki, M., Sumi, M., Nairn, A. C., Morita, R., Yamakawa, K., Greengard, P., and Ito, M. (1999) *PNAS* **96**, 2467-2472
3. Aitken, A., Bilham, T., Cohen, P., Aswad, D., and Greengard, P. (1981) *The Journal of Biological Chemistry* **256**, 3501-3506
4. Horton, P., Park, K.-J., Obayashi, T., and Nakai, K. (2006) *Proceedings of the 4th Annual Asia Pacific Bioinformatics Conference APBC06, Taipei, Taiwan*, 39-48
5. Kunau, W.-H. (2005) *Current Biology* **15**, R774-R776
6. J.A.Wanders, R., and R.Waterham, H. (2006) *Annual Review of Biochemistry* **75**, 295-332
7. Schlichter, D. J., Detre, J. A., Aswad, D. W., Chehrazi, B., and Greengard, P. (1980) *PNAS* **77**, 5537-5541
8. Endo, S., Nairn, A. C., Greengard, P., and Ito, M. (2003) *Neuroscience Research* **45**, 79-89
9. Hall, K. U., Collins, S. P., Gamm, D. M., Massa, E., DePaoli-Roach, A. A., and Uhler, M. D. (1999) *The Journal of Biological Chemistry* **274**, 3485-3495
10. Nakazawa, T., Endo, S., Shimura, M., Kondo, M., Ueno, S., and Tamai, M. (2005) *Brain Research Molecular Brain Research* **135**, 58-68
11. Swanson, L. W. (1995) *Trends in Neurosciences* **18**, 471-474
12. Nawrocki, R. A., Shaalan, M., Shaheen, S. E., and Lorenzon, N. M. (2012) *PLoS ONE* **7**, e45581
13. Singer, H. S., Mink, J. W., Gilbert, D. L., and Jankovic, J. (2010) 2 - Cerebellar Anatomy, Biochemistry, and Physiology. in *Movement Disorders in Childhood*, W.B. Saunders, Philadelphia. pp 9-15
14. Endo, S., Shutoh, F., Dinh, T. L., Okamoto, T., Ikeda, T., Suzuki, M., Kawahara, S., Yanagihara, D., Sato, Y., Yamada, K., Sakamoto, T., Kirino, Y., Hartell, N. A., Yamaguchi, K., Itohara, S., Nairn, A. C., Greengard, P., Nagao, S., and Ito, M. (2009) *PNAS* **106**, 3525-3530
15. Vibert, N., and Vidal, P. P. (2001) *European Journal of Biochemistry* **13**, 735-748
16. Purves, D., Augustine, G. J., Fitzpatrick, D., Katz, L. C., LaMantia, A.-S., McNamara, J. O., and Williams, S. M. (2001) *Neuroscience*, 2nd ed., Sinauer Associates, Sunderland (MA)
17. Voogd, J., and Glickstein, M. (1998) *Trends in Neurosciences* **21**, 370-375
18. Purves, D., Augustine, G. J., Fitzpatrick, D., Hall, W. C., Lamantia, A.-S., Mcnamara, J. O., and White, L. E. (2007) *Neuroscience*, 4th ed.,
19. Sillitoe, R. V., Fu, Y., and Watson, C. (2012) Chapter 11 - Cerebellum. in *The Mouse Nervous System* (Charles, W., George, P., Luis PuellesA2 - Charles Watson, G. P., and Luis, P. eds.), Academic Press, San Diego. pp 360-397
20. Ito, M. (2008) *Nature* **9**, 304-313
21. Chung, C. Y., Koprich, J. B., Endo, S., and Isacson, O. (2007) *The Journal of Neuroscience* **27**, 8314-8323
22. Altman, J., and Bayer, S. A. (1977) *Experimental Brain Research* **29**, 265-274
23. Altman, J., and Bayer, S. A. (1978) *Journal of Comparative Neurology* **179**, 49-75

24. Altman, J., and Bayer, S. A. (1985) *Journal of Comparative Neurology* **231**, 27-41
25. Seidler, R. D., Bernard, J. A., Burutolu, T. B., Fling, B. W., Gordon, M. T., Gwin, J. T., Kwak, Y., and Lipps, D. B. (2010) *Neuroscience & Biobehavioral Reviews* **34**, 721-733
26. Duong, J. K., Gardner, K., and Rucker, L. M. (2010) *Journal of the Canadian Dental Association* **76**, a25
27. Hillier, L. W., Fulton, R. S., Fulton, L. A., Graves, T. A., Pepin, K. H., Wagner-McPherson, C., Layman, D., Maas, J., Jaeger, S., Walker, R., Wylie, K., Sekhon, M., Becker, M. C., O'Laughlin, M. D., al., e., and (2003) *Nature* **424**, 157
28. Ono, S., Ezura, Y., Emi, M., Yuko, F., Takada, D., Sato, K., Ishigami, T., Umemura, S., Takahashi, K., Kamimura, K., Bujo, H., and Saito, Y. (2003) *Journal of Human Genetics* **48**, 447-450
29. Aswad, D. W., and Greengard, P. (1981) *The Journal of Biological Chemistry* **256**, 3494-3500
30. Hofmann, F., Bernhard, D., Lukowski, R., and Weinmeister, P. (2009) cGMP Regulated Protein Kinases (cGK). in *cGMP: Generators, Effectors and Therapeutic Implications* (Schmidt, H. H. H. W., Hofmann, F., and Stasch, J.-P. eds.), Springer Berlin Heidelberg, Heidelberg. pp
31. Alverdi, V., Mazon, H., Versluis, C., Hemrika, W., Esposito, G., Heuvel, R. v. d., Scholten, A., and Heck, A. J. R. (2008) *Journal of Molecular Biology* **375**, 1380-1393
32. Taylor, M. K., and Uhler, M. D. (2000) *Journal of Biological Chemistry* **275**, 28053-28062
33. Janssens, V., Longin, S., and Goris, J. (2008) *Trends in Biochemical Sciences* **33**, 113-121
34. Fong, N. M., Jensen, T. C., Shah, A. S., Parekh, N. N., Saltiel, A. R., and Brady, M. J. (2000) *The Journal of Biological Chemistry* **275**, 35034-35039
35. Cohen, P. T. W. (2002) *Journal of Cell Science* **115**, 241-256
36. Bollen, M., Peti, W., Ragusa, M. J., and Beullens, M. (2010) *Trends in Biochemical Sciences* **35**, 450-458
37. O'Connell, N., Nichols, S. R., Heroes, E., Beullens, M., Bollen, M., Peti, W., and Page, R. (2012) *Structure* **20**, 1746-1756
38. Wakula, P., Beullens, M., Ceulemans, H., Stalmans, W., and Bollen, M. (2003) *The Journal of Biological Chemistry* **278**, 18817-18823
39. Hendrickx, A., Beullens, M., Ceulemans, H., Abt, T. D., Eynde, A. V., Nicolaescu, E., Lesage, B., and Bollen, M. (2009) *Chemistry and Biology* **16**, 365–371
40. Slupe, A. M., Merrill, R. A., and Strack, S. (2011) *Enzyme Research* **2011**, 8
41. Berridge, M. J. (2012)
42. Junttila, M. R., and Westermarck, J. (2008) *Cell Cycle* **7**, 592-596
43. Howlett, G. J., Minton, A. P., and Rivas, G. (2006) *Current Opinion in Chemical Biology* **10**, 430–436
44. Laue, T. M. (1995) *Methods in Enzymology* **259**, 427–452
45. Cole, J. L., Lary, J. W., Moody, T. P., and Laue, T. M. (2008), 143-179
46. Corrêa, D. H. A., and Ramos, C. H. I. (2009) *African Journal of Biochemistry Research* **3**, 164-173
47. Kelly, S. M., Jess, T. J., and Price, N. C. (2005) *Biochimica et Biophysica Acta* **1751**, 119 – 139

48. Bracewell, R. N. (1978.) *The Fourier Transform and its Application*, McGraw-Hill Book Co., New York
49. Farrar, T. C. (1989) *Introduction to Pulse Nmr Spectroscopy*, Farragut Press
50. Marr, D. (1969) *The Journal of Physiology* **202**, 437-470
51. Ito, M. (1989) *Annual Review of Neuroscience* **12**, 85-102
52. Chartier-Harlin, M.-C., Crawford, F., Houlden, H., Warren, A., Hughes, D., Fidani, L., Goate, A., Rossor, M., Roques, P., Hardy, J., and Mullan, M. (1991) *Nature* **353**, 844 - 846
53. Yoshida, H., and Goedert, M. (2012) *Journal of Neurochemistry* **120**, 165-176
54. Planel, E., Yasutake, K., Fujita, S. C., and Ishiguro, K. (2001) *The Journal of Biological Chemistry* **276**, 34298-34306
55. Nussbaum, R. L., and Polymeropoulos, M. H. (1997) *Human Molecular Genetics* **6**, 1687-1691
56. Hughes, A. J., Daniel, S. E., Ben-Shlomo, Y., and Lees, A. J. (2002) *Brain* **125**, 861-870
57. Cookson, M. R. (2005) *Annual Review of Biochemistry* **74**, 29-52
58. Harding, A. E. (1982) *Brain* **105**, 1-28
59. Zoghbi, H. Y., and Orr, H. T. (2010) *Annual Review of Neuroscience* **23**, 217-247
60. Matilla-Dueñas, A., Goold, R., and Giunti, P. (2008) *The Cerebellum* **7**, 106-114
61. Banfi, S., Chung, M.-Y., Jr., T. J. K., Ranum, L. P. W., McCall, A. E., Chinault, A. C., Orr, H. T., and H.Y. Zoghbi*. (1993) *Genomics* **18**, 627-635
62. Chung, M.-y., Ranum, L. P. W., Duvick, L. A., Servadio, A., Zoghbi, H. Y., and Orr, H. T. (1993) *Nature Genetics* **5**, 254-258
63. Jodice, C., Malaspina, P., Persichetti, F., Novelletto, A., Spadaro, M., Giunti, P., Morocutti, C., Terrenato, L., Harding, A. E., and Frontali, M. (1994) *The American Journal of Human Genetics* **54**, 959-965
64. Serra, H. G., Byam, C. E., Lande, J. D., Tousey, S. K., Zoghbi, H. Y., and Orr, H. T. (2004) *Human Molecular Genetics* **13**, 2535-2543
65. Hanahan, D. (1983) *Journal of Molecular Biology* **166**, 557-580
66. King, J., and Laemmli, U. K. (1971) *Journal of Molecular Biology* **62**, 465-477
67. Tung, H. Y. L., Resink, T. J., Hemmings, B. A., Shenolikar, S., and Cohen, P. (1984) *European Journal of Biochemistry* **138**, 635-641
68. Li, H. C., Hsiao, K. J., and Sampathkumar, S. (1979) *Journal of Biological Chemistry* **254**, 3368-3374
69. Whitmore, L., and Wallace, B. A. (2008) *Biopolymers* **89**, 392-400
70. Sreerama, N., and Woody, R. W. (2000) *Analytical Biochemistry* **287**, 252-260
71. Provencher, S. W., and Glockner, J. (1981) *Biochemistry* **20**, 33-37
72. Stokkum, I. H. M. V., Spoelder, H. J. W., Bloemendal, M., Grondelle, R. V., and Groen, F. C. A. (1990) *Analytical Biochemistry* **191**, 110-118
73. Sents, W., Ivanova, E., Lambrecht, C., Haesen, D., and Janssens, V. (The biogenesis of active protein phosphatase 2A holoenzymes: a tightly regulated process creating phosphatase specificity) *FEBS Journal*
74. Trinkle-Mulcahy, L., Andersen, J., Lam, Y. W., Moorhead, G., Mann, M., and Lamond, A. I. (2006) *The Journal of Cell Biology* **172**, 679-692
75. Hinds, T. D., and Sánchez, E. R. (2008) *The International Journal of Biochemistry and Cell Biology* **40**, 2358–2362

76. Gong, C.-X., Liu, F., Wu, G., Rossie, S., Wegiel, J., Li, L., Grundke-Iqba, I., and Iqbal, K. (2004) *Journal of Neurochemistry* **88**, 298–310
77. Dancheck, B., Nairn, A. C., and Peti, W. (2008) *Biochemistry* **25**, 12346–12356
78. Harms, M. B., Ori-McKenney, K. M., Scoto, M., Tuck, E. P., Bell, S., Ma, D., Masi, S., Allred, P., Al-Lozi, M., Reilly, M. M., Miller, L. J., Jani-Acsadi, A., Pestronk, A., Shy, M. E., Muntoni, F., Vallee, R. B., and Baloh, R. H. (2012) *Neurology* **78**, 1714-1720
79. Willemsen, M. H., Vissers, L. E. L., Willemsen, M. A. A. P., Bon, B. W. M. v., Kroes, T., Ligt, J. d., Vries, B. B. d., Schoots, J., Lugtenberg, D., Hamel, B. C. J., Bokhoven, H. v., Brunner, H. G., Veltman, J. A., and Kleefstra, T. (2012) *Journal of Medical Genetics* **49**, 179-183
80. Mikami, A., Tynan, S. H., Hama, T., Luby-Phelps, K., Saito, T., Crandall, J. E., Besharse, J. C., and Vallee, R. B. *Journal of Cell Science* **115**, 4801-4808
81. Dessaud, E., McMahon, A. P., and Briscoe, J. (2008) *Development* **135**, 2489-2503
82. Wang, S. S.-H., Denk, W., and Häusser, M. (2000) *Nature Neuroscience* **3**, 1266 - 1273
83. Shouval, H. Z., Bear, M. F., and Cooper, L. N. (2002) *PNAS* **99**, 10831–10836
84. Berridge, M. J. (2008) *Biochimica et Biophysica Acta* **1793**, 933–940
85. Khachaturian. (1994) *Annals of the New York Academy of Sciences* **15**, 1-11
86. Anekonda, T. S., and Quinn, J. F. (2011) *Biochimica et Biophysica Acta (BBA) - Molecular Basis of Disease* **1812**, 1584-1590
87. Kishimoto, A., Kajikawag, N., Shiotan, M., and Nishizuka, Y. (1983) *Journal of Biological Chemistry* **258**, 1156-1164
88. Nakazawa, T., Shimura, M., Mourin, R., Kondo, M., Yokokura, S., Saido, T. C., Nishida, K., and Endo, S. (2009) *Journal of Neuroscience Research* **87**, 1412-1423
89. Veldhoven, P. P. V. (2010) *Journal of Lipid Research* **51**, 2863-2895
90. Mahrus, S., Trinidad, J. C., Barkan, D. T., Sali, A., Burlingame, A. L., and Wells, J. A. (2008) *Cell* **134**, 866-876
91. Hackam, A. S., Yassa, A. S., Singaraja, R., Metzler, M., Gutekunst, C.-A., Gan, L., Warby, S., Wellington, C. L., Vaillancourt, J., Chen, N., Gervais, F. G., Raymond, L., Nicholson, D. W., and Hayden, M. R. (2000) *The Journal of Biological Chemistry* **275**, 41299-41308.
92. Zha, J., Zhou, Q., Xu, L.-G., Chen, D., Li, L., Zhai, Z., and Shu, H.-B. (2004) *Biochemical and Biophysical Research Communications* **319**, 298–303
93. Sirover, M. A. (2011) *Biochimica et Biophysica Acta* **1810**, 741–751
94. Jabůrek, M., Costa, A. D. T., Burton, J. R., Costa, C. L., and Garlid, K. D. (2006) *Circulation Research* **99**, 878-883
95. Yonekawa, H., and Akita, Y. (2008) *FEBS Journal* **275**, 4005-4013
96. Ottolini, D., Calì, T., Negro, A., and Brini, M. (2013) *Human Molecular Genetics*, 1-17
97. Rodriguez, F. J., Giannini, C., Asmann, Y. W., K.Sharma, M., Perry, A., Tibbetts, K. M., Jenkins, R. B., Scheithauer, B. W., Anant, S., Jenkins, S., Eberhart, C. G., Sarkaria, J. N., and Gutmann, D. H. (2008) *Journal of Neuropathology and Experimental Neurology* **67**, 1194–1204
98. Oleinik, N. V., Krupenko, N. I., Priest, D. G., and A.Krupenko, S. (2005) *The Biochemical Journal* **391**, 503-511

99. Peng, J., Dong, W., Chen, Y., Mo, R., Cheng, J.-F., Hui, C.-c., Mohandas, N., and Huang, C.-H. (2006) *Biochimica et Biophysica Acta* **1759**, 562–572
100. Junttila, M. R., Puustinen, P., Niemela, M., Ahola, R., Arnold, H., Bottzauw, T., Ala-aho, R., Nielsen, C., Ivaska, J., Taya, Y., Lu, S.-L., Lin, S., Chan, E. K. L., Wang, X.-J., Grenman, R., Kast, J., Kallunki, T., Sears, R., Kahari, V.-M., and Westermarck, J. (2007) *Cell* **130**, 51-62
101. Chen, J., Li, L., and Chin, L.-S. (2010) *Human Molecular Genetics* **19**, 2395–2408
102. Arnouk, H., Merkley, M. A., Podolsky, R. H., Stöppler, H., Santos, C., Álvarez, M., Mariategui, J., Ferris, D., Lee, J. R., and Dynan, W. S. (2009) *Proteomics. Clinical Applications.* **3**, 516-527
103. Myers, M. P., Pass, I., Batty, I. H., Kaay, J. v. d., Stolarov, J. P., Hemmings, B. A., Wigler, M. H., Downes, C. P., and Tonks, N. K. (1998) *PNAS* **95**, 13513-13518
104. Mackay, J. P., Sunde, M., Lowry, J. A., Crossley, M., and Matthews, J. M. (2007) *Trends in Biochemical Sciences* **32**, 530-531
105. Chatr-aryamontri, A., Ceol, A., Licata, L., and Cesareni, G. (2008) *Trends in Biochemical Sciences* **33**, 241-242
106. Welch, G. R. (2009) *Trends in Biochemical Sciences* **34**, 1-2
107. Tompa, P., and Fuxreiter, M. (2008) *Trends in Biochemical Sciences* **33**, 2-8
108. Wilson, M. A., Collins, J. L., Hod, Y., Ringe, D., and Petsko, G. A. (2003) *PNAS* **100**, 9256-9261
109. Bandopadhyay, R., Miller, D. W., Kingsbury, A. E., Jowett, T. P., Kaleem, M. M., Pittman, A. M., deSilva, R., Cookson, M. R., and Lees, A. J. (2005) *Neuroscience Letters* **383**, 225-230
110. Wagenfeld, A., Yeung, C. H., Shivaji, S., Sundareswaran, V. R., Ariga, H., and Cooper, T. G. (2000) *Journal of Andrology* **21**, 954-963
111. Hod, Y., Pentyala, S. N., Whyard, T. C., and El-Maghrabi, M. R. (1999) *Journal Cellular Biochemistry* **72**, 435-444
112. Mitsumoto, A., and Nakagawa, Y. (2001) *Free Radical Research* **35**, 885-893
113. Mitsumoto, A., Nakagawa, Y., Takeuchi, A., Okawa, K., Iwamatsu, A., and Takanezawa, Y. (2001) *Free Radical Research* **35**, 301-310
114. deNobel, H., Lawrie, L., Brul, S., Klis, F., Davis, M., Alloush, H., and Coote, P. (2001) *Yeast* **18**, 1413-1428
115. Rocha, M., Rovira-Llopis, S., Bañuls, C., Bellod, L., Falcon, R., Castello, R., Morillas, C., Herance, J. R., Hernandez-Mijares, A., and ., V. M. V. (2013) *Current Pharmaceutical Design*
116. Bonifati, V. (2003) Autosomal recessive, early-onset Parkinson's disease. Department of Clinical Genetics, Erasmus MC Rotterdam,The Netherlands
117. Tao, X., and Tong, L. (2003) *Journal of Biological Chemistry* **278**, 31372-31379
118. Baulac, S., LaVoie, M. J., Strahle, J., Schlossmacher, M. G., and Xia, W. (2004) *Molecular and Cellular Neuroscience* **27**, 236-246
119. Olzmann, J. A., Brown, K., Wilkinson, K. D., Rees, H. D., Huai, Q., Ke, H., Levey, A. I., Li, L., and Chin, L.-S. (2004) *The Journal of Biological Chemistry* **279**, 8506-8515
120. Aleyasin, H., Rousseaux, M. W. C., Marcogliese, P. C., Hewitt, S. J., Irrcher, I., Joselin, A. P., Parsanejad, M., Kim, R. H., Rizzu, P., Callaghan, S. M., Slack, R. S., Mak, T. W., and Park, D. S. (2010) *PNAS* **107**, 3186–3191
121. Leau, O., and Ducrot, R. (1957) *Comptes Rendus la Societe Francaise Biologie* **151**, 1365-1367

122. Leger, A., Schnerb, A., Lejeune, D., Glisse, J. C., and Vieillefond, H. (1986) *Medecine Des Armees* **13**, 269-273
123. Lacour, M. (1995) Influence d'un traitement pharmacologique a l'acetyl-DL- leucine dans la compensation des deficits vestibulaires chez le chat. Etude neurophysiologique., Pierre Fabre Medicaments, Castres, France, Laboratoires Pierre Fabre
124. Neuhauser, H. K., and Lempert, T. (2009) *Seminars in Neurology* **29**, 473-481
125. Tanimukai, H., Grundke-Iqbal, I., and Iqbal, K. (2005) *The American Journal of Pathology* **166**, 1761–1771

Chapter 11: Appendix

```
1   atg gct tcc aaa aga gct ctg gtc atc ctg gct aaa gga gca gag gaa atg gag acg gtc
    tac cga agg ttt tct cga gac cag tag gac cga ttt cct cga ctc ctt tac ctc tgc cag
61  atc cct gta gat gtc atg agg cga gct ggg att aag gtc acc gtt gca ggc ctg gct gga
    tag gga cat cta cag tact cc gct cga ccc taa ttc cag tgg caa cgt ccg gac cga cct
121 aaa gac cca gta cag tgt agc cgt gat gtg gtc att tgt cct gat gcc agc ctt gaa gat
    ttt ctg ggt cat gtc aca tcg gca cta cac cag taa aca gga cta cgg tcg gaa ctt cta
181 gca aaa aaa gag gga cca tat gat gtg gtg gtt cta cca gga ggt aat ctg ggc gca cag
    cgt ttt ttt ctc cct ggt ata cta cac cac caa gat ggt cct cca tta gac ccg cgt gtc
241 aat tta tct gag tct gct gct gtg aag gag ata ctg aag gag cag gaa aac cgg aag ggc
    tta aat aga ctc aga cga cga cac ttc ctc tat gac ttc ctc gtc ctt ttg gcc ttc ccg
301 ctg ata gcc gcc atc tgt gca ggt cct act gct ctg ttg gct cat gaa ata ggc tgt gga
    gac tat cgg cgg tag aca cgt cca gga tga cga gac aac cga gta ctt tat ccg aca cct
361 agt aaa gtt aca aca cac cct ctt gct aaa gac aaa atg atg aat gga ggt cat tac acc
    tca ttt caa tgt tgt gtg gga gaa cga ttt ctg ttt tact ac tta cct cca gta atg tgg
421 tac tct gag aat cgt gtg gaa aaa gac ggc ctg att ctt aca agc cgg ggg cct ggg acc
    atg aga ctc tta gca cac ctt ttt ctg ccg gac taa gaa tgt tcg gcc ccc gga ccc tgg
                                          K175STP FWD 3′ccg atc ctc cac cgc cg 5′
481 agc ttc gag ttt gcg ctt gca att gtt gaa gcc ctg aat ggc Tag gag gtg gcg gct caa
    tcg aag ctc aaa cgc gaa cgt taa caa ctt cgg gac tta ccg atc ctc cac cgc cga gtt
                                          5′gcc ctg aat ggc tag gag g 3′K175STP REV
541 gtg aag gct cca ctt gtt ctt aaa gac tag
    cac ttc cga ggt gaa caa gaa ttt ctg atc
```

Figure 11.1: Design of K175Stop mutant from wild type DJ-1.

Point mutation is shown in red and primers are underlined.

```
1   atg gct tcc aaa aga gct ctg gtc atc ctg gct aaa gga gca gag gaa atg gag acg gtc
    tac cga agg ttt tct cga gac cag tag gac cga ttt cct cga ctc ctt tac ctc tgc cag
61  atc cct gta gat gtc atg agg cga gct ggg att aag gtc acc gtt gca ggc ctg gct gga
    tag gga cat cta cag tact cc gct cga ccc taa ttc cag tgg caa cgt ccg gac cga cct
121 aaa gac cca gta cag tgt agc cgt gat gtg gtc att tgt cct gat gcc agc ctt gaa gat
    ttt ctg ggt cat gtc aca tcg gca cta cac cag taa aca gga cta cgg tcg gaa ctt cta
181 gca aaa aaa gag gga cca tat gat gtg gtg gtt cta cca gga ggt aat ctg ggc gca cag
    cgt ttt ttt ctc cct ggt ata cta cac cac caa gat ggt cct cca tta gac ccg cgt gtc
241 aat tta tct gag tct gct gct gtg aag gag ata ctg aag gag cag gaa aac cgg aag ggc
    tta aat aga ctc aga cga cga cac ttc ctc tat gac ttc ctc gtc ctt ttg gcc ttc ccg
301 ctg ata gcc gcc atc tgt gca ggt cct act gct ctg ttg gct cat gaa ata ggc tgt gga
    gac tat cgg cgg tag aca cgt cca gga tga cga gac aac cga gta ctt tat ccg aca cct
361 agt aaa gtt aca aca cac cct ctt gct aaa gac aaa atg atg aat gga ggt cat tac acc
    tca ttt caa tgt tgt gtg gga gaa cga ttt ctg ttt tact ac tta cct cca gta atg tgg
421 tac tct gag aat cgt gtg gaa aaa gac ggc ctg att ctt aca agc cgg ggg cct ggg acc
    atg aga ctc tta gca cac ctt ttt ctg ccg gac taa gaa tgt tcg gcc ccc gga ccc tgg
   3′CG AAG CTC AAA CGC GGA CG 5′ – L166P FWD
481 agc ttc gag ttt gcg cCt gca att gtt gaa gcc ctg aat ggc aag gag gtg gcg gct caa
    tcg aag ctc aaa cgc gGa cgt taa caa ctt cgg gac tta ccg ttc ctc cac cgc cga gtt
                    5′CG CCT GCA ATT GTT GAA GCC C 3′ – L166P REV
541 gtg aag gct cca ctt gtt ctt aaa gac tag
    cac ttc cga ggt gaa caa gaa ttt ctg atc
```

Figure 11.2: Design of L166P mutant from wild type DJ-1.

Point mutation is shown in red and primers are underlined.